Controlling the Stability of Colloidal Drug Aggregates for Chemotherapeutic Delivery

by

Ahil Naban Ganesh

A thesis submitted in conformity with the requirements
for the degree of Doctor of Philosophy

Chemical Engineering and Applied Chemistry
Institute of Biomaterials and Biomedical Engineering
University of Toronto

Controlling the Stability of Colloidal Drug Aggregates for Chemotherapeutic Delivery

Ahil Naban Ganesh

Doctor of Philosophy

Chemical Engineering and Applied Chemistry
Institute of Biomaterials and Biomedical Engineering

University of Toronto

2019

Abstract

Colloidal aggregation presents a significant nuisance in drug discovery programs; the self-assembly of hydrophobic compounds into colloidal particles leads to numerous artifactual results in screening assays. In biochemical enzyme inhibition assays colloids non-specifically adsorb proteins leading to partial unfolding and enzyme inactivation. In cell-based cytotoxicity assays colloids are unable to cross cell membranes leading to the drug being unable to bind to its intracellular target, resulting in apparent inactivity. Colloidal aggregation is not only common among drug screening candidates but also among clinically used drugs. Being composed entirely of active drug, colloidal drug aggregates have many properties that make them suitable as nanoparticle drug formulations. In this work, two methods to stabilize colloidal drug aggregates were developed to enable targeted delivery and in vivo utility.

First, exploiting the ability of drug colloids to adsorb proteins, we formed controlled protein coronas to stabilize colloids in both buffered solutions and serum-containing media. Coronas comprising antibodies not only stabilized colloids but also enabled their specific internalization by target cells. Second, incorporation of amphiphilic surfactants during colloid formation resulted in a hydrophilic polymer layer that sterically stabilized drug colloids. Incorporation of

surfactants significantly reduced protein adsorption, stabilizing drug colloids in serum-containing media. We designed methods to test colloid stability in high serum media in vitro based on co-aggregation with fluorescent FRET pairs. Finally, we investigated the influence of stable colloidal drug aggregates on the in vivo pharmacokinetics of chemotherapeutics. Stable colloidal formulations showed increased plasma circulation half-lives compared to solubilized, monomeric formulations. Overall, we demonstrate methods to stabilize, study and utilize colloidal drug aggregates, turning a nuisance into an opportunity for drug formulation.

Acknowledgments

I would first and foremost like to thank my supervisor, Dr. Molly Shoichet for the unwavering support, guidance, and mentorship throughout my PhD. She was a constant source of encouragement when things weren't working and excitement when challenging experiments finally worked. When I first approached her as an undergrad about staying in the lab for graduate studies, she wanted me to make sure I wasn't just picking the easiest option. This is something that has continued to resonate with me and allowed me to think critically about junctures in research and elsewhere. I would also like to thank Dr. Brian Shoichet for a great collaboration over the course of my PhD. With his encouragement I was able to let my curiosity go free and ask questions that might have been a shot in the dark. Thank you to the many other scientists that I had the pleasure of collaborating with, for enriching my science with your own experience and expertise. I would like to thank the members of my committee over the years who simultaneously encouraged and challenged me, ultimately improving the quality of this thesis.

I owe a lot of gratitude to the member of the Shoichet lab, whose mentorship and friendship have been the most fruitful reward of this PhD journey. I would not be the scientist or person I am today without the relationships I've built in the lab. I am thankful to each and every member of the lab over the years but in particular I am grateful to a few people who have impacted my life in more ways than one. I am indebted to Team Colloid for directly making this thesis possible: Shawn, for introducing me into the world of colloids and teaching me how to be a scientist; Chris, for being a pillar of strength during the early years as we struggled together to wrap our heads around getting colloids to do what we wanted them to; Jenn, (who we brought over to the dark side) started out as a mentor but became a great friend; and Eric, for helping me, in recent years, consider the mechanisms at play in my own work. I'd also like to thank: Sam, for her sassy, yet genuine, friendship; Anup, for his refreshing perspective on the world; Nick, for our honest and open conversations about science and the world; and Alex, for keeping me motivated till the end. I haven't named everyone, but you have all become cherished friends, without whom I wouldn't be here today. These relationships are ones that I'm sure will last a lifetime and I look forward to reminiscing over the good (and not so good) times we've had together in the lab.

Lastly, but most importantly, I'd like to thank my parents, brother, and grandma for their constant support in pursuing my dreams. I'm finally done – for now.

Table of Contents

List of Figures

1 Introduction

Portions of this chapter are derived from the following manuscript:

Ganesh, A.N., Donders, E.N., Shoichet, B.K., and Shoichet, M.S. (2018) Colloidal aggregation: From screening nuisance to formulation nuance. *Nano Today*. 19:188-200.

Reprinted with permission from Elsevier. ANG, END, BKS and MSS wrote and edited the manuscript. This manuscript is included in section 1.3.

1.1 Rationale

Over the past decade and a half, the colloidal aggregation of hydrophobic, small molecule compounds has emerged as the leading cause of false-hits in early-stage drug discovery[1,2]. It was found that many hydrophobic, small molecule compounds self-assemble into colloidal particles with diameters typically between 50 – 1000 nm[3,4]. Their formation is governed by a critical aggregation concentration (CAC), akin to a critical micelle concentration, where colloidal particles are formed once this critical concentration has been exceeded[5]. This phenomenon is not only observed with compounds being investigated in the high-throughput screening (HTS) stage of drug discovery, but also with approved drugs that are used in the clinic[6-8]. Colloidal aggregates result in a number of artifactual results in screening assays. In enzyme inhibition assays, as those used in HTS, colloidal aggregates result in false positives; enzymes, such as β-lactamase and malate dehydrogenase, are inhibited by aggregates through their non-specific adsorption to the colloid surface[4]. In addition to causing false-positive results in early biochemical enzyme inhibition assays, colloids have also been shown to cause false-negative results in cell-based assays[7,9]. As drug concentration increases above the CAC and colloidal particles are formed, the potency of the drug is lost; the formation of colloidal drug aggregates prevents these compounds from entering cells where they would elicit cytotoxic effects.

Although the formation of colloidal aggregates is typically associated with undesirable results, their unique self-assembly properties give rise to the potential for use as an intentional nanoparticle drug formulation. Colloidal aggregates are nano-sized particles composed entirely of active, unmodified drug. Taking advantage of such drug-rich particles would yield formulations with significantly higher drug loadings than conventional micellar or liposomal formulations. Their physical properties can be optimized for passive tumor targeting and their unique interactions with

proteins can be harnessed to confer active targeting capabilities. While, colloidal aggregates have many advantages in this regard, their transient stability has limited their study and use thus far. Strategies to stabilize colloidal drug aggregates would enable turning this nuisance phenomenon into a useful formulation strategy.

1.2 Hypothesis and Objectives

The hypothesis governing this thesis is:

Controlled formulation of colloidal drug aggregates with proteins and polymers will improve their in vitro serum stability and in vivo pharmacokinetics.

To test this hypothesis, this work was divided into three primary objectives:

1. **To design stable antibody-modified drug colloids for targeted in vitro delivery**

   In Chapter 2, I demonstrate that colloidal drug aggregates can be stabilized by taking advantage of their innate ability to adsorb proteins. Formation of a protein corona stabilizes colloids in both buffered solutions and serum-containing media. Furthermore, coronas comprising targeted antibodies, such the anti-HER2 trastuzumab, can elicit uptake by target, HER2-overexpressing cells leading to internalization and increased efficacy of the colloidal formulation.

2. **To enhance the stability of colloidal drug aggregates with polymeric excipients**

   In Chapter 3, I demonstrate that a variety of amphiphilic surfactants can be used to stabilize colloidal drug aggregates. Incorporation of polymers significantly reduces protein adsorption and increases stability of drug colloids in serum-containing media. Additionally, stable colloidal formulations do not passively diffuse into cells and are internalized in a different manner to non-colloid forming soluble drugs.

3. **To investigate the in vivo utility of stable colloidal drug formulations**

   In Chapter 4, I further investigate the stability of polymer-stabilized drug colloids under plasma-mimicking conditions and in vivo. I measure, for the first time, the critical aggregation concentration of a colloid-forming compound under high serum conditions. After demonstrating that colloids can be formulated to be stable in 90% serum in vitro, I

show that colloidal formulations extend the plasma half-life of drugs in vivo compared to monomeric formulations.

1.3 Colloidal Aggregation

Drug discovery often begins with screening libraries of over one million molecules to find early compounds that may become leads to drug candidates[1,10]. While they remain the most widely used strategy in pharmaceutical research to discover new disease-related targets, these high-throughput screening (HTS) campaigns are dominated by false-positive "hits"[3,11,12]. Often, far more time and resources are spent distinguishing between true and false positives, and prioritizing well-behaved hits for progression, than was spent developing and executing the HTS in the first place.

Among the most common mechanisms for false-positive hits in HTS is the colloidal aggregation of small molecules, first discovered 15 years ago[3] and now widely accepted[2]. Subsequent mechanistic work demonstrated that aggregation occurs via phase separation and particle formation when the small molecules are present above a compound-specific critical aggregation concentration (CAC)[5]. The resulting colloidal aggregates non-specifically bind proteins to their surface causing local unfolding events, which, in the case of enzymes, result in loss of catalytic activity[5,13]. Compound aggregation alone explained the flat structure-activity relationships and high sensitivity to assay conditions that had been a common feature of the HTS false positives[1,12]. A third widespread feature of these pathological hits, their steep Hill coefficients in concentration-response curves, was explained by the aggregates having binding affinities for their target proteins that were substantially higher than the concentration of the targets in the assays[12].

The formation of colloidal particles in biochemical buffers and their interactions with biological molecules have had many implications for drug discovery, formulation and activity. While many of these properties have rendered colloidal aggregates to be considered as nuisance artifacts, they can also be exploited to turn colloidal aggregation into an advantage. The unique properties of colloidal aggregates, their implications in biochemical assay and drug development will be discussed herein.

1.3.1 Properties of Colloids

Many organic small molecules spontaneously self-assemble in aqueous media into nano-sized colloidal aggregates without chemical manipulation. These molecules cover a range of chemical properties and structures, and include compounds from screening libraries, dyes (e.g. Congo red and Trypan blue), and even clinically approved drugs (e.g. chemotherapeutic vemurafenib and anti-retroviral ritonavir)[3,4,8]. In the following sections, properties that make colloidal aggregates unique as nanostructures and different from other self-assembled drug nanoparticles are highlighted.

1.3.1.1 Colloidal particle formation

The formation of stable, amorphous, nano-sized particles is a characteristic property of colloidal aggregation[3]. These colloids have diameters typically between 50 and 1000 nm and form through spontaneous phase separation on addition to aqueous media from, often, an organic stock solution such as DMSO. Aggregation is concentration dependent; at low concentrations, the compound is fully solubilized, but as the concentration increases, spontaneous self-assembly occurs at a critical concentration (Figure 1.1)[5].

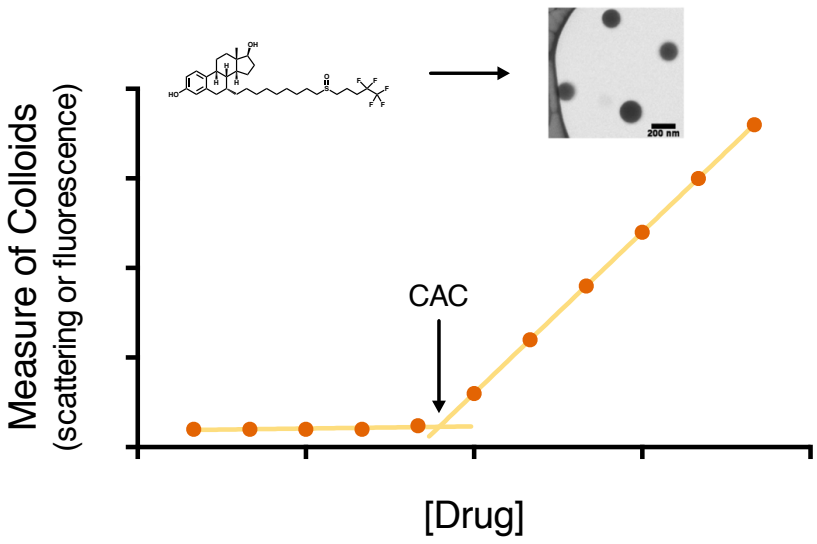

Figure 1.1. Onset of colloidal aggregation determined by the critical aggregation concentration (CAC) of the compound. At low concentrations, the drug is fully soluble and only baseline scattering is observed. Once the CAC has been exceeded, scattering increases indicating the formation of colloidal particles. Insert, electron micrograph of colloidal drug aggregates of fulvestrant (scale bar represents 200 nm).

This critical aggregation concentration (CAC) appears to correspond to the amorphous solubility of the compound[14]. Notably, this concentration is higher than the crystal solubility of the compound, at least in those cases where the two have been carefully compared. The CAC is analogous to the critical micelle concentration for surfactants; like micelles, when diluted below the CAC the aggregates will spontaneously disassemble and return to a monomeric state[3,15]. At least transiently, the concentration of free molecules that remain in solution is defined by the CAC, even once aggregates have formed, as is the case with micelles[5]. This can be shown by centrifugation, for instance, where the colloidal aggregates may be spun down and separated from the soluble molecule, with the concentration in the supernatant remaining constant at the CAC.

Taylor et al. demonstrated that colloidal aggregates are liquid-liquid phase-separated solutions[14], unlike nanocrystals where the drug molecules are tightly packed into an organized lattice. The amorphous nature of colloidal aggregates allows them to interact with hydrophobic dyes akin to micelles, and unlike nanocrystals. Fluorescent probes, such as pyrene, change their emission characteristics depending on the polarity of their environment[16,17]. Such dyes preferentially associate with the hydrophobic core of micelles and allow measurement of the CMC[16-18]. Similarly, these dyes associate with hydrophobic colloids at concentrations that correlate with the CAC[14,19-22]. The ability of fluorophores to incorporate into colloidal aggregates supports their liquid nature, as dyes are unable to penetrate crystal lattices.

While the actual molecular structure of colloidal aggregates is poorly understood, some studies have provided a preliminary glimpse into their structure. By small-angle X-ray scattering, the structure of the colloidal aggregates fit the expected pair distance distribution function for well-packed, rather than hollow, spheres[23]. This result is supported by the ratio of the radius of gyration to the hydrodynamic radius from light scattering[23]. Additional studies are needed to fully understand the molecular organization (if any) of colloidal aggregates.

1.3.1.2 Aggregation thermodynamics

The self-assembly of molecules into colloidal aggregates is driven by their relative inability to form energetically favorable interactions with water[24]. Practically, these aggregates form when water is added to a hydrophobic aggregator dispersed in a water-miscible organic solvent (e.g. DMSO)[5,24], or blended in a water-soluble polymer matrix[14,25,26]. In these conditions, the mixture spontaneously separates to generate a liquid or glassy colloidal phase along with a small

molecule-depleted aqueous phase. The exact mechanism by which colloidal aggregates form has not been studied for all aggregators, or under all conditions however some mechanisms for colloid formation, during which the organic and aqueous phases are mixed together, have been proposed[24,25,27]. Phase separation will occur whenever local supersaturation is achieved during mass exchange between organic and aqueous phases. Since phase separation will occur when the local composition is supersaturated, the aggregator concentration in the organic phase and the solubility parameters of the aggregator and organic matrix (which influence the shape of the unstable and metastable regions) likely dictate where phase separation will occur[25]. When the aggregator concentration is low, phase separation occurs only after a relatively large amount of water has penetrated the organic phase as aggregator-in-polymer formulations dissolve[27]. Conversely, when the aggregator concentration is high, phase separation occurs after only a small amount of water diffuses into the organic phase[25].

1.3.1.3 Factors that influence the critical aggregation concentration

The CAC of an aggregator is determined by both its intrinsic properties and the conditions of the continuous phase. Equation 1 estimates the CAC as a function of the crystal solubility (C_{sat}), enthalpy of fusion (ΔH_f), melting temperature (T_m), temperature (T), gas constant (R), and a correction factor that accounts for the aggregator-rich phase containing solutes such as water ($\exp(-I(a_2))$)[14,28]. This approach generally yields a good approximation of the CAC; more rigorous methods are more predictive when the degree of undercooling ($T_m - T$) is high[22].

$$CAC = C_{sat}\, exp\left(\frac{\Delta H_f (T_m - T)}{R T_m^2}\right) exp\big(-I(a_2)\big) \qquad 1$$

For a single-aggregator system, the enthalpy of fusion, melting temperature, and correction factor are static and intrinsic to each aggregator. However, the CAC is also affected by extrinsic factors. For example, the CAC can be indirectly altered by factors that affect the crystal solubility (C_{sat}), as is evident from Equation 1. This property, while heavily dependent on the nature of the aggregator, is strongly affected by the solvent conditions[3,14,24]. For example, crystal solubility is increased with increasing temperature, which increases the CAC. Additionally, adding salts to the aqueous phase reduces the solubility of relatively non-polar aggregators, and the CAC will be reduced, similar to self-assembled micelle systems[29,30]. Conversely, adding an organic solvent that is miscible with water (e.g. ethanol, DMSO or THF) will increase the aggregator solubility, and the CAC will increase. Addition of solubilizing excipients such as

cyclodextrins or surfactants can greatly increase the effective CAC of an aggregator because the aggregator partitions with the solubilizer, reducing the concentration of aggregator in the continuous phase[4,19,27,31,32]. Similarly, changing the pH can appear to change the CAC of an aggregator with ionizable groups[33,34]. This phenomenon is often due to conversion of the neutral aggregator to a generally more soluble charged species. In pH conditions that favour the charged species, a higher overall aggregator concentration is needed for the neutral aggregator to reach its CAC; however, the true value of the CAC is unaffected by pH[21]. Taken together, this means that the observed CAC of an aggregator depends on the composition of the media.

1.3.1.4 Macromolecule adsorption onto colloidal aggregates

At least partly due to their high surface area, and perhaps to the apolar nature of that surface, colloidal aggregates sequester macromolecules such as proteins, as illustrated in the following examples. The interaction of colloids with proteins was first observed through their non-specific and time-dependent enzyme inhibition[4] (further discussed in Section 1.3.2.1). Enzymes adsorb onto the surface of colloids and are partially unfolded, resulting in a loss of enzymatic activity[13]. The binding of proteins to the colloid is driven by surface interactions between the colloid and proteins, and often has dissociation constants in the picomolar range[12,35]. Intriguingly, adsorption to colloids is specific to proteins, and has not been observed with other common biomolecules. Comparing fluorescently labeled proteins and DNA, only proteins were observed to be substantially adsorbed to colloidal aggregates; all DNA (single- or double-stranded) remained fully solubilized[23]. Full proteins also adsorbed more strongly than peptide fragments. For example, in a competitive assay in which the full β-lactamase protein and its peptide fragments were incubated with colloids, the presence of peptides had little impact on the inactivation of the enzyme by the colloids, demonstrating the preferential binding of full proteins to the colloidal surface. While protein adsorption to nanoparticles is not unique to colloidal aggregates, their reversible formation provides a unique method for enzyme re-activation[36].

1.3.1.5 Detergent reversibility

A defining property of colloidal aggregates is their detergent reversibility. When detergents are added to the colloids, at concentrations greater than the aggregator concentration, the colloids can be disrupted[3,37]. Typically Triton X-100 (0.01% (v/v)) and polysorbate 80 (0.025% (v/v)) are used to disrupt aggregation in enzyme- and cell-based assays, respectively[7,38]. Lower concentrations can prevent enzyme inhibition while still maintaining intact colloids[4]. The true

biological effects of colloid-forming compounds in enzyme and cell-based assays can be probed using detergents to disrupt colloid formation[4,7].

1.3.2 Biological Implications of Colloidal Aggregates

In addition to their interesting physical properties, colloidal aggregates have unique interactions with biological environments. As mentioned in Section 1.3.1.4, their interactions with proteins can result in false hits in HTS. Furthermore, their stability in the presence of high-protein milieus impacts both in vitro and in vivo analyses. Proteins are abundant in biological systems, where their interactions with other macromolecules drive important biochemical pathways and physical transport phenomena. Understanding the interactions of colloids with proteins and cells is key to understanding in vitro and in vivo data.

1.3.2.1 Interactions of colloidal aggregates with proteins

A characteristic of colloidal aggregates is their strong surface adsorption of proteins. Direct association of colloids with proteins has been shown by centrifugation of solutions with both colloids and proteins, where the protein is concentrated in the colloid pellet[4,36]. TEM imaging of the colloid-protein complex has also confirmed their direct association[4]. Colloids are stable in high-protein milieus and even form in the presence of proteins[7,39].

In the case of enzymes, adsorption to the colloid surface typically leads to a loss of catalytic activity. This phenomenon is non-specific and colloid-forming compounds inhibit many unrelated enzymes at micromolar concentrations[3,23,38]. Enzyme inhibition is typically time-dependent and partly reversible, as demonstrated by adsorption kinetics studies. Liu et al. showed that initial rates of the reaction were inhibited by aggregates, and were suggestive of non-competitive inhibition wherein the aggregate binds to both free enzyme and the enzyme-substrate complex[40]. Upon disruption of the colloids (either by dilution or solubilization with detergents), the majority of enzyme activity returns[4]. Intriguingly, colloidal aggregates can actually stably sequester enzymes, preserving their activity until the colloid is disrupted[36].

The origins of protein inhibition by colloidal aggregates appears to be sequestration followed by partial unfolding, though the importance of the second, unfolding step, remains to be fully determined. The occurrence of partial enzyme unfolding has been demonstrated in several ways[13,39]. First, incubation of a β-lactamase-colloid complex with the irreversible inhibitor moxalactam led to no observable effect on the reactivated enzyme after colloid disruption,

indicating that there is no significant exchange between bound and free enzyme. Second, binding of β-lactamase to colloids followed by deuterium-hydrogen exchange, led to increased incorporation of deuterium into the enzyme, as measured by mass spectroscopy after protease digestion. Such increased incorporation into the peptide backbone suggests increased accessibility to the solvent due to at least local unfolding. Third, β-lactamase bound to colloids was much more susceptible to trypsin degradation than was the free enzyme, further supporting denaturation of the enzyme on colloid binding. Because the enzyme regains much of its activity rapidly on colloid disruption, within the dead-time of a spectrophotometric assay, it seems likely that the unfolding that the enzyme suffers on the colloids surface is local and transient.

Based on particle counting methods combined with enzyme activity assays, Coan et al. concluded that colloidal particles had sufficient surface area to adsorb all the protein used in their study, but this observation does not rule out protein absorption into the colloid core[5]. While the molar ratio of protein to colloid-forming compounds in these systems may be on the order of 1:1000, the ratio of enzyme to colloidal particle is much higher since each particle contains millions of drug molecules. This higher ratio of enzyme to colloid also makes it possible for the particle surface to become saturated. For example, pre-incubation of colloids with albumin significantly reduces enzyme inhibition because albumin adsorbs to the colloid surface, leaving less surface area for enzymes[3,36]. Notably, the addition of protein to the already formed colloid-enzyme complex neither frees adsorbed protein nor restores catalytic activity[39], likely due to the slow dissociation of already bound enzyme (picomolar dissociation constants).

1.3.2.2 Membrane transport of colloidal drug aggregates

Drug transport across cell membranes is key to efficacy. Studying membrane transport of drugs using a standard diffusion cell, with the donor and receiver chambers separated by a semipermeable membrane, Taylor et al. found that when colloidal drug aggregates form, there is an upper limit for flux across the synthetic membrane[41]. When the donor chamber concentration was below the CAC, they found that the flux of felodipine increased linearly with increasing concentrations. However, when the donor cell concentration exceeded the CAC, the flux of drug remained constant over all concentrations tested. This observation supports the formation of colloidal drug aggregates, as any drug above the CAC self-assembles into particles, which cannot cross the membrane. Thus, the effective drug concentration that drives diffusion is limited at the CAC; only the non-colloidal drug amount is able to diffuse into the receiver chamber,

which leads to a constant flux when the total drug concentration is greater than the CAC. As diffusion occurs, the drug in the continuous phase is replenished by drug within the colloidal aggregates and thus flux is maintained over time.

Due to the reversible nature of colloidal aggregation, the presence of solubilizing excipients also influences the diffusive flux across membranes. When only low concentrations of micellar detergents are present, the thermodynamic activity of the drug and therefore the diffusive flux remain constant. When an excess of detergents is used to disrupt colloids, drug molecules partition with these detergents and there is a reduction in flux due to a decrease in the concentration of free, non-micelle-bound drug to below the CAC[31]. A similar observation is made when the aqueous environment itself affects the aggregation properties of the compounds. For example, Raina et al. observed a difference in diffusive flux of felodipine in phosphate buffer versus simulated intestinal fluid (SIF)[31]. Constant flux above a certain concentration was observed in both buffers; however, the concentration at which this plateau was observed was significantly higher in SIF, which is indicative of a higher CAC in this medium. While these studies have important implications in the context of oral drug delivery, the role of active transport processes and presence of biomacromolecules, such as proteins and lipids, remain sparsely studied.

1.3.2.3 Colloidal drug aggregates in cell culture

Colloidal aggregates are stable in high-protein milieus, and it is perhaps unsurprising that their presence would have an impact on drug activity in cell culture assays[7,9]. For instance, when aggregating chemotherapeutic compounds reach their CAC values and adopt a colloidal form in cell culture, a substantial decrease (in some cases a total loss) of cytotoxic activity is observed. Conversely, when a free drug monomer population is maintained, through the addition of detergents, the activity of the drug returns. The concentration at which loss of drug activity occurs coincides with the CAC of the compounds[9]. In contrast to the expected monotonic sigmoidal dose-response curve observed for many chemical inhibitors, a “bell-shaped” dose response curve was observed for many colloidal aggregators (Figure 1.2A). “Bell-shaped” curves are common in the literature, and are typically explained by the engagement of multiple cellular pathways. Undoubtedly this explanation holds for many molecules, but for at least some molecules these unusual curves will reflect the formation of colloidal aggregates[9].

The interactions between colloid-forming dyes and cells were investigated to further understand the mechanism of drug activity loss[9]. When colloidal dye particles were incubated with cells, little to no fluorescence was observed within the cell, indicating that colloids were not internalized by cells (Figure 1.2B). However, upon disruption of the dye colloids with detergents, solubilized dye molecules could freely cross the cell membrane (Figure 1.2C). Permeabilized membranes allowed both colloidal and monomeric dye solutions to enter cells. This observation suggests that the loss of drug activity in colloidal formulations is due to the inability of drug colloids to cross cell membranes. Consistent with previous work investigating nanoparticle-cell interactions, these results suggest that, in high-protein milieus, the strong affinity of the colloid surface for proteins leads to immediate protein adsorption. This formation of a protein corona prevents interactions between the colloid and cell surface, thus limiting entry of the drug into cells[42-44]. Furthermore, while drug dissolution from the colloid immediately replaces depleted free drug in the absence of proteins (as discussed above), the presence of serum and the formation of a protein corona appears to impede the ability of the colloid to replenish the free drug species in cell culture conditions. Thus, it seems that the colloid reduces the thermodynamic activity of the drug.

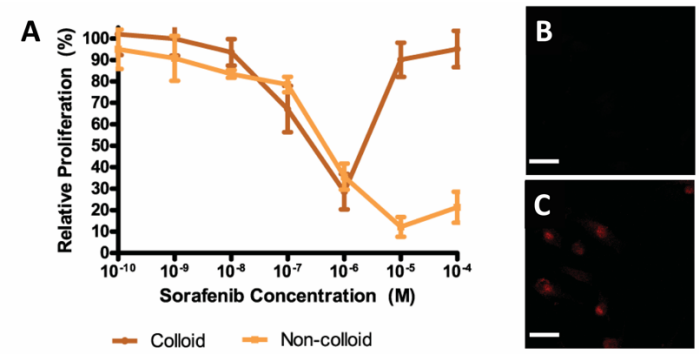

Figure 1.2. (A) "Bell-shaped" dose-response curve of the colloid-forming anti-neoplastic drug, sorafenib. Upon colloid formation, loss of anti-proliferative activity is observed. Intracellular fluorescence after incubation with (B) colloidal and (C) monomeric formulations of Evans blue shows inability of colloids to permeate cell membrane. Reprinted with permission from Ref. [9]. Copyright 2014 American Chemical Society.

1.3.2.4 Persistence of colloidal drug aggregates in vivo

Based on expected gastric drug concentrations and the diversity of conditions under which colloidal aggregation occurs, it is not surprising that colloidal drug aggregates are in fact present

in vivo. Doak et al. observed that many compounds formed colloids at concentration relevant to in vivo dosing regimens in simulated gastric environments in vitro[45]. Work by Frenkel et al. suggests that not only do colloids form and persist in the gastrointestinal tract, but their presence also impacts the bioavailability of these compounds in vivo[33,46].

Frenkel et al. investigated the colloid-forming properties of a number of non-nucleoside reverse transcriptase inhibitors (NNRTIs) which have known pharmacokinetic parameters in rodent models and humans[33]. They identified a number of NNRTIs that form colloidal particles in simulated gastric environments at concentrations similar to those expected in the gastrointestinal tract after oral dosing. They classified these compounds into two groups based on aggregate size: small particles (60-220 nm diameters) and large particles (>500 nm diameters). They found good correlations between this classification of compounds and their known pharmacokinetic parameters. For example, compounds that formed aggregates with small diameters had good adsorption/bioavailability parameters (AUC > 5 μg·h/mL) while those that formed large aggregates had poor bioavailability (AUC < 1 μg·h/mL). The authors hypothesized that the smaller aggregates were absorbed by M cells of the Peyer's patch and then entered systemic circulation via lymphatic circulation. This result is consistent with other studies investigating nanoparticle formulations for oral delivery[47,48]. In contrast, larger aggregates appeared to have precipitated, thus limiting the bioavailability of the drug.

Since changes in pH play an important role in gastrointestinal drug absorption, Frenkel et al. also investigated the effect of pH on aggregation and subsequent bioavailability. For most of the compounds studied, an increase in pH led to an increase in aggregate size; however, the degree to which the aggregate size changed depended on the compound itself[33]. This pH-dependence on size change was correlated to bioavailability of the compound; the most bioavailable compounds were found to be the least affected by increasing pH while the least bioavailable compounds increased in size the most with increasing pH values.

1.3.3 Colloid-Forming Drugs

Although colloidal aggregates are currently viewed as a hindrance in the drug discovery process, a number of clinically used compounds also form colloidal drug aggregates. Colloid-forming drugs range in disease applications from anti-fungals (e.g. clotrimazole), to cardiovascular therapies (e.g. felodipine and nifedipine) and to chemotherapeutics (e.g. sorafenib and lapatinib). A number of chemotherapeutics have been shown to form colloidal aggregates with CACs in the

low micromolar range. Since colloidal drug aggregates are composed entirely of active, unmodified drug, this presents an opportunity to turn these screening artifacts into a formulation strategy for these compounds. Such strategies could also give “new-life” to colloid-forming lead candidates that have been rejected in the drug development process.

1.4 Cancer Chemotherapy

Chemotherapeutic regimens in cancer utilize cytotoxic agents to stop proliferation or kill cancerous cells. Numerous chemical compounds have been extracted from natural sources or chemically designed for this purpose[49]. Many compounds target DNA within the cell nucleus either causing its modification (e.g. alkylating agents such as nitrogen mustards and DNA cross-linkers such as cyclophosphamide) or preventing interactions with other proteins (e.g. antitumour antibiotics such as doxorubicin which inhibits topoisomerase II)[50]. The microtubules are an important target of many chemotherapeutics. The vinca alkaloids (vinblastine and vincristine) depolymerize microtubules, while the taxanes (paclitaxel and docetaxel) promote microtubule polymerization[51]. In both cases, cells are unable to escape the mitotic state and the cell cycle is stalled leading to apoptosis. Combined these chemotherapeutics are widely used to treat many cancers, both as single agents and in drug cocktails[52].

The aforementioned compounds typically target cancer cells due to their rapid rate of proliferation. However, they can also elicit cytotoxic effects on proliferating healthy cells, leading to dose-limiting side effects. In recent decades, with the elucidation of the genetic drivers of cancer, targeted therapies have been developed. These therapies are specific to cancer-driving proteins that are overexpressed in cancer cells, providing an opportunity to minimize off-target effects. Anti-hormone compounds are often used in the treatment of breast cancer, as two-thirds of breast cancers are estrogen-receptor positive and respond to such anti-estrogen therapies[53]. Estrogen acts primarily through binding to estrogen receptor-α (ERα)[53,54] where the ligand-receptor complex dimerizes and translocates to the cell nucleus (Figure 1.3A). Here, it binds to estrogen response elements in regulatory regions of genes responsible for cell proliferation and survival. Anti-estrogen therapies aim to block the interaction of estrogen with ERα; these include compounds such as the selective estrogen receptor modulator, tamoxifen, and the pure estrogen receptor antagonist, fulvestrant[53,55-57]. Fulvestrant is an analogue of estradiol (the most common form of estrogen in circulation) and competitively binds with ERα[54]. Once bound to the

receptor, fulvestrant blocks dimerization and nuclear translocation, in addition to promoting degradation of the receptor (Figure 1.3B).

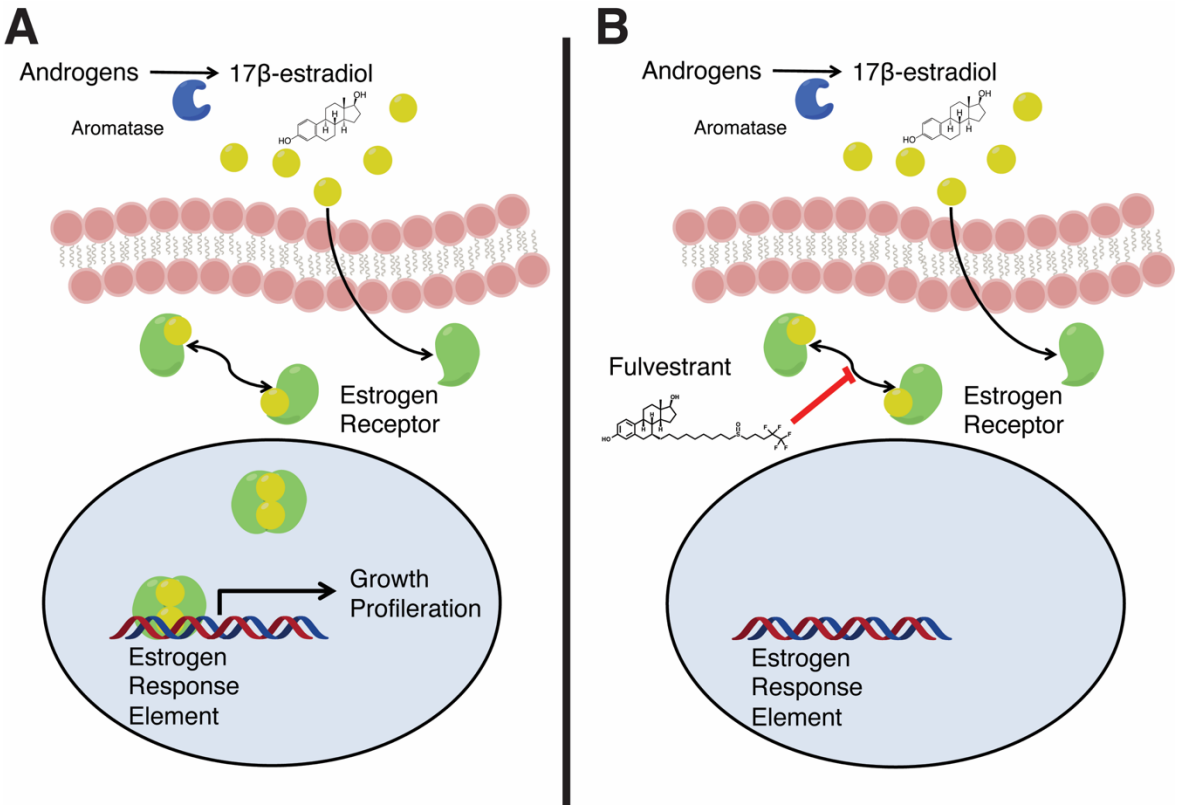

Figure 1.3. Mechanism of actions of estrogen and fulvestrant. (A) Estrogen induces estrogen receptor-α dimerization and subsequent activation of genes inducing cell proliferation and survival. (B) Fulvestrant binds to ERα, preventing dimerization and gene transcription.

Another class of targeted therapies that have been successful in a broad range of cancers (and other diseases) are the kinase inhibitors[58,59]. Many cancer cells depend on the downstream signal transduction of tyrosine kinases for their enhanced survival and proliferation. In breast cancer, the human epidermal growth factor receptor 2 (HER2) is over expressed in 20-30% of breast tumours[60]. Through heterodimerization with other members of the epidermal growth factor receptor family, kinase activity leads to autophosphorylation and signaling via Ras and PI3K pathways to stimulate cell division and cell growth, respectively[61,62]. HER2 kinase inhibitors, such as lapatinib, prevent autophosphorylation and have been clinically approved for the treatment of HER2-positive breast cancers[58,63,64].

Prodrug strategies can also be used to improve the solubility of chemotherapeutics as well as take advantage of tissue-specific enzymes for drug activation[65]. One such example is the investigational anthracycline-derived prodrug, pentyloxycarbonyl-(*p*-aminobenzyl)doxazolidinylcarbamate (PPD), developed by the Koch lab at the University of Colorado-Boulder[66]. PPD is activated by carboxylesterase 2 (CES2) which is overexpressed in a number of cancers including liver and ovarian cancer[67]. Upon activation by CES2, the drug undergoes self-immolative degradation releasing doxazolidine as an active metabolite (Figure 1.4). Such drugs are developed to limit drug activity at non-target tissues; dose-limiting cardiotoxicity associated with doxorubicin is overcome by modification with a pentyl-PABC linker that is only activated in the tumor[68].

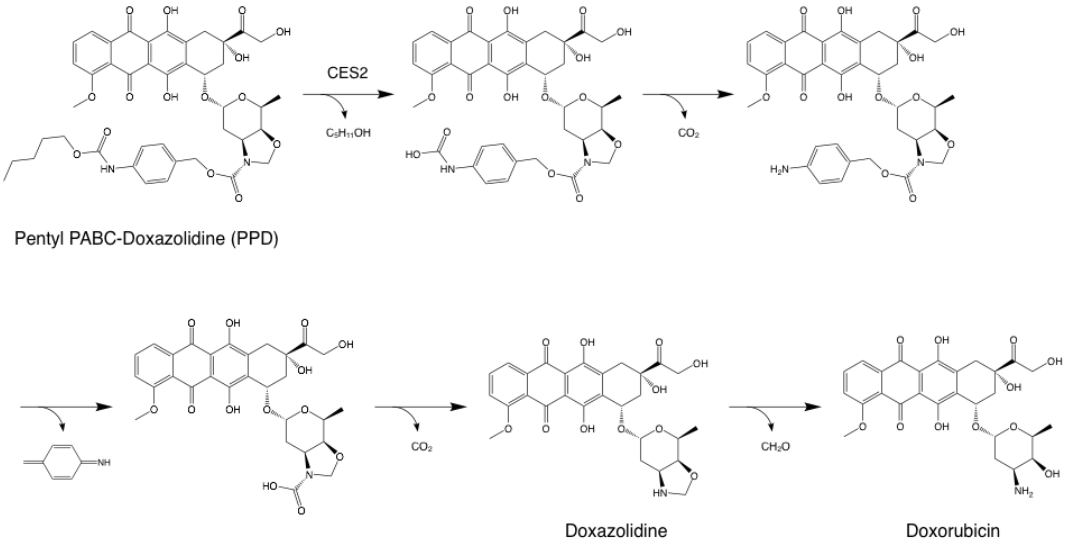

Figure 1.4. Activation of PPD by CES2 leads to active metabolites doxazolidine, which crosslinks DNA, and doxorubicin, which inhibits topoisomerase II.

With advances in protein engineering methods, monoclonal antibodies have become an important therapeutic in cancer treatment[69]. Antibodies target cancer-specific surface proteins and can be used to prevent signaling through receptor tyrosine kinases. The anti-HER2 antibodies, trastuzumab and pertuzumab, have been used with clinical success in HER2-postive breast cancers. These, and other antibodies, can have a number of different effects leading to selective cytotoxicity; they can block receptor dimerization, prevent receptor internalization and facilitate antibody-dependent cellular cytotoxicity through interactions between cancer cells and immune cells[70]. Antibodies have been a crucial aspect of recent immunotherapy efforts[71,72].

1.5 Chemotherapeutic Delivery Strategies

While a variety of formulation strategies are clinically used for small molecule chemotherapeutics, delivery remains a challenge due to excipient toxicity, poor bioavailability and off-target effects. Many of these agents are hydrophobic and often require toxic excipients for their formulation. For example, paclitaxel must be solubilized in CremophorEL, a surfactant that greatly affects the formulation pharmacokinetics and is associated with hypersensitivity reactions in many patients[73,74]. The poor bioavailability of chemotherapeutics often necessitates high and frequent dosing[75]. Finally, even with targeted therapies, some of these compounds can still have off target effects; many anti-HER2 therapies have associated cardiotoxicity concerns[70]. Thus, there still exists a need for innovative delivery strategies to minimize off-target effects and increase tumor-specificity.

1.5.1 Antibody-Drug Conjugates

In the past decade, the potential of antibody-drug conjugates (ADC) has generated excitement for the opportunity to deliver highly potent chemotherapeutics only to cancer cells[76,77]. Building off the success of monoclonal antibody therapy, conjugation of a highly potent small molecule chemotherapeutic to a target cell-specific monoclonal antibody has been shown to be an effective therapeutic strategy. There are currently a handful of ADCs approved for the cancer therapy and many more in preclinical and clinical trial stages[76]. For example, Kadcyla is a conjugate of the anti-HER trastuzumab and the anti-microtubule maytansinoid DM1[78]. Cell-specific delivery has allowed for the use of highly potent cytotoxic agents (IC50 values on range of 10^{-10}-10^{-12} M) such as auristatins and maytansinoids. However, ADCs are often limited to a low drug-to-antibody ratio, in order to minimize hydrophobicity of conjugates which can lead to accelerated plasma clearance[79]. This has limited the clinical translation of conjugates with less potent drugs, such as doxorubicin[80,81].

1.5.2 Nanoparticle Drug Delivery

Nanoparticles offer alternative formulations for a variety of chemotherapeutic agents improving drug solubility, reducing dose-limiting side-effects, and facilitating tumor targeting[82]. These characteristics of nanoparticles have made them highly attractive as drug carriers and current literature is filled with nanoparticle formulations in preclinical and clinical development[83,84]. Some types of nanoparticle formulations currently being studied include liposomes, polymeric micelles, drug nanocrystals, and self-assembled drug nanoparticles.

Liposomes consist of self-assembled, nano-sized lipid bilayers; this allows for the solubilization of both hydrophilic compounds (within the aqueous core) and hydrophobic compounds (within the bilayer itself)[85,86]. A liposomal formulation of doxorubicin, Doxil, was the first nanoparticle to receive FDA approval[87]. Polymeric micelles present a class of drug carriers well suited for delivery of hydrophobic or sparingly soluble drugs[88,89]. They are formed from amphiphilic polymers that self-assemble in aqueous solutions when present at concentrations above a critical micelle concentration (CMC). Genexol-PM, a micellar formulation of paclitaxel, is composed of a di-block copolymer of poly(D,L-lactide) and PEG; it is clinically approved in South Korea[83]. Drug nanocrystals are dispersions of crystalline drug particles on the order of 200-500 nm produced through high-pressure homogenization, wet milling or laser fragmentation[90,91]. One of the most successful example of a nano-formulation is Abraxane[87,92]. This nano-sized formulation of paclitaxel utilizes serum albumin as a solubilizing agent and is well tolerated by patients, allowing for a greater maximum tolerated dose that results in modest improvements in efficacy. Other self-assembled drug-based nanoparticles have also been recently reported[93-95].

1.5.2.1 Nanoparticle Pharmacokinetics

Upon entering systemic circulation, a drug is distributed to various tissues of the body in proportion to the blood flow to that specific tissue[96]. The main goal of drug delivery vehicles is to beneficially alter the pharmacokinetic profiles of their cargo. Upon intravenous administration, a number of biological processes dictate the fate of drug-carrying nanoparticles. Immediately upon injection, a protein corona forms on the surface of the nanocarrier[97-99]. The synthetic surface properties of the nanoparticle will dictate the composition of the protein corona[100,101]. This protein corona will dictate how the nanoparticle interacts with immune cells, organ parenchymal cells and target tumor cells. If a nanocarrier is designed to minimize interactions with off-target cells, increased circulation can be achieved. Two decades of work have demonstrated that reducing protein adsorption to nanoparticles through the use of poly(ethylene glycol) (PEG) can increase the circulation of PEGylated nanoparticles[102-104]. Recently other strategies such as zwitterionic polymers and biomimetic strategies utilizing cell membranes as an outer nanoparticle layer has shown significant improvements to circulation times[102,105]. While there is a need to increase the circulation times of many nanoparticles, it is important to consider that an upper limit exists to avoid hematological and other toxicities[106]. For example, the long plasma half-life of Doxil is attributed to the slow distribution of doxorubicin into skin resulting in palmar-plantar erythrodysthesia[107].

1.5.2.2 Tumor Targeting

Of particular importance in the design of drug delivery systems is the ability to reach the desired target. While the size of many nanoparticles can preclude them from clearance by the renal filtration (< 5.5 nm[108]), distribution to the other clearance organs, the liver and spleen, are the main route of elimination from circulation[96]. In the case of cancer nanomedicines, if nanoparticles are able to avoid clearance and remain in circulation for extended durations, targeting of the drug carrier to the tumor site is possible[109,110].

In cancer, the rapid growth of tumors results in blood vessels with defective architecture allowing for enhanced permeability of nanoparticles[111,112]. Additionally, the poor lymphatic drainage in tumors can limit clearance of nanoparticles from the tumor. Combined, the enhanced permeability and retention (EPR) effect has been exploited to increase the drug concentration in tumors using nanoparticles[113]. Many studies have shown that particle sizes less than 200 nm are required to observe increased accumulation in tumour tissue[114,115]. The EPR effect and tumour penetration are improved for even smaller particles (~50 nm)[116,117]. In recent years, the heterogeneity of the EPR effect in both human disease and pre-clinical mouse models has become accepted[118-121]. However there remains high interest in the application of nanomedicines for select patient groups that demonstrate leaky vasculature[122,123].

Active targeting methods functionally modify the surface of the drug delivery system with targeting moieties to allow preferential accumulation within specific cells or intracellular organelles[124]. Nanoparticles can be modified with a number of ligands for active targeting: monoclonal antibodies (e.g. anti-HER2 trastuzumab[125]), polysaccharides (e.g. hyaluronic targeting CD44-overexpressing breast and ovarian cancer stem cells[126]), small molecules (e.g. folic acid[127-129]), peptides (e.g. cyclic-RGD targeting tumour vasculature[130-132]). Through these mechanisms, targeted particles aim to deliver chemotherapeutic payloads directly into cancer cells where they can elicit effects on their intracellular target. This is particularly important for delivery of membrane-impermeable therapeutics such as oligonucleotides.

1.5.3 Limitations of Current Formulations

While many nanoparticle formulations are in development, a number of limitations exist and have contributed to the poor translation of these formulations to the clinic. Firstly, while many long circulating nanoparticles have been developed, a meta-analysis of nanoparticle tumor accumulation over the past ten years found that on average only 0.7% of the initial dose

accumulated at the tumor site[133]; this low accumulation was regardless of nanoparticle type, surface chemistry and active tumor targeting. However, it should be noted that while there remains opportunity to improve tumor accumulation, this 0.7% is still much higher that many solubilized drug formulations[134]. Secondly, while antibody targeting has been shown to be effective in antibody and ADC therapies, the utility of active targeting in nanoparticle drug delivery has been mixed at best. Studies that have directly compared targeted and non-targeted particles have not observed significant improvements to efficacy with targeted formulations[135]. Furthermore, recently it was shown that even with targeted particles, the majority of nanoparticles that reached the tumor were sequestered in the extracellular matrix or by tumor-associated macrophages[136]. Finally, while many nanoparticles have had success in improving the toxicity profile of chemotherapeutics such as doxorubicin or docetaxel through the use biocompatible nanoparticle systems, even among those formulations that have reached clinical use, many have not led to an improvement in efficacy compared to conventional formulations[87,92]. The recent approval of Vyxeos, a liposomal formulation of cytarabine and daunorubicin, marked the first liposomal formulation that showed improved overall survival in a Phase III trial[137]. The limited translation of nanomedicines underscores the need for further investigation of in vivo bio-nano interactions that can guide engineering of these drug delivery systems[138,139].

Additionally, although both micelles and liposomes are well studied in the literature, a major limitation is their low drug loadings. Typically only 5-10% of the total formulation consists of active drug[140-142]. Even antibody-drug conjugates are limited by low drug-to-antibody ratios[143]. Strategies that chemically modify drugs to promote self-assembly (e.g. squalenoylation of chemotherapeutics), can overcome some of these limitations but require chemical modification of established compounds which can lead to changes in pharmacodynamics and ultimately efficacy. A method for self-assembly that does not require drug modification would remove concerns over changes to it mechanism of action.

Notwithstanding these limitations, the development of stable, drug-rich and targeted nanoparticles still offers significant opportunities to improve chemotherapeutic delivery. This thesis focuses on the colloid-forming properties of two chemotherapeutics, fulvestrant and PPD (Figure 1.5), as proof-of-concept compounds where these findings may be extended to other colloid-forming drugs.

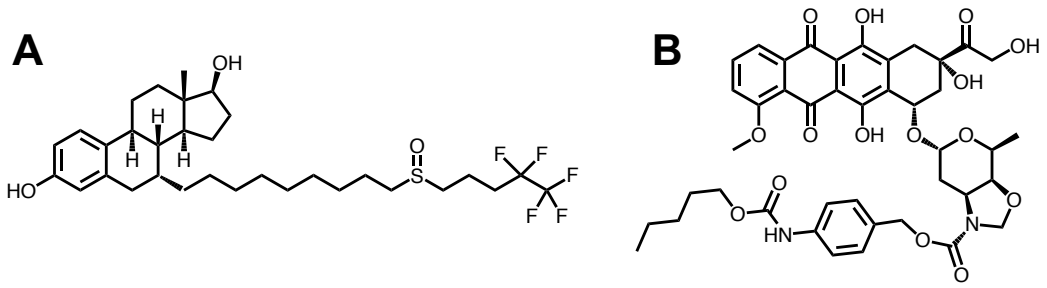

Figure 1.5. (A) Fulvestrant, an anti-estrogen used to treat ER-positive breast cancer. (B) PPD, an investigation anthracycline prodrug activated by carboxylesterase 2.

2 A new spin on antibody-drug conjugates: trastuzumab-fulvestrant colloidal drug aggregates target HER2-postive cells

*This chapter was published in ACS Applied Materials and Interfaces.

Ganesh, A.N., McLaughlin, C.K., Duan, D., Shoichet, B.K., and Shoichet, M.S. (2017) A new spin on antibody-drug conjugates: trastuzumab-fulvestrant colloidal drug aggregates target HER2-positive cells. *ACS Applied Materials and Interfaces*, 9: 12195-12202.

Reprinted with permission from the American Chemical Society. ANG, CKM, BKS, and MSS designed the research; ANG performed experiments and analysed the data; CKM performed transmission electron microscopy experiments; DD performed initial protein adsorption experiments; ANG, CKM, BKS, and MSS wrote and edited the manuscript.

2.1 Abstract

While the formation of colloidal aggregates leads to artifacts in early drug discovery, their composition makes them attractive as nanoparticle formulations for targeted drug delivery as the entire nanoparticle is composed of drug. The typical transient stability of colloidal aggregates has inhibited exploiting this property. To overcome this limitation, we investigated a series of proteins to stabilize colloidal aggregates of the chemotherapeutic, fulvestrant, including: bovine serum albumin, a generic human immunoglobulin G, and trastuzumab, a therapeutic anti-human epidermal growth factor receptor 2 antibody. Protein coronas reduced colloid size to <300 nm and improved their stability to over 48 hours in both buffered saline and media containing serum protein. Unlike colloids stabilized with other proteins, trastuzumab-fulvestrant colloids were taken up by HER2 overexpressing cells and were cytotoxic. This new targeted formulation reimagines antibody-drug conjugates, delivering mM concentrations of drug to a cell.

2.2 Introduction

Since their discovery, colloidal drug aggregates have been associated with artifacts in screening assays[144]. In enzyme[4] and cell-surface receptor assays[145], they lead to false-positive hits due to protein adsorption and inactivation on the colloid surface. Furthermore, colloidal aggregates lead to false-negative results in cell-viability assays due to an inability to cross the cell membrane, which inherently limits their efficacy[9]. The formation of colloidal particles has been reported for multiple compound classes of organic compounds and even for therapeutic drugs, including several anti-cancer chemotherapeutics[7]. Governed by a critical aggregation concentration, above which these compounds spontaneously self-assemble into amorphous particles, colloidal drug aggregates have several unique properties including their propensity for protein adsorption and detergent-reversible formation[5]. Intriguingly, while colloids are undesirable in screening assays, they are attractive as nanoparticle formulations. Composed entirely of drug molecules, they overcome the low loadings typically encountered with nanoparticle systems[140,146].

A number of nanoparticle drug formulations are being investigated for chemotherapeutic delivery. To address the issue of poor drug loading, drugs are being chemically modified to enhance their self-assembly[93,94,147-149]. While these methods have been used successfully in preclinical studies, the need to chemically modify compounds complicates their translation to the clinic, as they become new chemical entities. Exploiting drugs that self-assemble without modification would be an advantage in this respect.

Many drugs form colloidal drug aggregates in biologically relevant environments, including cell culture media and simulated gastrointestinal fluids[7,33,39,45]. Several of these drugs aggregate at micromolar or sub-micromolar concentrations, including chemotherapeutics such as the estrogen receptor (ER) antagonist, fulvestrant[7]. However, the colloids formed are often polydisperse and precipitate over several hours. Excipients, including polymers and even other colloid-forming compounds, such as azo-dyes, can control the size and stability of these colloidal drug aggregates[14,19,36]. We hypothesized that proteins themselves might be useful as stabilizing excipients due to their strong interactions with colloidal surfaces[12]. Protein excipients have been successfully used to stabilize other nanoparticle drug dispersions, such as Abraxane™, a formulation of the chemotherapeutic paclitaxel that is stabilized by human serum albumin[87]. In addition to stabilizing colloidal drug aggregates, proteins can also confer functionality. For

example, the adsorption of antibodies onto the surface of drug nanocrystals has been shown to promote selective uptake by target cells[150-152].

Here we investigate the use of proteins to both stabilize colloidal drug aggregates and to target them to specific cell populations. We demonstrate that the formation of a protein corona on the colloid controls the size of drug colloids in a concentration-dependent manner and improves their stability in many conditions, including serum-containing media. Antibody-based coronas lead to cellular targeting of colloids, thereby enhancing uptake by target cells and the efficacy of these formulations.

2.3 Materials and Methods

2.3.1 Materials

Fulvestrant (Cat No S1191) was purchased from Selleck Chemicals. Sorafenib (Cat No HY-10201) and vemurafenib (Cat No HY-12057) were purchased from MedChem Express. Cell culture grade DMSO (Cat No D2650), chlorotrianisene (Cat No C7128), bovine serum albumin (Cat No A7030), IgG from human serum (Cat No I4506), insulin from bovine pancreas (Cat No I0516) and RPMI 1640 cell culture media (R8758) were purchased from Sigma Aldrich. Trastuzumab (Herceptin) was obtained from Roche (Mississauga, Ontario, Canada). McCoy's 5A (Cat No 1660082) and DMEM F12 (Cat No 11330032) cell culture media, CholEsteryl BODIPY FL C12 (Cat No C3927MP), CholEsteryl BODIPY 542/563 C11 (Cat No C12680), Hoechst 33342 (Cat No H1399), wheat germ agglutinin Alexa Fluor 647 conjugate (Cat No W32466), dextran Alexa Fluor 647 conjugates (Cat No D22914) and PrestoBlue cell viability reagent (A12361) were purchased from Thermo Fisher Scientific. Cell lines SKOV-3 (Cat No HTB-77), MDA-MB-231 (Cat No HTB-26), BT-474 (Cat No HTB-20) and MCF-7 (Cat No HTB-22) were purchased from ATCC. Charcoal stripped fetal bovine serum (Cat No 080750) and Hank's balanced salt solution (Cat No 311515) were purchased from Wisent Bioproducts. Polysorbate 80 (HX2) was purchased from NOF America Corporation.

2.3.2 Colloid Formation

Stock solutions of each colloid-forming compound were prepared at 5 mM in DMSO. Colloid formation occurred after the rapid addition of double-distilled water (865 µL) to drug stock solution (10 µL). After colloid formation, proteins of interest (25 µL) and 10X PBS (100 µL) were added simultaneously to the colloid solution. Final drug concentration was 50 µM, DMSO

was kept to 1% (v/v) and protein concentrations ranged from 5 nM to 5 μM. For experiments including serum, charcoal stripped fetal bovine serum was added after colloid formation to a concentration of 5% (v/v). Formulations of colloids that include CholEsteryl BODIPY FL C12, CholEsteryl BODIPY 542/563 C11 or both were prepared by inclusion of the fluorophores into the compound stock solutions in DMSO. Final total concentration of fluorophore was 500 nM. For the stability study in buffers of different pH, citric acid was added to formulations to adjust pH to the desired value.

2.3.3 Dynamic Light Scattering

Colloid diameters, polydispersity and normalized scattering intensity were measured using a DynaPro Plate Reader II with a laser width optimized by the manufacturer for colloidal particle detection (Wyatt Technologies). Operating conditions were 60 mW laser at 830 nm and detector angle of 158°. Samples were measured in a 96-well format with 100 μL and 20 acquisitions per sample.

2.3.4 Colloid Centrifugation and Gel Electrophoresis

Colloids were formulated as described above and pelleted by centrifugation at 16000x *g* for 1 h at 4°C. Proteins in pellet and supernatant were reduced by addition of loading dye containing 2-mercaptoethanol and boiled for 5 min. Proteins were separated by sodium dodecyl sulfate polyacrylamide gel electrophoresis. Proteins were identified by staining with Coomassie Blue G-250.

2.3.5 Transmission Electron Microscopy

Colloid formulations (5 μL) were deposited onto a freshly glow-discharged 400 mesh carbon coated copper TEM grid (Ted Pella, Inc.) and allowed to adhere for 5 min. Excess liquid was removed with filter paper, followed by a quick wash with double-distilled water (5 μL). Particles were then stained with 1% ammonium molybdate (w/v, pH 7, 5 μL) for 30 sec. Stain was removed and samples imaged using a Hitachi H-7000 microscope operating at 75 kV. Images were captured using an Advanced Microscopy Techniques (AMT) XR-60 CCD camera with typical magnifications between 30000 – 100000x. Images were analyzed using ImageJ 64 software and processed with Photoshop.

2.3.6 XPS and TOF-SIMS

Colloids formulated with or without BSA were deposited on a silicon wafer and excess liquid was evaporated under vacuum. Surface analysis by XPS was carried out using an Escalab 250Xi XPS Spectrometer (ThermoFisher Scientific, East Grinstead, UK) and a monochromatized Al Kα X-ray source. Samples were cleaned using a 4000 eV high cluster size Ar cluster source and a nominal spot size of 400 x 400 μm^2 was analyzed. Charge compensation was applied using the combined low energy e^-/Ar^+ flood gun with the binding energy scale shifted to place the main C 1s peak (C-C) to 285.0. Both survey (pass energy 100 eV) and high resolution (pass energy 30 eV) spectra were obtained. All data collection and analysis was performed using Avantage v.5.957 software.

Negative polarity TOF-SIMS spectra were obtained using an Ion-ToF V spectrometer (ION-TOF GmbH, Muenster, Germany). Spectra were obtained using a 60 keV Bi_3^{++} cluster primary ion source. A depth profile was obtained in an interlaced, dual source mode run under high spatial resolution conditions[153]. An Ar cluster sources was used to generate the sputter crater (5000 eV, 4 nA, 100 x 100 μm^2) and spectra were obtained from an area of 20 x 20 μm^2 centred in the sputter crater. The mass scale was calibrated to standard peaks found in all spectra.

2.3.7 In vitro Serum Stability

Fulvestrant colloid stability in serum-containing media was assessed using fast protein liquid chromatography (FPLC), as previously described[154,155]. Fluorescent colloids were formulated of 50 μM fulvestrant, 875 nM BODIPY FL C12 and 125 nM BODIPY 542/563 C11. Protein concentrations were 100 nM BSA and 3.5 μM trastuzumab. Colloids were incubated in 20% charcoal-stripped FBS, 10 UI/mL penicillin and 10 μg/mL streptomycin. At selected time points, 500 μL of sample was separated on a Superdex 200 gel filtration column at a flow rate of 1.5 mL/min with PBS as the mobile phase. FRET signal was measured at excitation wavelength of 490 nm and emission wavelength of 575 nm. Integration of colloid peak area was performed using GraphPad software version 6.0.

2.3.8 Cell Culture

All cells were maintained at 37°C in 5% CO_2 in appropriate cell culture media supplemented with 10% FBS, 10 UI/mL penicillin and 10 μg/mL streptomycin. RPMI 1640 media was used for culture of MDA-MB-231 and BT-474 cells. McCoy's 5A media was used form SKOV-3 cells

and DMEM-F12 was used for MCF-7. Media for MCF-7 cells was additionally supplemental with 10 μg/mL of insulin.

2.3.9 Confocal Microscopy

Fluorescent fulvestrant colloids were prepared as described above with 500 nM BODPY 542/563 C11. Trastuzumab or IgG (3.5 μM) were added to formulation and incubated for 10 minutes prior to addition of charcoal-stripped FBS (5% final concentration). SKOV-3 and MDA-MB-231 were seeded at 10,000 cells/well and 7,500 cells/well, respectively, in 16-well glass chamber slides. Cells were incubated with appropriate formulations for 3 h at 37°C at 5% CO_2. Formulations were then removed and either replaced with fresh media for an additional 24 h or with 4% PFA solution for cell fixation. Following fixation cells membranes were stained with wheat germ agglutinin Alexa Fluor 647 conjugate (5 μg/mL) as per the manufacturer protocol and counter-stained with Hoechst. Cell lysosomes was visualized by incubating cells with Alexa Fluor 647 conjugated dextran (10,000 g/mol) overnight at 0.05 mg/mL prior to incubation with colloidal formulations and imaged under live-cell imaging conditions. Cells were imaged on an Olympus FV1000 confocal microscope at 60x magnification. Excitation and emission wavelengths are as follows: for Hoechst, excitation at 405 nm, emission at 460 nm; for colloids, excitation at 543 nm, emission at 572 nm; for WGA-647 and dextran-647, excitation at 633 nm, emission at 668 nm. Z-stacks of each field of view were obtained at 1 μm step-size and compressed into a single image.

2.3.10 Flow Cytometry

BT-474 cells were seeded at 50,000 cells/well in 24-well plates. Fluorescent colloids were formulated as above and incubated with cells for 3 h at 37°C at 5% CO_2. After incubation period, cells were washed with media and cells detached using accutase. Cells were counterstained with propidium iodide for exclusion of dead cells. Cell fluorescence was analysed using a BD Accuri C6 flow cytometer with excitation wavelength of 488 nm and emmisions filters of 533/30 nm (BODIPY) and 585/40 nm (propidium iodide). Data was analysed using FlowJo software and mean fluorescence intensity of the live cell fraction was measured for three biological replicates.

2.3.11 Cell Viability Study

BT-474 and MCF-7 cells were seeded at 10,000 cells/well in 96-well plates and allowed to adhere overnight in 10% charcoal-stripped FBS. Formulations were prepared as described above.

Monomeric formulations were prepared by the addition of ultrapure polysorbate 80 to a final concentration of 0.015% (v/v). Cells were incubated with formulations for 24 h followed by replacement with fresh media for an additional 48 h. Cell viability was assessed using Presto Blue viability assay according to manufacturer's protocols. Cell viability is reported as a percentage of the vehicle controls.

2.4 Results

Fulvestrant is a potent chemotherapeutic that forms transiently stable colloidal aggregates in buffer. Three different proteins were evaluated for their ability to stabilize fulvestrant colloids: bovine serum albumin (BSA), human immunoglobulin G (IgG), and trastuzumab, a clinical anti-human epidermal growth factor receptor 2 (HER2) antibody.

As with many other self-assembled particles, colloidal drug aggregate size and stability is influenced by ionic strength[144]. In water, fulvestrant colloids typically have nanometer-scale diameters (<200 nm) and narrow size distributions (<0.15 as measured by dynamic light scattering, DLS); however, when formulated in buffer, their diameters are greater than 1 µm (Figure 2.1).

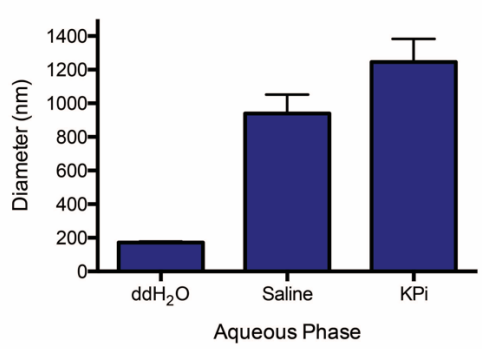

Figure 2.1. Formulation of 50 µM fulvestrant colloids in water, saline and 100 mM phosphate buffer (KPi). (n=3, mean + SD)

We hypothesized that proteins would form coronas on the colloid surface, thereby yielding stable colloids of uniform size in buffered solutions. Colloids were first formulated in water to obtain initial diameters <200 nm, followed by the simultaneous addition of protein and buffer salts. All three proteins controlled colloid size in a concentration-dependent manner, with a sigmoidal relationship consistent with saturation binding (Figure 2.2A). At low protein concentrations, colloid diameters were greater than 1 µm. As each protein concentration increased, colloid

diameters decreased. Each of the three proteins stabilized fulvestrant colloids over different concentration ranges; BSA controlled colloidal size at the lowest concentration, where as little as 25 nM was sufficient to achieve colloidal diameters <300 nm. IgG and trastuzumab required at least 1 μM and 5 μM, respectively, to reduce colloid size to similar diameters. To confirm the presence of a protein corona, colloids were centrifuged and proteins found in the resulting pelleted material were separated using gel electrophoresis, using this previously described method[4]. Proteins were associated with the pelleted colloids only, indicating that they had formed a tightly bound corona at the particle surface (Figure 2.3). Additionally, surface-sensitive techniques, such as X-ray photoelectron spectroscopy (XPS) and time-of-flight secondary ion mass spectrometry (TOF-SIMS), were used to investigate whether proteins were bound to the colloid surface. A nitrogen signal associated with proteins was only observed for BSA-stabilized colloids by XPS (Figure 2.4A). Depth profiling by TOF-SIMS shows a decrease in the protein-specific secondary CN- ion signal, suggesting that proteins are localized to the surface of colloids (Figure 2.4B). The control and stability conferred by protein coronas was not limited to colloidal drug aggregates of fulvestrant alone and was also observed for colloid-forming drugs such as sorafenib, vemurafenib and chlorotrianisene (Figure 2.5).

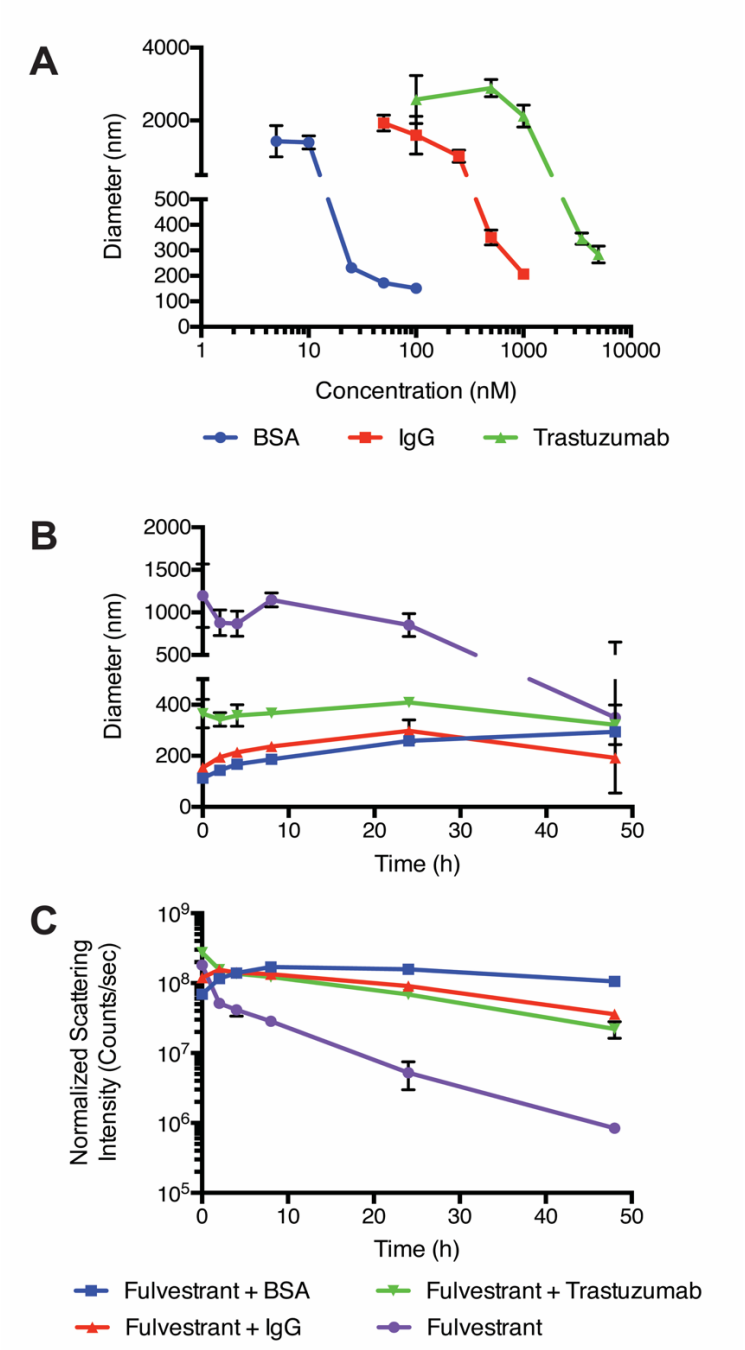

Figure 2.2. (A) Proteins control fulvestrant colloid size in a concentration-dependent manner. Size measured after a 4-h incubation by DLS. Proteins improve the stability of colloids during incubation in buffer salts at 37 °C as indicated by stability in (B) size and (C) scattering intensity by DLS. Colloids of fulvestrant alone precipitate over the 48-h incubation resulting in reduced scattering intensity. All formulations are 50 µM fulvestrant and 1% DMSO in PBS. For (B and C) [BSA] = 100 nM; = 1 µM; [trastuzumab] = 3.5 µM. (n=3, mean ± SD)

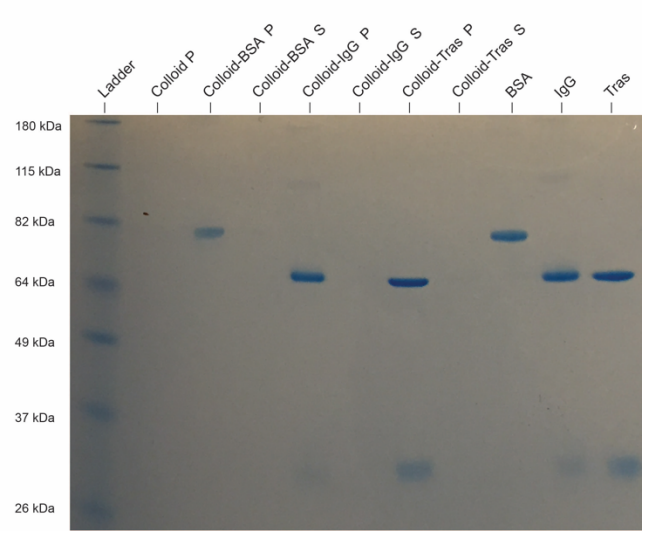

Figure 2.3. SDS-PAGE of protein corona based colloidal formulations (50 nM protein). Pellet (P) and supernatant (S) fractions of formulations were isolated by centrifugation at 16000x *g* for 1 h at 4 ºC. Proteins were only found associated with the pellet fraction indicating that they were bound to the colloid surface forming a protein corona. Protein-only controls indicate where protein was loaded directly onto gel (lanes 9-11): BSA is bovine serum albumin; IgG is immunoglobulin G; Tras is trastuzumab. Representative image of 3 repeats.

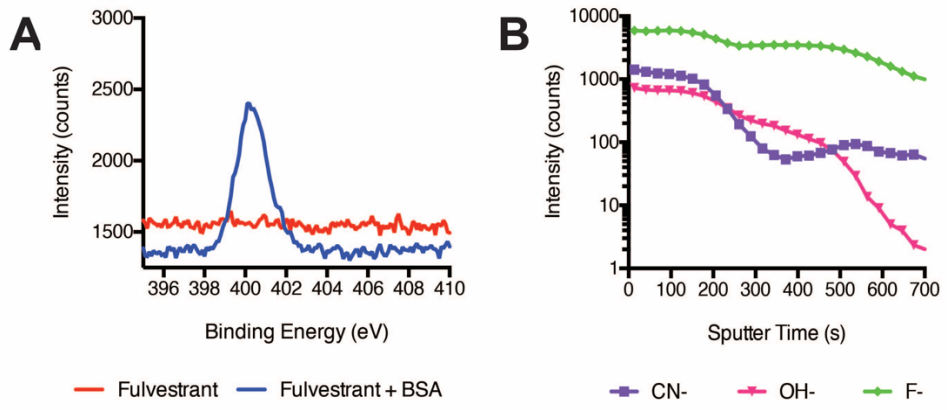

Figure 2.4. (A) Only fulvestrant colloids formulated with BSA, but not fulvestrant colloids alone, have a nitrogen peak by XPS, confirming the presence of surface-bound protein. (B) Depth profile of fulvestrant-BSA colloids by TOF-SIMS shows protein-specific secondary CN- ion signal decreasing in intensity through depth of sample, confirming surface-bound protein.

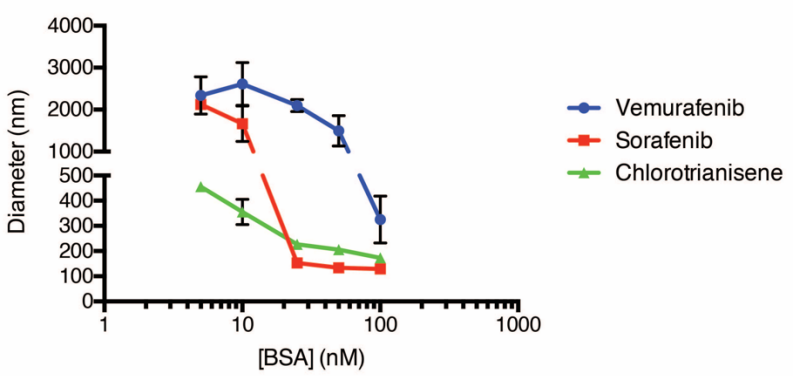

Figure 2.5. Formulations of 50 µM each of vemurafenib, sorafenib and chlorotrianisene form colloids in water that are stabilized with protein coronas of bovine serum albumin (BSA). The protein corona controls the size of all three colloid-forming compounds in a concentration-dependent manner. (n=3, mean ± SD)

We next studied the stability of the protein-fulvestrant formulations in solution using dynamic light scattering, in order to identify which protein formulation was sufficiently stable. Minimal changes in hydrodynamic diameters were observed for all three protein-stabilized formulations over a 48-h incubation at 37 ºC, with all diameters within 100 nm of the initial value (Figure 2.2B). Conversely, non-stabilized "bare" fulvestrant colloids maintained a large diameter, but a reduction in scattering intensity by two orders of magnitude was observed over 48 h due to precipitation of larger aggregates, reflecting their instability in the absence of proteins, as is typical of non-stabilized colloidal aggregates (Figure 2.2C). Conversely, protein-stabilized formulations maintained high scattering intensities, indicating that colloids were present and stable in buffered solutions over at least 48 h at 37 °C (Figure 2.2C).

We then evaluated the ability of protein coronas to stabilize fulvestrant colloids in serum-containing media. Since the high concentration and variety of proteins in serum results in a high background signal in DLS, we used transmission electron microscopy (TEM) and fast protein liquid chromatography (FPLC) to study colloidal stability. Significant morphological differences were observed by transmission electron microscopy (TEM) after incubation in 5% serum. Non-stabilized fulvestrant formulations appeared as large non-uniform aggregates, whereas protein-stabilized colloids maintained a spherical morphology of distinct particles (Figures 2.6A, 2.6B and 2.7).

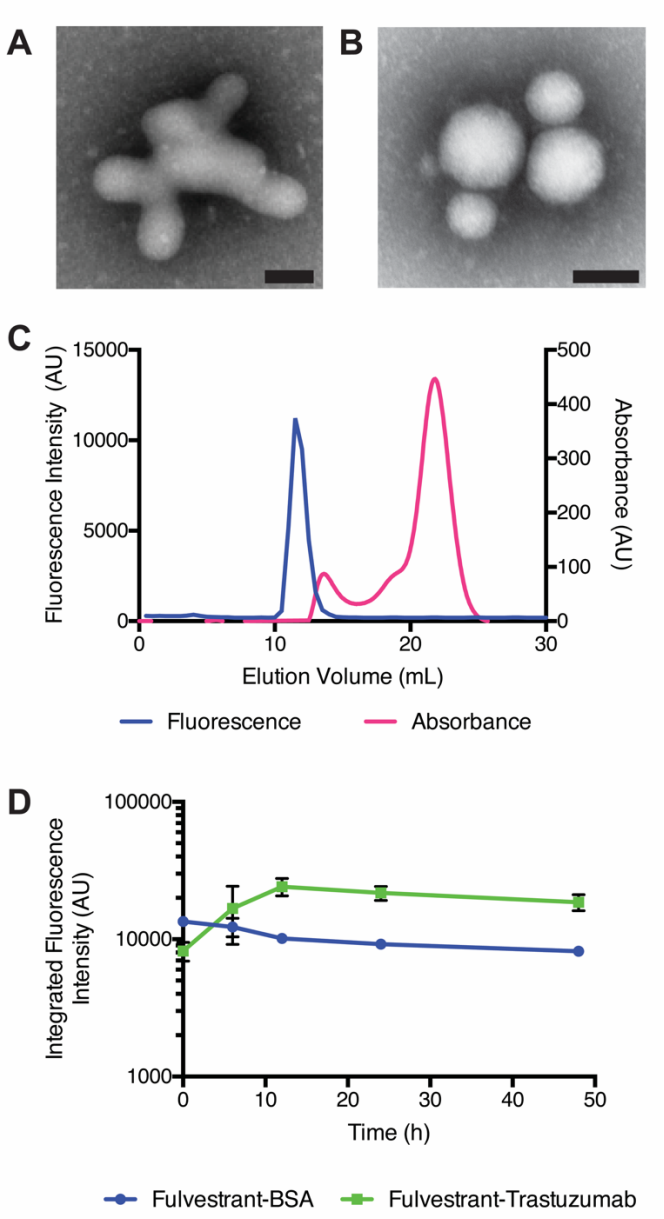

Figure 2.6. Protein corona formulation improves the stability of fulvestrant colloids in serum-containing media. (A) Non-stabilized and (B) trastuzumab-stabilized colloids show distinct morphologies after a 4-h incubation in 5% serum-containing media as shown by TEM. (C) Size exclusion chromatography traces show separation of BSA-stabilized colloids (blue, FRET fluorescence) from serum proteins (pink, absorbance at 280 nm). (D) After incubation in 20% serum, both BSA and trastuzumab-stabilized colloids maintain FRET fluorescence over 48 h, demonstrating their stability over this timeframe. Colloids were formulated at 50 µM fulvestrant and 1% DMSO in all cases. (n=3 mean ± SD, scale bar represents 100 nm)

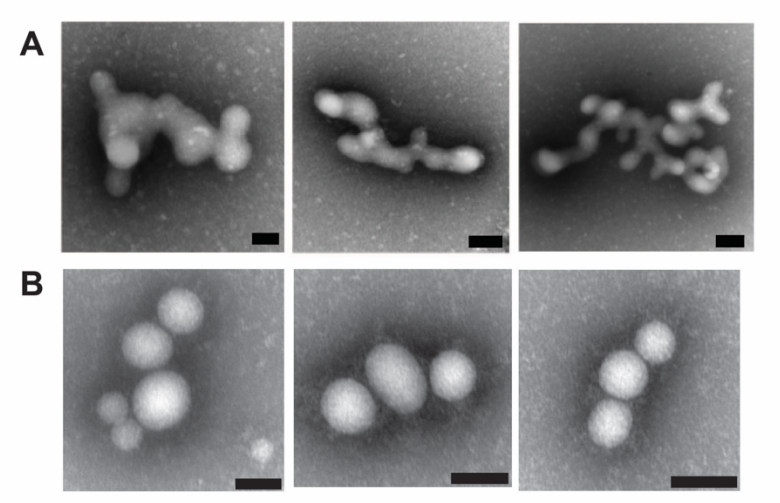

Figure 2.7. Additional TEM fields of view of (A) non-stabilized and (B) trastuzumab-stabilized fulvestrant colloids. 50 µM fulvestrant were formulated with 1% DMSO and 3.5 µM trastuzumab and incubated in 5% serum for 4 h prior to imaging. Scale bar represents 100 nm.

To study the stability of these formulations in higher serum concentrations (20%), size exclusion chromatography was used to separate intact colloids from serum proteins (Figure 2.6C). Co-formulations of fulvestrant colloids with a FRET pair consisting of cholesterol derivatives of BODIPY FL (FRET donor) and BODIPY 542/563 (FRET acceptor) provided a measure of intact colloids (Figure 2.8). These dyes have previously been used to study self-assembled particles[156] and were chosen for this study due to their physical and even structural similarity to fulvestrant. A high FRET signal, due to incorporation of these dyes within the colloids, corroborated their amorphous nature and correlated with the presence of intact particles, where exclusion of the dyes from the crystal lattice, due to precipitation, resulted in a low FRET signal (Figure 2.8)[14,16,17]. In serum-containing media, both BSA and trastuzumab-stabilized colloids had little dissociation over 48 h as indicated by the relatively constant fluorescence intensity of the colloid fraction (Figure 2.6D).. With this improved colloid stability, additional functionality can now be provided by adsorbed antibodies.

With colloidal formulations that were stable in serum, we investigated whether the antibody corona would lead to selective uptake by target cells. Previous studies showed that colloidal drug aggregates cannot diffuse across intact cell membranes[9]. We hypothesized that colloids loaded with a targeting antibody would be selectively internalized through receptor-mediated

endocytosis. We investigated the potential for colloids formulated with trastuzumab, an antibody against HER2, which is overexpressed in 25% of breast cancers[60,157], to selectively deliver fulvestrant, an estrogen receptor antagonist[56].

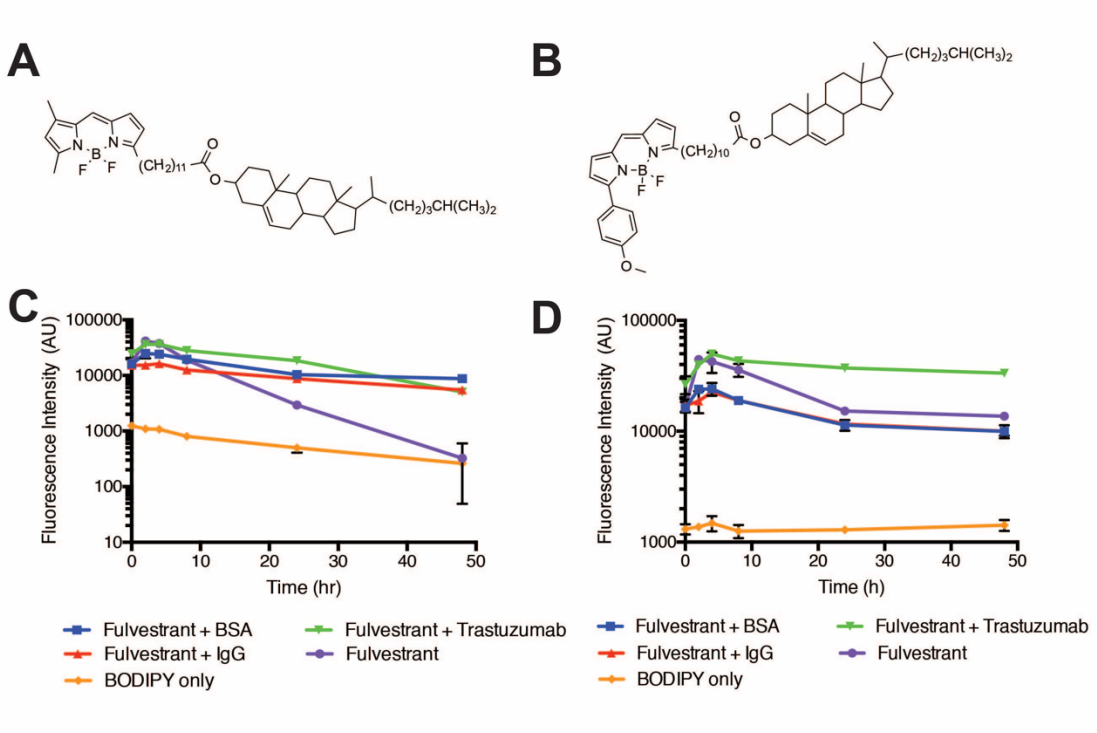

Figure 2.8. FRET donor (A) cholesteryl BODIPY FL C12 (1.75 mol%) and (B) acceptor cholesteryl BODIPY 542/563 C11 (0.25 mol%) dyes were co-formulated with fulvestrant colloids to measure of stability. (C) Fulvestrant colloids with or without stabilizing protein coronas were incubated in PBS over 48 hours at 37 ºC. The decrease in fluorescence for fulvestrant-only colloids corresponds to the decrease in colloidal species observed in solution. (D) In media containing 5% serum, all formulations remain relatively stable. (n=3, mean ± SD)

We first evaluated the cellular uptake of trastuzumab-stabilized fulvestrant colloids by confocal laser scanning microscopy. Co-formulation with a BODIPY dye aided in direct visualization of colloids after exposure to cells for 3 h in 5% serum. The trastuzumab-stabilized colloids (green, Figure 2.9A) were clearly internalized by SKOV-3 cells that overexpress HER2, whereas the control IgG-stabilized colloids showed no uptake in the same cell line (Figure 2.9B), indicating trastuzumab-mediated cell uptake of fulvestrant colloids. Quantification of colloid uptake by flow cytometry showed that trastuzumab-stabilized colloids had a 10-fold increase in uptake by

HER2-overexpressing cells compared to IgG stabilized colloids (Figure 2.10). Furthermore, pre-incubation with free trastuzumab, significantly reduced this uptake. Consistent with a HER2-mediated uptake mechanism, neither the trastuzumab nor the IgG stabilized formulations were taken up by HER2 low-expressing MDA-MB-231 cells (Figure 2.9C and 2.9D, respectively).

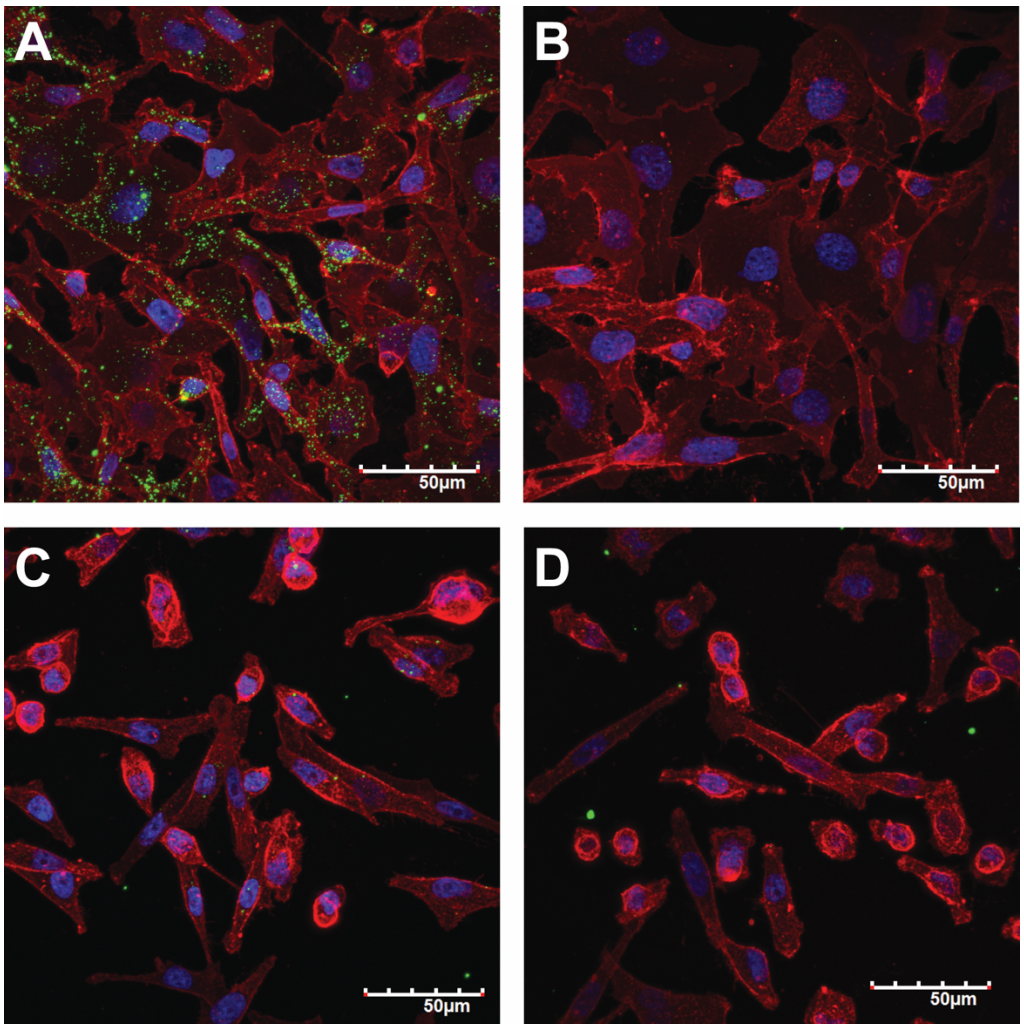

Figure 2.9. (A) Trastuzumab-modified colloids (BODIPY, green), but not (B) IgG-modified colloids, are taken up by HER2 overexpressing SKOV-3 cells (blue, Hoechst for cell nuclei and red, wheat germ agglutinin for cell membranes) after a 3 h incubation. Neither (C) trastuzumab-modified nor (D) IgG modified colloids are taken up by MDA-MB-231 cells that are HER2 low-expressing. Formulations used are 50 µM fulvestrant, 1% DMSO and 3.5 µM antibody in 5% serum. Representative confocal microscope images of at least 3 biological repeats. Scale bar represents 50 µm.

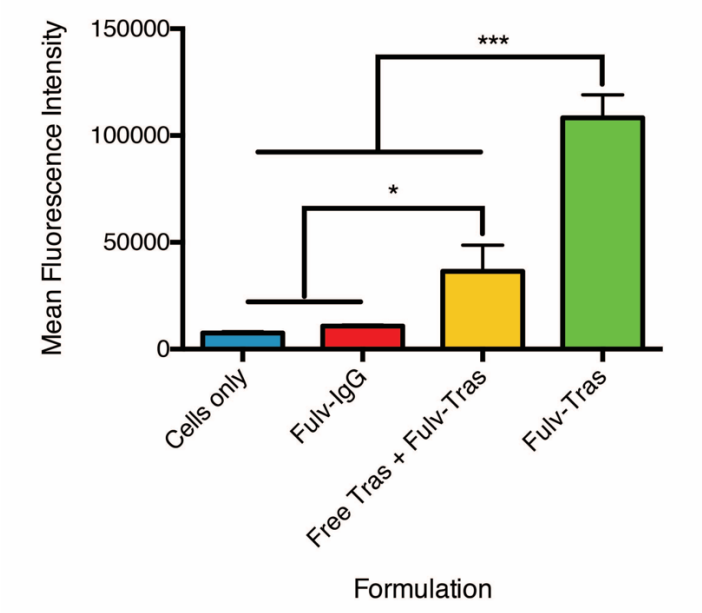

Figure 2.10. Quantification of colloid uptake by HER2 overexpressing BT-474 cells using flow cytometry. Trastuzumab-stabilized fulvestrant colloids (green) have significantly increased uptake by BT-474 cells compared to IgG-stabilized colloids (red) after 3-h incubation. Pre-incubation of cells with free trastuzumab (yellow) significantly reduced uptake of trastuzumab-stabilized colloids by cells. (n=3 biological replicates, mean + SD, *p<0.05, ***p<0.001)

Subsequent cell uptake studies revealed that trastuzumab-stabilized colloids are localized to endo-lysosomal compartments even 24 h after exposure (Figure 2.11). Trafficking to the lysosomal compartment was indicated by the co-localization of colloid fluorescence (green) with that of a lysosomal dextran marker (red). Lysosomal accumulation is only observed for trastuzumab-modified colloids (Figure 2.11A) and not for IgG-modified colloids (Figure 2.11B), consistent with the selective internalization of the former (Figure 2.9). Unexpectedly, the protein-formulated colloids appear to be mostly stable even in low pH environments of the endo-lysosomal pathway (Figure 2.12)[158].

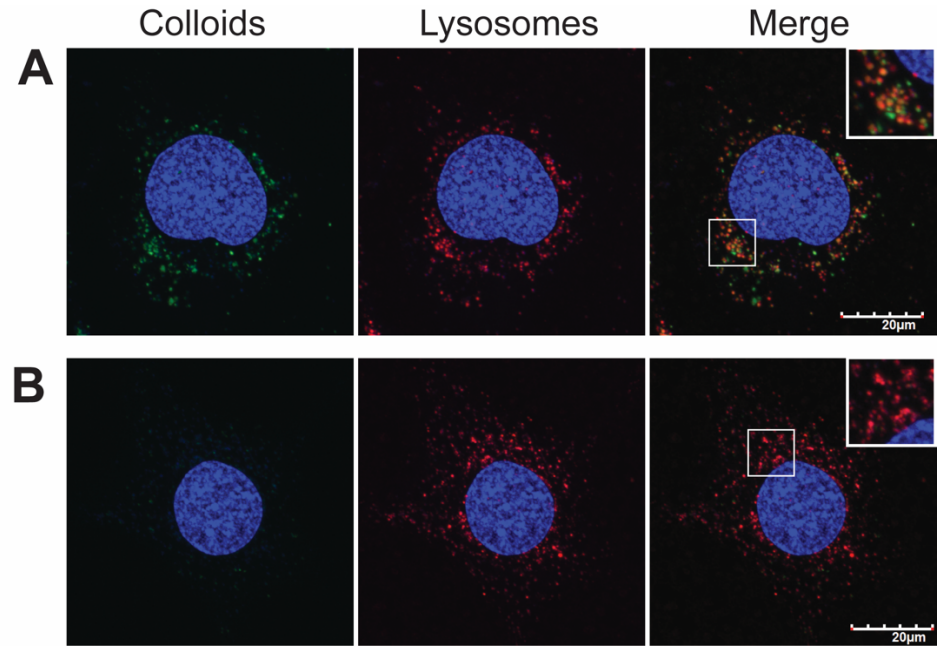

Figure 2.11. Internalized colloids are trafficked to lysosomal compartments of SKOV-3 cells. (A) Trastuzumab-modified colloids (BODIPY, green) co-localize with lysosomes (Dextran-647, red) after 24 h. (B) IgG-modified colloids have minimal cell uptake. Hoechst (blue) is used to stain cell nuclei. Formulations used are 50 µM fulvestrant, 1% DMSO and 3.5 µM antibody in 5% serum. Cells were pulsed with colloidal formulations for 3 h followed by chase with full media for 21 h. Representative confocal microscope images of at least 3 biological repeats. Scale bar represents 20 µm.

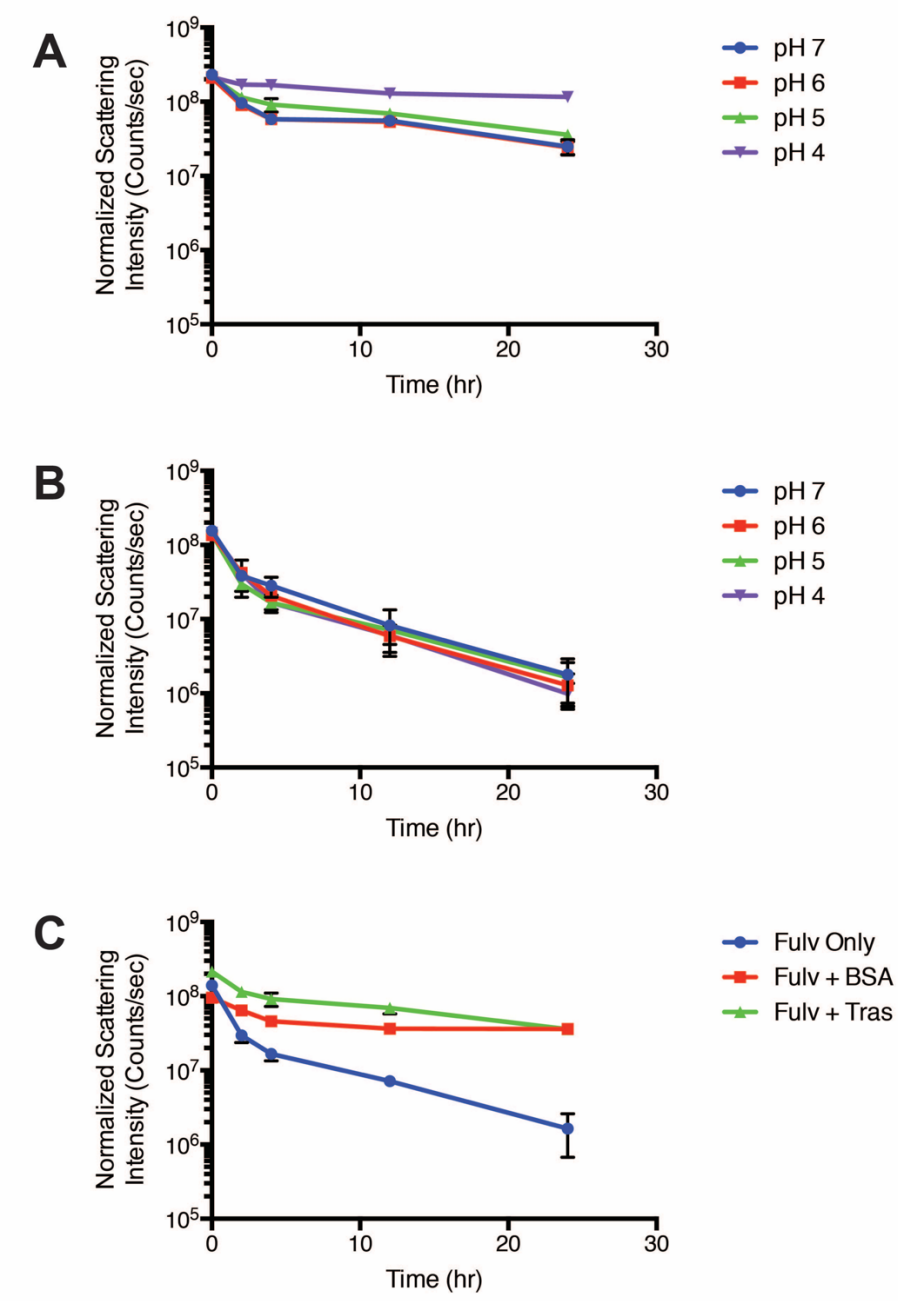

Figure 2.12. Proteins improve the stability of colloids in acidic environments such as those of the endo-lysosomal pathway. (A) Trastuzumab-stabilized fulvestrant colloids maintain scattering intensity over a 24-hour incubation in buffers of different pH while (B) non-stabilized colloids decrease in scattering indicating a decrease in colloidal species. (C) At pH 5, protein coronas stabilize colloids in a citric acid-phosphate buffer system. 50 µM fulvestrant, 1% DMSO, 100 nM BSA or 3.5 µM trastuzumab. (n=3, mean ± SD)

We next investigated whether these targeted colloidal formulations would improve drug efficacy relative to non-targeted colloids. Since trastuzumab-stabilized fulvestrant colloids showed selective uptake by HER2 overexpressing cells, we wondered whether they would increase efficacy against fulvestrant-sensitive BT-474 cells, which overexpress both HER2 and ER[159]. Fulvestrant colloids co-formulated with trastuzumab significantly reduced viability compared to controls, while colloids stabilized with a non-targeted antibody did not show the same effect (Figure 2.13). Non-stabilized colloidal fulvestrant formulations had a minimal effect on cell viability. High amounts of trastuzumab were required to stabilize colloids of fulvestrant compared to the other proteins investigated and, as a result, even the trastuzumab-only controls showed a significant reduction in cell viability relative to a 1% DMSO vehicle control (Figure 2.13). When these formulations were incubated with fulvestrant-sensitive cells that have low expression of HER2 (MCF-7), no differences between targeted and non-targeted colloidal formulations were observed (Figure 2.14). We note that whereas the targeted colloids significantly reduced cell viability versus the untargeted colloids, the difference did not reflect the substantially higher amount of colloids internalized by the cells. This perhaps reflects the integrity of the colloids long after internalization. This contrasts with the expected cytotoxicity observed for monomeric formulations of fulvestrant (Figures 2.14 and 2.15).

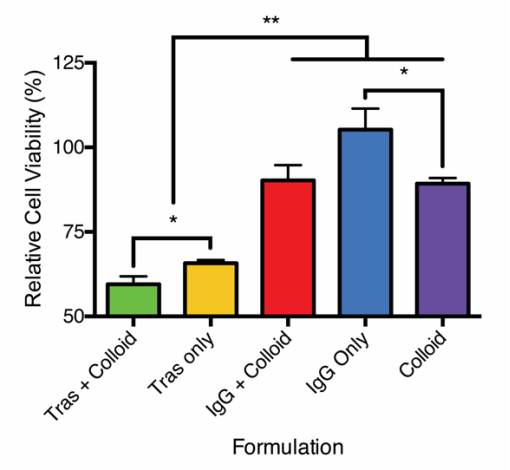

Figure 2.13. Fulvestrant colloids targeted with a trastuzumab corona reduce cell viability. BT-474 cells were exposed to 50 µM fulvestrant formulations with trastuzumab or IgG (3.5 µM) for 24 h followed by fresh media for an additional 48 h. 50 µM fulvestrant with 1% DMSO in 5% serum was used for all formulations. Cell viability is represented as a percentage of 1% DMSO vehicle control. * p<0.05, ** p<0.01. (n=4 biological replicates, mean + SD)

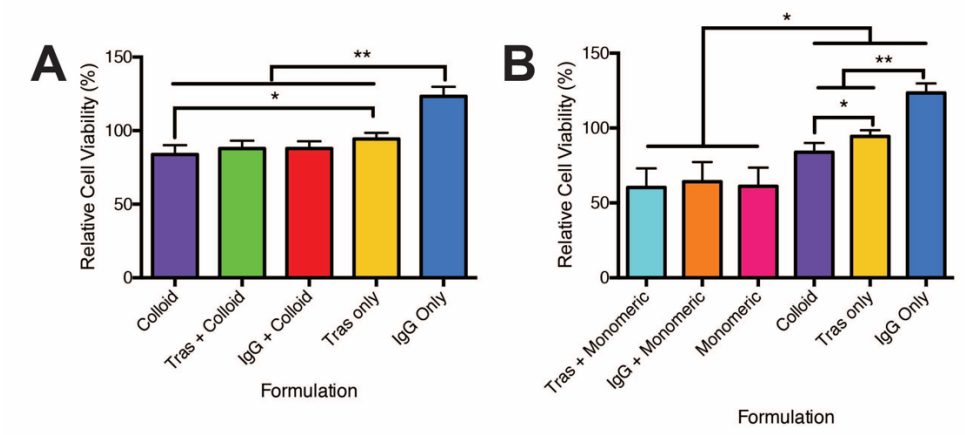

Figure 2.14. (A) Fulvestrant colloids formulated with trastuzumab do not selectively target low HER2-expressing MCF-7 cells as shown with similar cell viability as non-targeted fulvestrant colloids formulated with IgG. (B) All monomeric fulvestrant formulations reduce cell viability to the same extent irrespective of the presence of either trastuzumab or IgG. Cells were incubated with 50 µM fulvestrant, 3.5 µM antibody, 1% DMSO and 0.015% UP80 to maintain monomeric formulation for 24 hours. Cell viability was assessed by the PrestoBlue assay after a 72-hour total incubation. * p<0.05, ** p<0.01. (n=4 biological replicates, mean + SD)

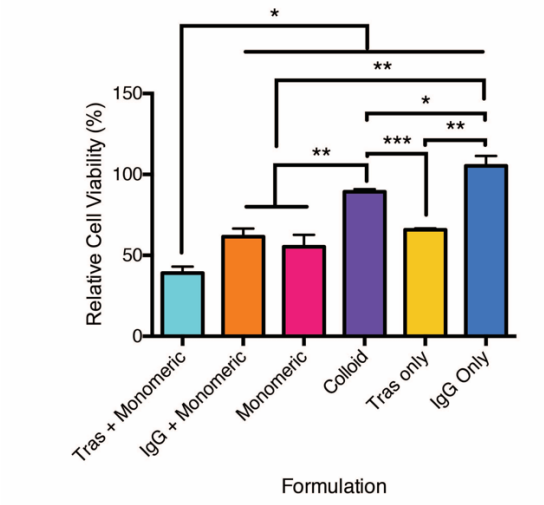

Figure 2.15. All monomeric formulations reduce cell viability of BT-474 cells. Cells were incubated with 50 µM fulvestrant, 3.5 µM antibody, 1% DMSO and 0.015% UP80 to maintain monomeric formulation for 24 hours. Cell viability was assessed by the PrestoBlue assay after a 72-hour total incubation and represented as percentage of vehicle control. * p<0.05, ** p<0.01, *** p<0.001. (n=4 biological replicates, mean + SD)

2.5 Discussion

Two key results emerge from this study. First, colloidal drug aggregates may be stabilized by protein adsorption, converting them from polydisperse particles prone to precipitation into more monodisperse species with multi-day stability. Second, colloids can be co-formulated with proteins that are themselves active, like the anti-HER2 antibody trastuzumab, and can be used to target colloids to specific cell types. This antibody colloidal drug formulation is specifically internalized by target cells, increasing the toxicity of the colloids versus colloids without the targeting antibody and relative to non-target cells. These antibody-colloidal drug formulations are analogous to antibody drug conjugates, but deliver orders of magnitude more drug per active antibody while maintaining the drug in an inactive form prior to cell internalization.

Proteins form coronas on nanoparticle formulations upon exposure to biological media[160,161]. Both the nature of the protein and colloidal surface determine the strength of this interaction and, as a result, several factors may contribute to the differences in interaction between fulvestrant colloids and the three proteins studied here[98,99,162]. Many studies have shown that proteins readily bind to hydrophobic colloidal surfaces. Albumin, for example, can bind to a number of colloidal particles and in most cases improves their stability[39,163-165]. The diversity in chemical groups and specifically the hydrophobic pockets of BSA could account for the superior ability of albumin to stabilize the hydrophobic fulvestrant colloids compared to the antibodies investigated here[162,166-169]. Differences in post-translational modifications, such as glycosylation, can change the properties of proteins and could explain the differences observed between IgG and trastuzumab[170,171]. The properties of the colloids also influence interactions with proteins. For example, the zeta potential of the colloidal surface dictates the strength of electrostatic interactions[98]. Although we have focused on fulvestrant colloids in this study, we observed the same ability of proteins to stabilize colloidal aggregates of other drugs , namely sorafenib, vemurafenib and chlorotrianisene.

The concentration of the protein is an important factor in colloid stabilization; at low protein concentrations, colloidal particles agglomerate with one another, perhaps due to changes in electrostatic interactions and bridging effects[164]. The colloidal diameters observed in this study at low protein concentrations are in fact larger than those of fulvestrant colloids alone. At higher protein concentrations, however, the protein corona increases colloidal stability by saturating the surface, resulting in repulsive steric and entropic forces that arise from the displacement of

surface-bound water molecules upon protein adsorption[164,172,173]. Both forces favor inter-colloid repulsion and lead to colloidal stability.

Importantly, protein coronas stabilize colloids upon serum incubation. Indeed, some stabilization was even observed for the bare fulvestrant colloids in serum-containing media, reflecting some corona formation by serum proteins themselves. This is consistent with previous studies, which have found that colloidal drug aggregates can persist in these conditions over 24 h[7]. However, the differences between the morphologies of bare and protein-stabilized colloids reflect the superior stability conferred by controlled corona formation. The observation that trastuzumab-modified colloids preferentially targeted HER2 overexpressing cells indicates that the antibody is stably bound to the colloid surface, even after exposure to serum, and that a substantial amount of antibody is oriented such that the Fab region can interact with the target receptor. These results suggest that it should be possible to find other protein-colloid pairs that can optimally stabilize monodisperse colloidal drug aggregates for targeted delivery and improved efficacy.

While we have shown that protein adsorption can stabilize colloidal drug aggregates, it is likely that differences in protein and colloid surface characteristics will demand optimization for different protein-colloid combinations. The formulation of fulvestrant and trastuzumab investigated here is clinically relevant for breast cancer patients with HER2 and ER positive tumors[157]. Combinations of other colloid-forming chemotherapeutics and targeting ligands may prove useful for other cancers. Additionally, although we have shown that trastuzumab-stabilized colloids are specifically internalized by HER2-expressing cells and decrease cell viability, the current protein-stabilized fulvestrant colloids seem to persist in the endo-lysosomal pathway, limiting their efficacy[174].

2.6 Conclusions

Colloidal drug aggregates, typically thought of as a nuisance artifact of early drug discovery, can be stabilized by complexation with proteins and targeted for selective cell uptake with functional antibodies. Since the colloidal aggregates act as both the active agent and the vehicle, antibody-stabilized colloidal drug formulations may address key limitations of nanoparticle formulations, namely their poor drug loading and necessity for massive amounts of nanoparticle material in the formulation. Many chemotherapeutics form colloidal aggregates[7,36,45] and protein corona formation may reveal opportunities to convert what has been considered a weakness into an opportunity for targeted delivery. In the last decade, both antibody-drug conjugates and

nanoparticle formulations have emerged as promising avenues for targeted drug delivery. We demonstrated specific uptake by target cancer cells in vitro, yet, like many other nanoparticle formulations, the stabilized fulvestrant colloids will likely be non-specifically internalized to some extent by phagocytic cells in vivo[100,175]. Notwithstanding, what may be thought of as "antibody colloidal drug conjugates" may deliver many more orders of magnitude of drug molecules per antibody, improving efficacy.

2.7 Acknowledgements

This work was supported by grants from the US National Institutes of General Medical Sciences (GM71630 to B.K.S and M.S.S.) and the Canadian Cancer Society Research Institute (to M.S.S. and B.K.S.). A.N.G. is supported by a Natural Sciences and Engineering Research Council (NSERC) Postgraduate Research Scholarship and C.K.M. is supported, in part, by an NSERC postdoctoral fellowship. We thank S. Boyle and B. Calvieri from the University of Toronto Microscopy Imaging Laboratory for assistance with TEM imaging, Dr. R. Sodhi from the Ontario Centre for the Characterization of Advanced Materials for XPS and TOF-SIMS analysis, Dr. P. Gilbert and S. Davoudi for use and assistance with their flow cytometer and members of the Shoichet labs for thoughtful discussion.

3 Leveraging colloidal aggregation for drug-rich nanoparticle formulations

*This chapter was published in Molecular Pharmaceutics and appears in the thesis entitled "Design and Synthesis of Self-Assembled Polymeric Nanoparticles for Cancer Drug Delivery" submitted to the University of Toronto © Jennifer Logie 2017.

Ganesh, A.N.[#], Logie, J. [#], McLaughlin, C.K. [#], Barthel, B.L., Koch, T.H., Shoichet, B.K., and Shoichet, M.S. (2017) Leveraging colloidal aggregation for drug rich nanoparticle formulations. *Molecular Pharmaceutics*. 14: 1852-1860.

Reprinted with permission from the American Chemical Society. #These authors contributed equally to this work. ANG, JL, CKM, BKS, and MSS designed the research; ANG performed experiments with fulvestrant and protein adsorption experiments; JL performed PPD stability experiments, CKM performed PPD stability experiments and transmission electron microscopy; BBL and THK synthesized and provided PPD; ANG, JL, CKM, and MSS wrote and edited the manuscript.

3.1 Abstract

While limited drug loading continues to be problematic for chemotherapeutics formulated in nanoparticles, we found that we could take advantage of colloidal drug aggregation to achieve high loading when combined with polymeric excipients. We demonstrate this approach with two drugs - fulvestrant and pentyl-PABC Doxazolidine (PPD) – a prodrug of doxazolidine, a DNA crosslinking anthracycline; and two polymers, respectively - polysorbate 80 (UP80) and poly(D,L-lactide-co-2-methyl-2-carboxytrimethylene carbonate)-graft-poly(ethylene glycol) (PLAC-PEG) – a custom-synthesized, self-assembling, amphiphilic polymer. In both systems, drug-loaded nanoparticles had diameters <200 nm, were stable for up to 2 days in buffered saline solution and for up to 24 h in serum-containing media at 37°C. While colloidal drug aggregates alone are typically unstable in saline and serum-containing media, we attribute colloid stability herein to the polymeric excipients and consequent decreased protein adsorption. We expect that this strategy of polymer-stabilized colloidal drug aggregates to be broadly applicable in delivery formulations.

3.2 Introduction

The inefficient formulation of hydrophobic small molecule drugs continues to be a barrier between drug development and clinical use. Although excipients can solubilize drugs for in vivo delivery, the high excipient concentrations necessary are associated with dose-limiting adverse effects, such as hypersensitivity and hemolysis[74,176,177]. While nanoparticle delivery systems have been developed to overcome this toxicity and to improve drug bioavailability and biodistribution[178-180], these strategies are themselves limited by low drug loading[42,133,140,142,181].

To produce more drug-rich systems and to overcome the limitations of excipient toxicity, an alternative approach has emerged to exploit the intrinsic physicochemical properties of a drug directly in formulation. These formulations generally take advantage of the immiscibility of hydrophobic drugs in aqueous media, which results in self-aggregation to produce a particle core[93,148]. More recently, co-formulation strategies have been developed that use macromolecules, either during or after particle formation, to suppress Ostwald ripening through stabilization of the drug-particle surface[182]. However, less attention has been given to the potential self-assembly parameters of the drugs themselves.

In the past decade, many drugs have been shown to self-assemble into colloidal drug aggregates. In early drug discovery[5] this leads to artifacts including both false positives in biochemical assays[4,145] and false negatives in cellular assays[7,9]. Though hard to predict[183], the mechanism of self-assembly for these colloidal aggregators is governed by a critical aggregation concentration (CAC). At concentrations above their CAC, self-assembly of these compounds by solvent-exchange methods leads to the generation of amorphous liquid-liquid phase-separated particles rather than crystalline precipitate[5,14]. While the assembling properties have been well studied, the utility of these aggregates is hindered by their instability[9,144]. We and others have attempted to stabilize colloidal drug aggregates in order to further study their biological implications[36,182]. Previously, we demonstrated that co-aggregation with azo-dyes can stabilize colloids, resulting in a maintenance of structural integrity in high ionic strength solutions and serum-containing media[36]. The incorporation of polymeric excipients, such as pluronics and polysorbates, remains an attractive method to stabilize colloidal aggregates due to the chemical diversity of polymers available and their ubiquity in pharmaceutical formulations. Work by Taylor et al. has shown that polymeric excipients can modulate the colloidal properties of drug aggregates; however, only modest improvements in stability have been achieved thus far[19,184].

Here, we investigate how small molecule colloidal drug aggregation properties can be combined with polymeric excipients to substantially improve particle stability. Using pharmaceutical excipients and biocompatible amphiphilic polymers, we demonstrate that colloidal drug aggregates can be formulated for multi-day stability in both buffered saline and serum-containing media. With this strategy, we not only stabilize colloidal drug aggregates, but overcome the low drug loading typically found in traditional polymeric nanoparticle systems. Monodisperse and stable colloidal formulations are achieved using polymeric excipients of two chemotherapeutics: the estrogen receptor antagonist fulvestrant[9,56] and the novel anthracycline-derived prodrug of doxazolidine, pentyloxycarbonyl-(p-aminobenzyl) doxazolidinylcarbamate (PPD)[68]. After screening a series of polymers, we found that the optimal polymer-colloid combination is specific to each drug; however, this approach should be broadly applicable to other colloidal drug aggregators. As a proof of concept for use in drug delivery, we investigate the stability in serum-containing media, variations in protein adsorption properties, and interactions with cancer cells of these colloidal formulations.

3.3 Materials and Methods

3.3.1 Materials

PPD was synthesized from expired clinical samples of doxorubicin (FeRx Inc, Aurora, CO) as previously described[68]. Fulvestrant was purchased from Selleckchem. Poly(D,L-lactide-co-2-methyl-2-carboxy-trimethylene carbonate)-graft-poly(ethylene glycol) (PLAC-PEG) was synthesized by a ring-opening polymerization using a pyrenebutanol initiator to a molecular weight of 12,000 g/mol and conjugated with an average of 3 PEG chains/backbone (10,000 g/mol PEG) as previously described[155]. Polysorbate 80 (H2X, UP80) was purchased from NOF America Corporation. Vitamin E-PEG 1000 (VitEPEG), Pluronic F68, Pluronic F127, Brij L23 and Brij 58 were purchased from Sigma Aldrich. McCoy's 5A cell culture media, CholEsteryl BODIPY 542/563 C11, Hoechst 33342 were purchased from Thermo Fisher Scientific. The SKOV-3 cell line was purchased from ATCC. Charcoal stripped fetal bovine serum and Hank's balanced salt solution were purchased from Wisent Bioproducts.

3.3.2 Colloid Formation

Colloids of both fulvestrant and PPD were formulated upon dilution of organic stock solutions into an aqueous phase. Fulvestrant colloids were prepared by adding double-distilled water (880 μL) to DMSO stock solution (10 μL at 5 mM) followed by the addition of 10X PBS (100 μL).

Final fulvestrant drug and organic concentrations were 50 μM and 1% (v/v), respectively. PPD colloids were prepared in a similar manner with drug stock solution at 12.5 mM in DMF leading to formulations with a final drug concentration of 500 μM and an organic concentration of 4% (v/v). Excipients were incorporated into formulations prior to colloid formation. Since the concentration of organic solvents are in the same range as those typically found in pharmaceutical formulations (up to 10%), we do not anticipate any toxicity. PLAC-PEG was added to the organic phase while all other excipients studied were dissolved in the aqueous phase. Amounts of polymers were chosen based on the initial concentration of drug being formulated. For fulvestrant colloids formulated at 50 μM, excipients were used at the following concentrations: 0.001% (w/v) UP80, 0.01% F127, 0.01% F68, 0.01% Brij L23, 0.01% Brij 58, 0.01% VitE-PEG and 0.004% PLAC-PEG. For PPD colloids formulated at 500 μM, excipients were used at the following concentrations: 0.01% UP80, 0.05% F127, 0.05% F68, 0.01% Brij L23, 0.01% Brij 58, 0.01% VitE-PEG and 0.04% PLAC-PEG. Precipitate formation was inspected visually during screening of excipients.

3.3.3 Colloid Characterization

Colloid diameter, polydispersity and normalized scattering intensity were measured by dynamic light scattering (DLS) using a DynaPro Plate Reader II (Wyatt Technologies) with a laser width optimized for colloidal aggregate detection (i.e., particles in the 100 to 1000 nm radius range) by the manufacturer. Operating conditions were 60 mW laser at 830 nm wavelength and detector angle of 158°. Samples were measured in a 96-well format with 100 μL and 20 acquisitions per sample.

Colloids (5 μL) were deposited from 50 μM and 500 μM solutions of fulvestrant and PPD, respectively, onto glow discharged transmission electron microscope (TEM) grids and allowed to adsorb for 5 min. The solution was then wicked away and the grid was washed briefly with water (5 μL). Grids were then allowed to dry and negatively stained with either uranyl acetate (5 μL, 10 sec, 2 % solution, pH ~4) for PPD colloids or ammonium molybdate (5 μL, 30 sec, 1% solution, pH 7) for fulvestrant colloids prior to imaging on a Hitachi H-7000 microscope operating at 75 kV.

3.3.4 In Vitro Serum Stability

The stability of fulvestrant and PPD colloids under serum conditions was determined using fast protein liquid chromatography (FPLC) using a previously established method[142,154]. Colloids

were incubated with 20% fetal bovine serum (FBS, Charcoal stripped) and 1% penicillin - streptomycin at 37°C. At 0, 6, 12, 24 and 48 h, 500 µL aliquots were removed and injected onto a Superdex 200 gel filtration column. Samples were run with a flow rate of 1.5 mL/min and 1x PBS as the mobile phase. For fulvestrant, colloids were co-formulated with the FRET pair of CholEsteryl BODIPY FL and BODIPY 542/563 (500 nM) and fluorescent emission at 575 nm was determined using a Tecan plate reader followed by integration of colloid peak area using GraphPad software version 6.0. For PPD, elution peak areas at 480 nm were calculated using UNICORN software version 5.31. Peak area is used as a measurement of intact colloid population. Protein components of FBS, drugs and polymer excipients will all contribute to the absorbance at 280 nm. Neither the polymer nor the FBS contribute to the absorbance at 480 nm or the fluorescence at 575 nm. Without polymer, PPD and fulvestrant colloids precipitate rapidly in PBS and thus their stability could not be assessed by FPLC.

3.3.5 In Vitro Protein Adsorption

Fulvestrant and PPD colloids were prepared at 50 µM (1 mL) as before in the presence or absence of UP80 and PLAC-PEG, respectively. Colloids were then incubated with 50 nM bovine serum albumin, human immunoglobulin G or fibrinogen for 10 min. Colloids were then pelleted by centrifugation for 1 h at 16000x *g* at 4 °C. After centrifugation, 950 µL of supernatant was removed and the pellet was resuspended in the remaining 50 µL. To prepare samples for SDS-PAGE, 10 µL of supernatant or 10 µL of resuspended pellet was mixed with 10% glycerol, 2% sodium dodecyl sulfate (SDS) and 100mM β-mercaptoethanol. This process effectively breaks up colloids and releases any colloid-bound protein. Each sample was boiled at 100 °C for 5 min. Proteins (15 µL sample volume) were then separated by sodium dodecyl sulfate polyacrylamide gel electrophoresis and identified using Coomassie Blue G-250 staining. Protein band intensities were quantified using ImageJ software. Data are expressed as the relative protein band intensities of the pellet to that of the supernatant.

3.3.6 In Vitro Cell Uptake

SKOV-3 cells were maintained at 37 ºC in 5% CO_2 in McCoy's 5A media supplemented with 10% FBS, 10 UI/mL penicillin, and 10 µg/mL streptomycin. Cells were seeded at 12,000 cells/well in 8-well borosilicate glass chamber slides and allowed to adhere overnight. Cells were incubated with 50 µM of appropriate formulations for 45 min in serum-free or 10% serum conditions. Fulvestrant colloids were co-formulated with CholEsteryl BODIPY 542/563 C11

(500 nM) for visualization. Following incubation, cells were rinsed and counterstained with Hoechst 33342. Cells were imaged on an Olympus FV1000 confocal laser-scanning microscope at 60X magnification under live-cell imaging conditions. Excitation and emission wavelengths were as follows: for Hoechst, excitation at 405 nm, emission at 460 nm; for fulvestrant colloids co-formulated with BODIPY, excitation at 559 nm, emission at 572; for PPD colloids and doxorubicin (DOX) formulations, excitation at 488 nm, emission at 520 nm.

3.4 Results

Hydrophobic chemotherapeutics, such as fulvestrant and PPD, form colloidal aggregates with CACs of 0.5 μM[7] and 14 μM (Figure 3.1), respectively.

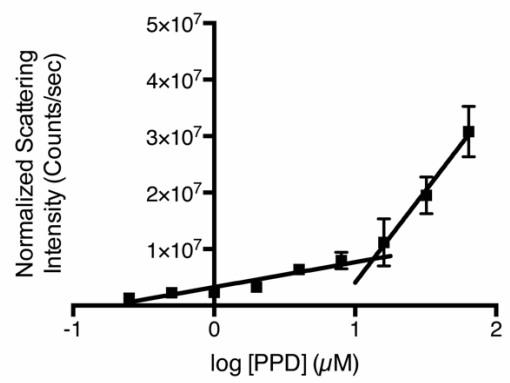

Figure 3.1. The critical aggregation concentration of PPD is 14 μM in PBS as determined by dynamic light scattering. Formulations contain 2% DMF. (n=3, mean ± SD).

Consistent with other colloidal drug aggregates[144], the addition of salt causes massive aggregation and precipitation of both drugs (Figure 3.2C and 3.2D, pink bars). In an effort to prevent colloid precipitation and improve stability in the presence of salts, each drug was co-formulated with one of seven different polymers ranging from clinically used excipients (polysorbate 80, Pluronics F68 and F127, Brij 58 and L23) to amphiphilic polymers used in micelle systems (PLAC-PEG, VitE-PEG) as a screening tool to identify formulations warranting further investigation. Polymers were used at 0.001-0.05% (w/v), a low weight percent relative to that used in traditional drug formulations, which are orders of magnitude higher[185]. All formulations in water had an initial diameter of <200 nm regardless of the presence of excipient or type of excipient used (Figure 3.2C and 3.2D). When formulated in PBS buffer, the addition of polymers prevented or reduced the aggregation of colloids. In contrast, the absence of

polymers led to the formation of drug aggregates larger than 1 μm, which precipitated from solution within minutes.

In the presence of polymeric excipients, colloids were stable over 48 h at 37 ºC (Figure 3.2E and 3.2F). For fulvestrant, formulation with polysorbate 80 (UP80) resulted in homogeneous colloids stable over 48 h. Fulvestrant-UP80 colloids had initial diameters of 109±7 nm, which increased to 168±18 nm over 48 h. Other polymers, such as PLAC-PEG, partially inhibited the growth rate of fulvestrant colloids in high salt buffer compared to the drug alone; however, the initial fulvestrant colloid diameter doubled over a 48 h period, demonstrating that UP80 was a more effective stabilizing agent. In contrast, PLAC-PEG was the optimal polymer to stabilize PPD colloids over 48 h. PPD-PLAC-PEG colloids had initial diameters of 93±8 nm, which grew to 122±6 nm. While other polymers stabilized PPD colloids, they were not as effective as PLAC-PEG. For example, Pluronic F68 showed a doubling in size within minutes of exposure to a high salt buffer (Figure 3.2D). Both fulvestrant-UP80 and PPD-PLAC-PEG maintained a narrow size distribution over the incubation period (PDI<0.2). Fulvestrant-UP80 and PPD-PLAC-PEG formulations have drug loadings of 75 and 50 wt%, respectively, calculated as the absolute amount of drug per total mass (drug and excipient mass).

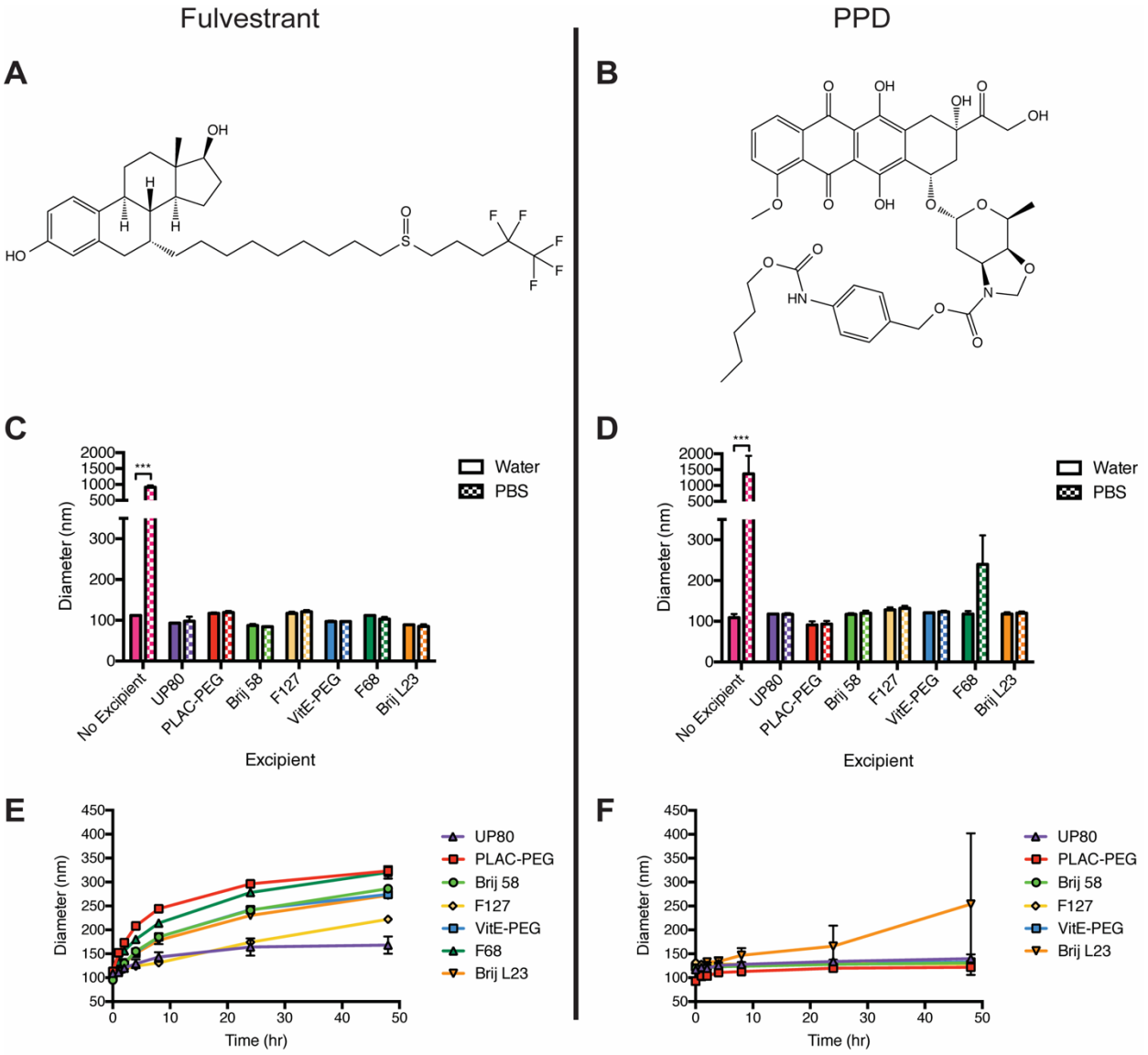

Figure 3.2. (A) Fulvestrant and (B) PPD were selected for their intrinsic chemotherapeutic efficacy and aggregation properties. Formulation of (C) fulvestrant and (D) PPD colloids in water or PBS in the presence of the following polymeric excipients: UP80, PLAC-PEG, Brij 58, Pluronic F127, VitE-PEG, Pluronic F68 and Brij L23. Initial diameters of the formulations are shown. Incubation of (E) fulvestrant and (F) PPD formulations at 37 °C, showing size changes over 48 h. UP80 was the optimal polymer to maintain the size of fulvestrant overtime in buffered salt solution (PBS) compared to other polymers. Stability of PPD with F68 could not be assessed due to precipitation. PLAC-PEG was the optimal polymer to maintain the size of PPD, with the smallest nanoparticle size over the incubation period. (n=3, mean + SD, *** p<0.001)

We characterized the morphology of our most stable and monodisperse formulations, fulvestrant-UP80 and PPD-PLAC-PEG, using TEM. Imaging confirmed the spherical morphology of the resulting particles, with multiple fields of view used to determine particle size distributions for each formulation (Figure 3.3); fulvestrant-UP80 colloids had diameters of 53±15 nm and PPD-PLAC-PEG had diameters of 60±16 nm. Thus, we observed smaller diameters by TEM than those determined by DLS, which is consistent with the drying effects that occur in the vacuum environment used for TEM compared to the hydrated state in DLS. Even small amounts of polymer excipients (0.001% UP80 and 0.04% PLAC-PEG) for these two formulations significantly improved stability in buffered aqueous solutions. This prompted us to investigate stability in more biologically relevant conditions, such as serum-containing media.

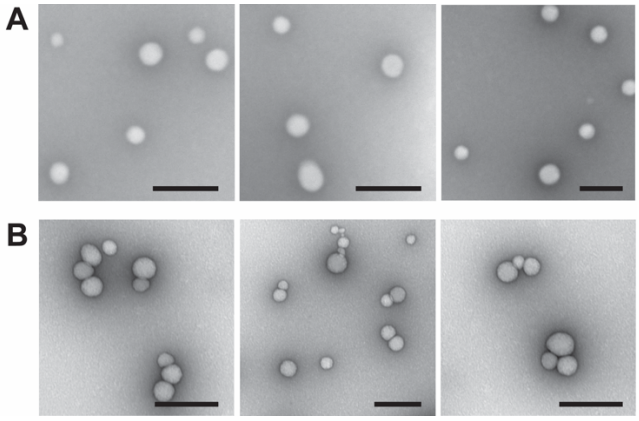

Figure 3.3. Representative fields of view of (A) fulvestrant-UP80 and (B) PPD-PLAC-PEG colloids in PBS. Scale bar represents 200 nm.

Encouraged by the enhanced stability of fulvestrant-UP80 and PPD-PLAC-PEG colloids in buffered solutions, we sought to better assess the structural integrity and stability of these formulations over time in serum-containing media using both TEM imaging and FPLC separation. Representative fields of view from TEM imaging (Figure 3.4A, 3.4B and additional fields of view in Figure 3.5) show that both formulations are present in 10% serum over a 48-h time period; fulvestrant-UP80 colloids (Figure 3.4A and 3.4C) increased in size and dispersity during the incubation from an initial diameter of 67±17 nm to a final diameter of 222±77 nm (Figure 3.4C). PPD-PLAC-PEG colloids maintained their size and distribution over time (Figure 3.4B and 3.4D), with initial and final diameters of 36±10 nm and 36±11 nm, respectively. Importantly, the spherical morphology of the colloids was retained for both formulations over the incubation period.

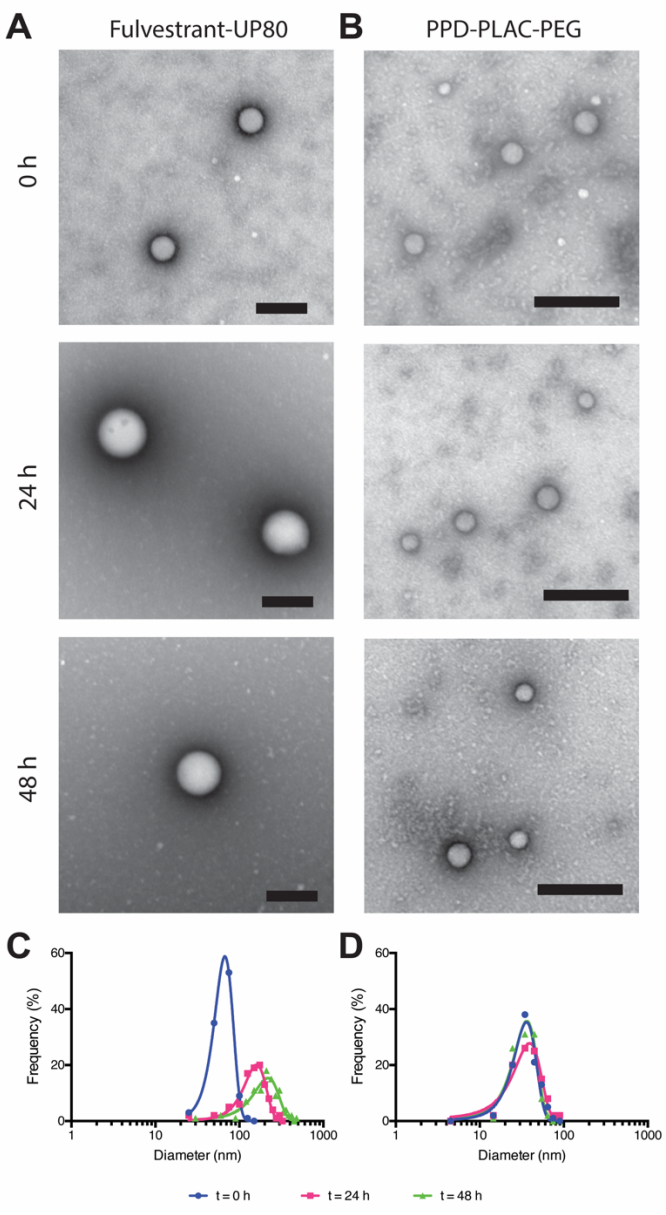

Figure 3.4. Fulvestrant-UP80 and PPD-PLAC-PEG characterization in 10% serum. (A,B) Representative TEM images of particles in serum at 0, 24 and 48 h. (A) Fulvestrant-UP80 colloids were stained with ammonium molybdate while (B) PPD-PLAC-PEG colloids were stained with uranyl acetate, scale bars are 200 nm. (C,D) TEM frequency distribution shows mean diameter increase and peak broadening of (C) fulvestrant-UP80 colloidal aggregates over time, while (D) PPD-PLAC-PEG maintains size and distribution over time.

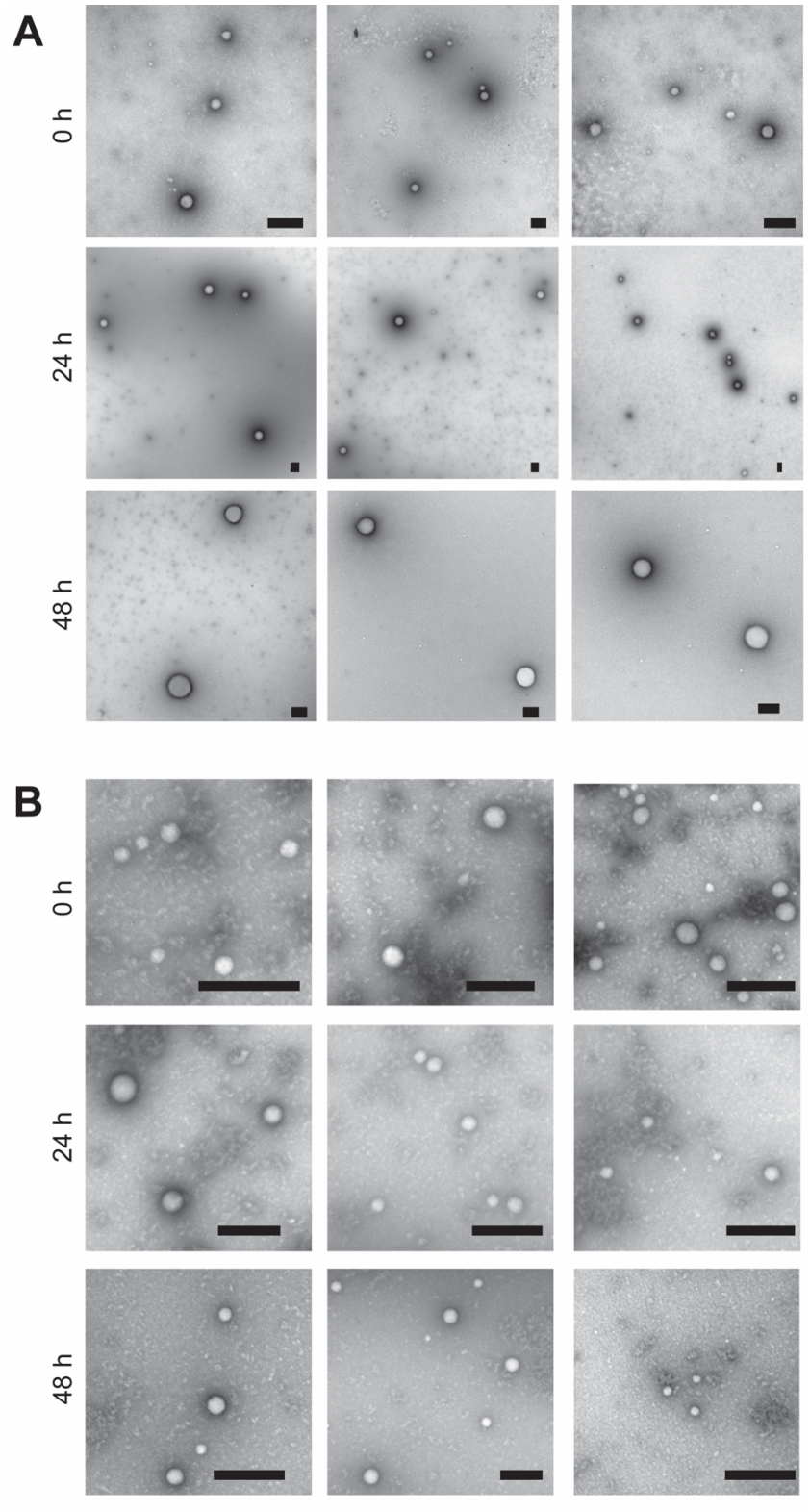

Figure 3.5. Additional TEM fields of view for (A) fulvestrant-UP80 and (B) PPD-PLAC-PEG during incubation in 10% serum as a function of time. Scale bar represents 200 nm.

The protein corona that forms on particle surfaces can cause premature drug release due to partitioning of the drug into the hydrophobic pockets of proteins, and thus we investigated drug release in the stabilized colloidal formulations in serum. To quantify the drug release, our two formulations were incubated in 20% serum, which is representative of in vivo serum conditions and allows colloids to be separated and quantified by FPLC directly[155]. At select time points, up to 48 h, the colloidal population was separated from serum proteins and free drug using size exclusion chromatography (SEC) and the colloid peak area was used as a proxy for drug concentration (Figure 3.6A, 3.6B and 3.7). Notably, bare colloids could not be separated by this method due to their rapid precipitation in salt conditions. Fulvestrant-UP80 was co-formulated with a BODIPY FRET pair (Figure 3.8), enabling fluorescence emission detection, while PPD-PLAC-PEG colloids were quantified by absorbance at 480 nm. Both formulations showed little dissociation over 24 h (Figure 3.6C). Fulvestrant-UP80 colloidal aggregates began to dissociate after this time, with almost 50% of the drug released at 48 h. PPD-PLAC-PEG aggregates showed no dissociation over the 48-h time period. Encouragingly, the stability data obtained for the colloids by FPLC separation reflect the trends observed by TEM (Figure 3.4).

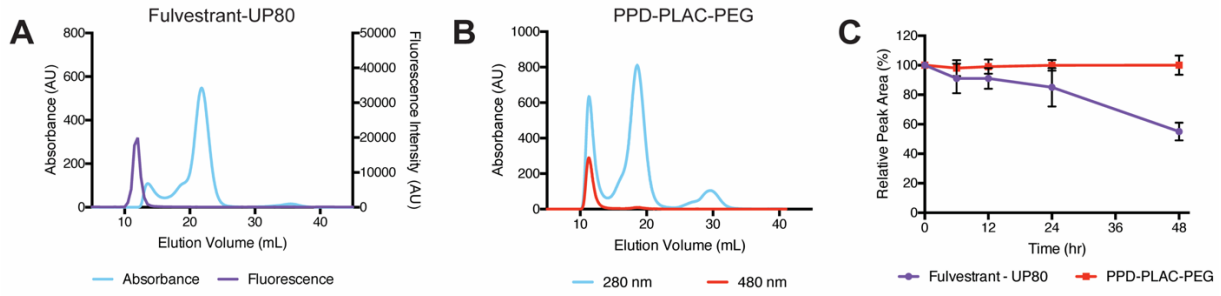

Figure 3.6. Serum stability of colloidal formulations by FPLC. Traces show separation between serum proteins (absorbance at 280 nm) and (A) fulvestrant-UP80 colloids (tracked by fluorescence using a BODIPY FRET pair) and (B) PPD-PLAC-PEG colloids (unique absorbance at 480 nm) at t=0. (C) The peak area under the colloid curve over time is compared to the area at t=0 h to determine colloid stability as a function of time. Both colloids are stable up to 24 h, with fulvestrant-UP80 colloids dissociating between 24 and 48 h, and PPD-PLAC-PEG colloids showing no evidence of dissociation over 48 h.

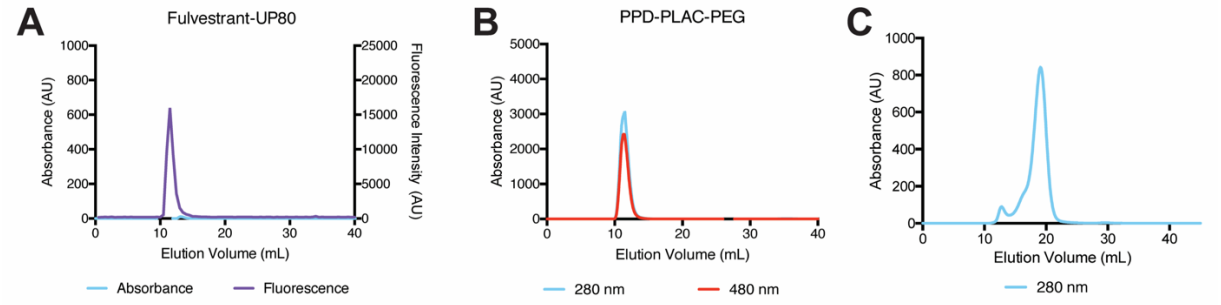

Figure 3.7. Representative chromatograms of (A) fulvestrant-UP80, (B) PPD-PLAC-PEG and (C) 20% serum following size exclusion chromatography. Fulvestrant-UP80 and PPD-PLAC-PEG were separated in serum-free conditions.

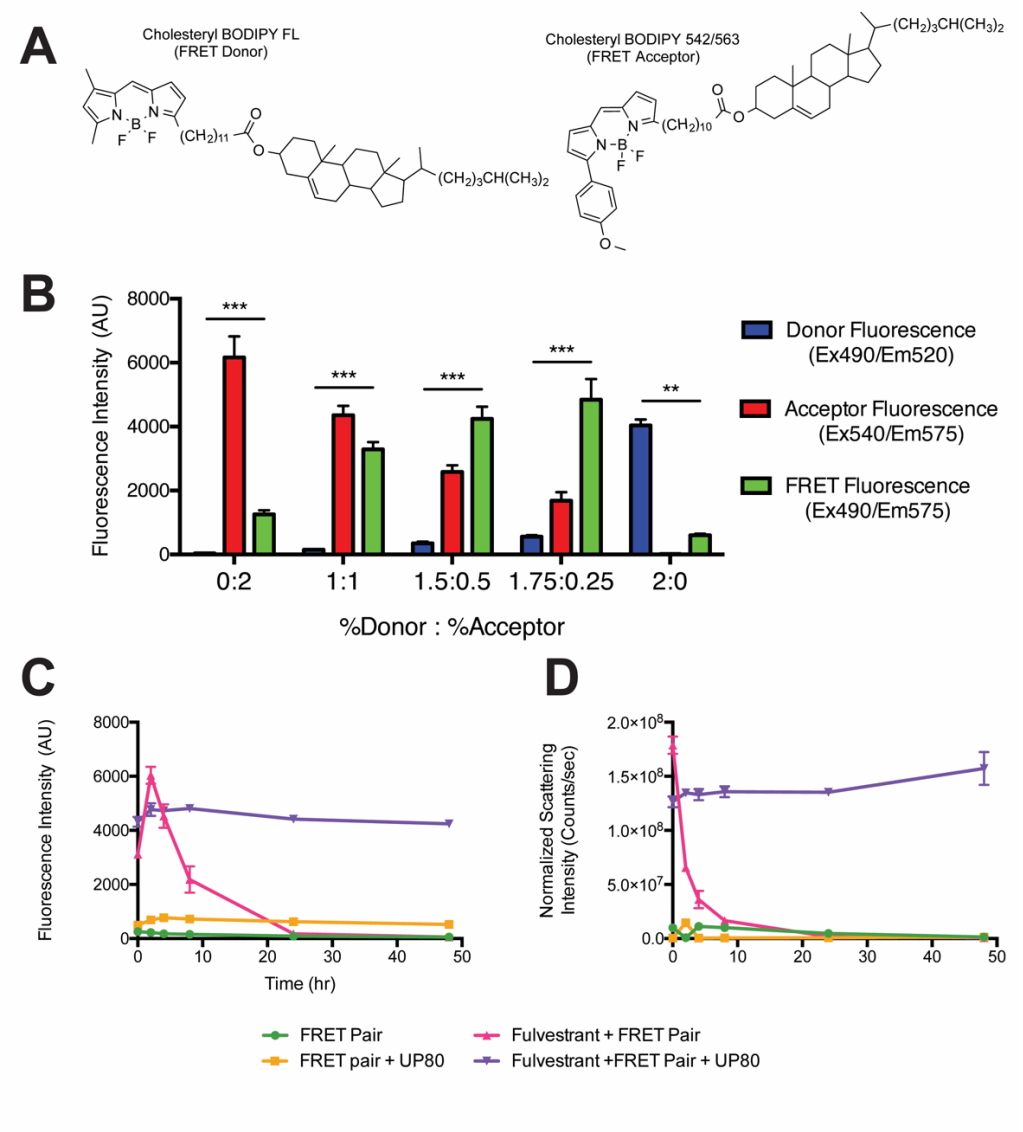

Figure 3.8. (A) Structure of FRET pair of CholEsteryl BODIPY FL (Donor) and CholEsteryl BODIPY 542/563 (Acceptor). (B) Fluorescence properties of BODIPY dyes (2 mol%) co-formulated with 50 µM fulvestrant and 0.001% UP80 in PBS. (n=3, mean±SD, ** p<0.01, ***p<0.001 between donor, acceptor and FRET fluorescence within formulations) (C) Stability of fulvestrant-UP80 colloids in PBS measured by FRET fluorescence correlates with stability measured by (D) dynamic light scattering. Decrease in fluorescence and scattering intensity of non-stabilized colloids indicates crystallization and precipitation over time. UP80-stabilized colloids maintain fluorescence intensity, indicating an amorphous state throughout. Dye incorporation is unlikely within nanocrystalline particles. Formulations comprise 50 µM fulvestrant, 1.75 mol% donor, 0.25 mol% acceptor, 0.001% UP80 in PBS (n=3, mean±SD).

We hypothesized that the polymeric excipients used to stabilize the colloidal formulations reduced protein adsorption and thereby provided stability in serum. To test this hypothesis, we used a previously reported method of centrifugation and gel electrophoresis of colloidal formulations to identify surface-bound proteins[144]. We studied the interaction of colloidal aggregates of fulvestrant vs. fulvestrant-UP80 and PPD vs. PPD-PLAC-PEG with the main serum proteins: bovine serum albumin (BSA), immunoglobulin G (IgG) and fibrinogen. Colloids were incubated with each protein and then pelleted by centrifugation. Proteins in the supernatant and those in the pelleted colloid fractions were identified by gel electrophoresis (Figure 3.9). All three proteins studied were concentrated (at a 5-15 fold increase) in the pelleted fraction when incubated with bare colloids, indicating significant adsorption to the colloid surface (Figure 3.10). In contrast, none of the three proteins studied were concentrated in the pelleted fraction when incubated with polymer-stabilized colloidal formulations of both fulvestrant-UP80 and PPD-PLAC-PEG, indicating minimal protein adsorption (Figure 3.10). These data are consistent with several other particle systems that use high-density PEG surfaces to reduce protein adsorption and particle opsonization[100,186,187].

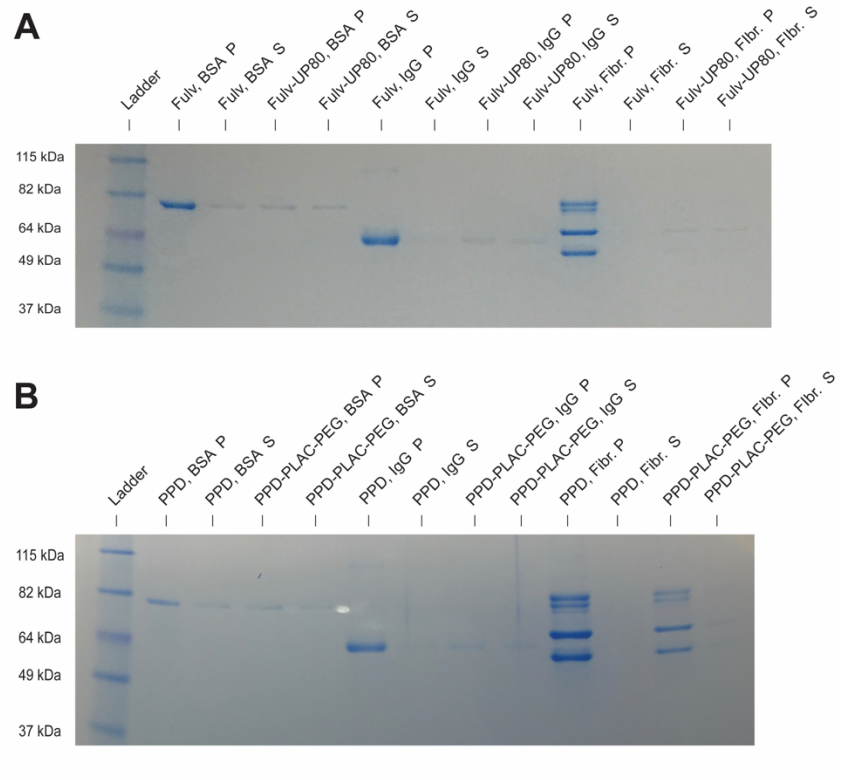

Figure 3.9. Representative SDS-PAGE images of (A) fulvestrant and (B) PPD colloids after incubation with 50 nM bovine serum albumin (BSA), immunoglobulin G (IgG) and fibrinogen (Fibr.). Pellet (P) and supernatant (S) fraction were separated by centrifugation of formulation at 16000x *g* for 1 h at 4 ˚C. Representative image of 3 repeats.

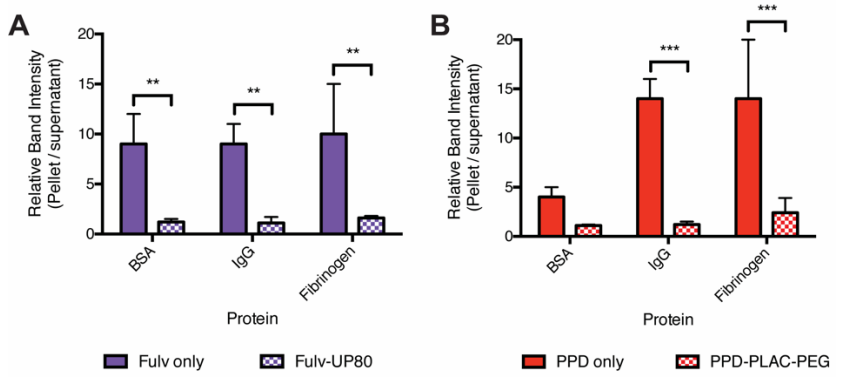

Figure 3.10. Formulation of colloids with excipient polymers reduces protein adsorption. BSA, IgG and fibrinogen (50 nM) adsorption are significantly increased on the surface of bare colloids of (A) fulvestrant and (B) PPD (filled bars) compared to colloids stabilized with the appropriate polymer (checkered bars): fulvestrant-UP80 and PPD-PLAC-PEG (n=3, mean + SD, **p<0.01, ***p<0.001).

In order to investigate the cell uptake of colloidal aggregates vs. drug monomers, which typically diffuse across cell membranes, fulvestrant-UP80 and PPD-PLAC-PEG were incubated with the human epithelial ovarian cancer SKOV-3 cell line (Figure 3.11) both in the absence and presence of serum. Doxorubicin, an anthracycline chemotherapeutic from which PPD is derived, does not form colloidal aggregates and was used as a positive control that can freely permeate cell membranes. Doxorubicin and PPD were directly tracked by excitation at 488 nm while fulvestrant-UP80 colloids were co-formulated with a BODIPY dye that was visualized by excitation at 559 nm. Fluorescence of the non-colloid forming doxorubicin was diffuse, co-localizing with cell nuclei under both serum-free and serum conditions. Conversely, intracellular fluorescence of fulvestrant-UP80 and PPD-PLAC-PEG colloids was only observed under serum-free conditions. Even then, the fluorescence was observed as punctate features within the cell body. In serum-containing media, little to no fluorescence was observed for the colloidal formulations.

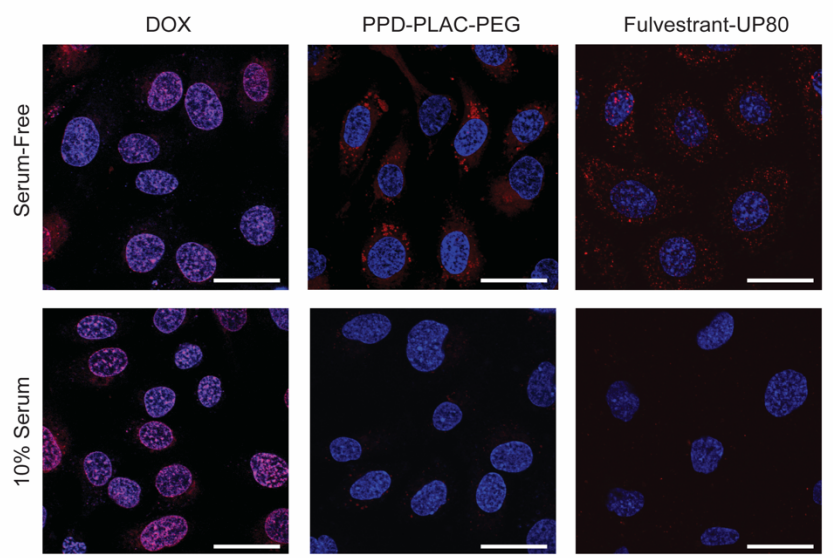

Figure 3.11. Representative images of the cell uptake of doxorubicin (monomer) and the colloidal formulations of PPD-PLAC-PEG and fulvestrant-UP80 (tracked by BODIPY). SKOV-3 cells were used for all experiments. Doxorubicin monomer freely permeates the cell membrane, showing localized fluorescence within the cells' nuclei. PPD and fulvestrant colloids show uptake only in serum-free conditions, with punctate fluorescence within the cell body. There is no evidence of cell uptake of colloids in serum-containing media. (scale bar represents 30 µm)

3.5 Discussion

While the intrinsic colloidal aggregation properties of hydrophobic small molecule drugs are often unpredictable, this phenomenon can be exploited and controlled with the addition of excipients. Using a nanoprecipitation method to formulate colloidal aggregates with polymeric excipients, we can produce stable high drug loaded particles resistant to changes in salt and serum conditions. Absolute drug loadings of our two formulations, fulvestrant-UP80 (75 wt%) and PPD-PLAC-PEG (50 wt%), are an order of magnitude higher than conventional micelle formulations, which are typically <10 wt%[140]. By incorporating polymeric excipients, the particles are stabilized and aggregation is prevented through steric repulsion between hydrophilic polymer chains[155,187]. In the absence of polymer, salts in the solution lead to charge shielding at the surface of colloidal species causing particle fusion and rapid aggregation, leading to eventual crystallization and precipitation[188]. The use of amphiphilic polymers allows hydrophobic segments of the polymer to interact with the hydrophobic colloidal core and hydrophilic segments of the polymer to extend into the aqueous phase to provide steric stability. Due to mixing of the drug and polymer during colloid formation, the hydrophobic segments of the polymer may be entangled within the colloid.

At present, the limited number of colloid-polymer combinations studied here prevent general predictions on optimal drug-polymer pairs. We hypothesize that the solubility parameters play an important role in determining which polymer would be best suited to stabilize a drug colloid, as has been shown by computational approaches used in other studies[189,190]. The concentration of polymer used in these formulations plays an important role in stabilizing colloidal species[191,192]. If the polymer concentration is too low, there is insufficient coverage of the colloidal surface to prevent aggregation and coalescence of the drug colloids. If the polymer concentration is too high and above the critical micelle concentration (CMC), the polymers themselves form micelles and solubilize the drug rather than stabilize the colloid. Accordingly, polymer concentrations near their CMCs were chosen for this study, providing adequate surface coverage without colloid disruption.

While the stability in salts is essential, we sought to characterize these colloidal aggregates in biologically relevant serum-containing media. Blood proteins destabilize particles, and premature drug release often results from drugs partitioning into the hydrophobic pockets of proteins adsorbed to the particle surface[193]. In fact, the non-stabilized colloids could not be

assayed in 20% serum due to their inherent instability and rapid precipitation. In contrast, we show that polymers stabilize these colloidal particles for at least 24 h in 20% fetal bovine serum by monitoring the drugs using their spectral properties. We hypothesized that this stability is due to a reduction in protein adsorption to the colloidal surface, consistent with the use of hydrophilic polymers, such as PEG, in other particle platforms[100,194]. To evaluate the interaction between the main components of serum – albumin, globulins and fibrinogens – and the particle surface, we used a centrifugation method to identify surface-bound proteins, as has been previously used to study the inhibition of enzymes by colloid surface sequestration[4,13]. This method is limited by the concentration of proteins that can be evaluated; however, non-stabilized colloids showed significant adsorption of proteins to their surface, whereas polymer stabilized colloids showed reduced protein adsorption. While colloidal drug aggregates have been previously defined by their ability to adsorb proteins, the use of polymers alters this property and yields formulations with increased stability.

To further probe the stability of the colloidal aggregates, we investigated their interactions with cells in vitro. Under serum-free conditions, distinct punctate fluorescence was observed intracellularly for both fulvestrant and PPD colloidal formulations, which is typical of internalized particles that are trafficked through the endo-lysosomal pathway[127,156]. Corroborating previous literature, doxorubicin, a compound that does not form colloidal aggregates, freely permeated lipid membranes and localized in the nucleus[195]. In serum-containing media, while the cellular uptake of doxorubicin was not significantly influenced, fulvestrant-UP80 and PPD-PLAC-PEG colloids were not internalized by cells. This is consistent with our previous observations that compounds in colloid form are not internalized by cells and thus lose their efficacy in cell culture[9]. The presence of proteins precludes the non-specific uptake of particles due to decreased adhesion of particles to the cell surface and supports the need for cellular targeting agents on the particles[42-44].

It is clear from this study that the combination of hydrophobic drug and polymer strongly influences particle size and stability over time. This is consistent with other polymer-based nanoparticle formulations where similar drug and vehicle compatibility leads to optimized drug loading, stability and in vivo circulation[196-200]. Of the formulations tested here, the combinations of fulvestrant-UP80 and PPD-PLAC-PEG are optimal for colloidal stability in both high ionic strength aqueous and serum containing solutions. Chemical modifications of both the drug and the polymeric excipient have been used previously to enhance molecular interactions that

provide improved particle stability[93,94,148]. However, this strategy often requires re-validation of materials, especially with respect to the drug. Directly screening for and exploiting the colloidal aggregation properties of drugs, as demonstrated here, can provide a mechanism to significantly increase drug loading and stability, without the need for chemical modification. With a continued increase in chemical diversity of both colloid-forming drugs and polymeric excipients, the methods outlined here will find further application in formulating drug-rich nanoparticle delivery systems.

3.6 Conclusions

By incorporating polymeric excipients into colloidal formulations of two relevant chemotherapeutics, fulvestrant and PPD, we demonstrated stability in both salt and serum containing-media. This enhanced stability can be attributed to reduced adsorption of serum proteins to the surface of the particles. We anticipate that this strategy of using polymers to stabilize colloidal drug aggregates is broadly applicable, thereby opening up new opportunities to achieve high drug loadings for drug delivery applications.

3.7 Acknowledgements

This work was supported by grants from the Canadian Cancer Society Research Institute (to M.S.S and B.K.S), the US National Institutes of General Medical Sciences (GM71630 to B.K.S. and M.S.S.) and the US National Cancer Institute (CA143549 to T.H.K.). A.N.G. and J.L. were supported, in part, by the Natural Sciences and Engineering Research Council (NSERC) of Canada Postgraduate Research Scholarships and C.K.M was supported, in part, by an NSERC postdoctoral fellowship. We thank S. Boyle and B. Calvieri from the University of Toronto Microscopy Imaging Laboratory for assistance with TEM imaging and members of the Shoichet labs for thoughtful discussion.

4 Colloidal drug aggregates stability in high serum conditions and pharmacokinetic consequence

*This manuscript has been submitted to *ACS Chemical Biology*

Ganesh, A.N., Aman, A., Logie, J., Barthel, B.L., Cogan, P., Al-awar, R.S., Koch, T.H., Shoichet, B.K., Shoichet, M.S. (2019) Colloidal drug aggregate stability in high serum conditions and pharmacokinetic consequence. Submitted to *ACS Chemical Biology*.

ANG, AA, RSA, BKS, and MSS design the research; ANG performed experiments; ANG and AA analysed the data; BBL, PC, and THK synthesized and provided PPD; ANG, and MSS wrote and edited the manuscript.

4.1 Abstract

Colloidal drug aggregates have been a nuisance in drug screening, yet, because they inherently comprise drug-rich particles, they may be useful in vivo if issues of stability can be addressed. As the first step toward answering this question, we demonstrate colloidal drug aggregate stability in high (90%) serum conditions with two chemotherapeutics, fulvestrant and an investigational pro-drug, pentyloxycarbonyl-(*p*-aminobenzyl) doxazolidinylcarbamate (PPD). We show, for the first time, that the critical aggregation concentration of fulvestrant depends on media composition and increases with serum concentration. Excipients, such as polysorbate 80, stabilize fulvestrant colloids in 90% serum in vitro for over 48 h. Consequently, the in vivo half-life of stabilized fulvestrant and PPD colloids were greater than their respective monomeric forms, demonstrating the potential of turning this nuisance into an opportunity for drug-rich formulations

4.2 Introduction

Colloidal aggregation of small, hydrophobic compounds is the leading cause of false hits in early screening and drug discovery[1,2]. The formation of these self-assembled colloids is characterized by a critical aggregation concentration (CAC), above which small molecules self-assemble into liquid-liquid phase-separated particles[5,14]. Colloidal aggregates cause both false-positives in enzyme- and receptor-based assays, and false-negatives in cell-based assays[4,7,145]. The formation of colloidal particles has been reported for thousands of compounds (http://advisor.bkslab.org)[183], including those from screening libraries and from clinically used drugs, such as anti-cancer, cardiovascular, and anti-retroviral therapeutics[6-8,22,201,202].

Few studies have investigated the implications of colloidal aggregates in biological milieus and for drug delivery. Doak et al. found that many biopharmaceutics classification system (BCS) class II and IV drugs form colloidal aggregates in simulated intestinal fluid, suggesting colloid formation could play a role in drug formulation and bioavailability[45]. The presence of proteins can further impact colloidal drug transport. For example, Owen et al. demonstrated that in standard cell culture conditions (10% serum), colloidal chemotherapeutics did not cross into cells, resulting in an apparent loss in cytotoxicity of the drug[9]. Recently, Wilson et al. demonstrated that colloid formation from amorphous solid dispersions can act as reservoirs and enhance plasma drug exposure after oral delivery[203]. Frenkel et al. found colloid-forming non-nucleoside reverse transcriptase inhibitors were more potent than expected after oral administration, speculating that this reflected their absorption in the Peyer's patch, directing the antiviral drugs to lymphatic circulation[33].

Efforts to exploit and study colloidal aggregates in high protein milieus have been hindered by their transient stability. Even in biochemical buffers, most small molecule aggregates are only transiently stable, often flocculating and precipitating over several hours. Recently, strategies to stabilize colloidal particles under physiologically relevant conditions have been developed. Co-aggregation with polymeric surfactants, azo-dyes, or protein coronas all stabilized drug colloids over many days in buffered and serum-containing media[36,204,205]. Colloids of the estrogen receptor antagonist, fulvestrant, and the investigational anthracycline prodrug, pentyloxycarbonyl-(*p*-aminobenzyl) doxazolidinylcarbamate (PPD), can be stabilized by co-aggregation with polysorbate 80 (UP80) and poly(D,L-lactide-*co*-2-methyl-2-carboxytrimethylene carbonate)-*g*-poly(ethylene glycol) (PLAC-PEG), respectively[205].

While these efforts have yielded drug aggregates that are stable under in vitro conditions, the in vivo fate of stable colloidal drug aggregates has not been investigated. Here, for the first time, we measure the critical aggregation concentration in high-serum content media, demonstrating that fundamental drug colloid properties, such as those that dictate the onset of aggregation, are significantly changed under in vivo-mimetic conditions. We further demonstrate that serum-stable colloidal drug aggregates influence in vivo drug circulation properties and increase the plasma half-life compared to monomeric formulations.

4.3 Materials and Methods

4.3.1 Materials

Fulvestrant was purchased from Selleckchem and PPD was synthesized as previously described[68]. Polysorbate 80 (H2X, UP80) was purchased from NOF America Corporation. Poly (D,L-lactide-*co*-2-methyl-2-carboxy-trimethylene carbonate)-*graft*-poly(ethylene glycol) (PLAC-PEG) was synthesized as previously described[155]. CholEsteryl BODIPY FL C12 and 543/563 C11 were purchased from Thermo Fisher Scientific. Charcoal-stripped fetal bovine serum was purchased from Wisent Bio Products. RPMI and DMEM-F12 media was purchased from Sigma Aldrich. Growth factor-reduced Matrigel was purchased from Corning.

4.3.2 Colloid Formation and Stability Studies

Colloids of fulvestrant and PPD were formed as previously described[205]. Briefly, a typical formulation comprised 880 µL of double-distilled water (ddH_2O), 20 µL drug stock solution (in DMSO) followed by the addition of 10X PBS (100 µL). Drug stock solutions were prepared to obtain the desired final concentration. Excipients were incorporated into ddH_2O prior to colloid formulation. Fluorescent colloids were prepared by including the FRET pair of CholEsteryl BODIPY dyes (FL C12 and 542/563 C11) in the drug stock solution. Final total dye content was limited to 2 mol%. For CAC measurement and stability experiments, colloids were formulated in PBS, as above, and then diluted 10-fold into various media. Colloids were incubated at 37 °C for the duration of the stability studies.

4.3.3 Colloid Characterization

Diameter, polydispersity and normalized scattering intensity were measured using dynamic light scattering (DLS). A DynaPro Plate Reader II (Wyatt Technologies), with a laser width optimized for colloidal aggregate detection by the manufacturer, was used with a 60 mW laser at 830 nm

wavelength and a detector angle of 158°. Fluorescence intensity of colloids co-formulated with the BOPDIY dye FRET pair was measured using the Tecan Infinite 200 Pro plate reader. The FRET pair was excited at 490 nm and the acceptor emission was measured at 575 nm.

For transmission electron microscopy, 5 µL of colloid solution were deposited on glow-discharged 400 mesh carbon-coated copper grids (Ted Pella Inc.) and allowed to adhere for 3 min. Excess liquid was removed and grids washed with 5 µL of double-distilled water. Grids were stained with 1% ammonium molybdate (pH 7, 5 µL) for 30 s. After excess stain removal, samples were imaged using Talos L120C transmission electron microscope operating at 80 kV. Images were captured using CETA CMOS camera and images analyzed using ImageJ software.

4.3.4 Cell Maintenance and Preparation for Xenografts

Cells were maintained at 37 °C in 5% CO_2 in media supplemented with 10% FBS, 10 units/mL penicillin and 10 µg/mL streptomycin. MCF-7 cells were purchased from ATCC and cultured in DMEM-F12 media. To prepare cells for injection, cells were detached using trypsin-ethylenediamine tetraacetic acid (trypsin-EDTA) followed by pelleting and washing with PBS (3 times). MCF-7 cells were resuspended at 10^8 cells/mL in 50% Matrigel.

4.3.5 Orthotopic Breast Tumor Model

Animal study protocols were approved by the University Health Network Animal Care Committee and performed in accordance with current institutional and national regulations. Mice were housed in a 12 h light/dark cycle with free access to food and water. NOD-*scid-Il2rg*^{null} (NSG) female mice were bred in-house and received tumor xeno-transplantation at 9-weeks old. Slow release 17β-estradiol pellets (0.72 mg/pellet, 60-day release) were subcutaneously implanted in mice 4 days prior to tumor cell transplantation. For orthotopic mammary fat pad surgeries, mice were anaesthetized with isoflurane-oxygen and the surgical area was depilated and cleaned with betadine. An incision in the skin of the lower abdomen to the right of the midline was made to reveal the mammary fat pad. Cells were injected into the right inguinal region (50 µL injection, 5 x 10^6 cells/mouse). The incision was then sutured and lactate Ringer's solution and buprenorphine were post-operatively administered for pain management and recovery.

4.3.6 Intravenous Injection

Tumors were allowed to grow for 3 weeks until palpable (100 mm^3). Formulations were injected intravenously using a BD324702 insulin syringe. The volume of injection was based on the weight of the mouse in order to administer the intended dose and no more than 10% of the blood volume.

4.3.7 Pharmacokinetics and Biodistribution Study

In each study, mice received either a colloidal formulation as described or a monomeric formulation comprising the same dose of drug solubilized with 5% polysorbate 80. Formulations were administered at the intended dose via tail vein injection. At time points after the injection, blood was drawn via the saphenous vein (< 30 µL) into EDTA-coated microcuvette tubes (Sarstead 16.444.100) such that each mouse was not sampled more than three times. At terminal time points, blood was collected by cardiac puncture after CO_2 asphyxiation. After collection of blood, tubes were immediately centrifuged, and isolated plasma was flash-frozen. For biodistribution, organ tissue (tumor, heart, lung, liver, kidney, spleen, brain) at terminal time points of PK studies were collected in pre-weighed vials after rinsing with PBS and flash frozen.

4.3.8 Drug extraction and Protein Precipitation

Drug concentrations were determined by HPLC-MS/MS following drug extraction and protein precipitation. Plasma samples (10 µL) were diluted with 10 µL of 1% formic acid solution and 10 µL of internal standard at 10x the final concentration in acetonitrile (ACN) followed by vortexing (10 s, 2 times). Samples were further diluted with 70 µL ACN followed by a second round of vortexing and then centrifuged at 16,000 x *g* for 15 min at 4 °C. The resulting supernatant was collected for analysis by HPLC-MS/MS. Standard curves were prepared in a similar manner with 10 µL of a 10x-concentrated standard solution spiked into blank plasma prior to the first round of vortexing.

To prepare organ tissue, samples were thawed and weighed followed by the addition of 20 zirconia beads (1.0 mm diameter) to facilitate homogenization. To each vial were added, 100 µL of 1% formic acid solution and 100 µL of 10x-concentration internal standard solution. Samples were then homogenized for 1 min (2 times) using a bead beater with 1 min on ice between each run. Cold ACN was then added (800 µL) followed by an additional round of homogenization. Samples were centrifuged at 16,000 x *g* for 15 min at 4 °C and supernatant collected for analysis.

Standard curves were prepared by spiking blank liver tissue with 100 µL of 10x-concentration drug solution.

4.3.9 Drug Quantification by HPLC-MS/MS

Fulvestrant and PPD concentrations were determined by HPLC-MS/MS. Chromatographic separation was performed using a Waters XTerra C8 column (5 µm) on an Agilent 1100 HPLC equipped with an AB Sciex API 4000 triple quadrupole mass spectrometer with electrospray ionization source detector. Mobile phases of 0.1% formic acid in water (solvent A) and methanol (solvent B) were used. Fulvestrant and PPD standard curves were prepared in blank plasma or liver as described above (0.5 ng/mL – 500 ng/mL) using norethindrone or docetaxel (50 ng/mL) as an internal standard, respectively. If necessary, samples were diluted to be within the standard curve with blank plasma or liver that had been spiked with IS solution.

4.3.10 PK and Statistical Analysis

PK parameters were determined using Phoenix WinNonlin software. Statistical analysis was performed using GraphPad Prism 5.0 software.

4.4 Results and Discussion

Few techniques are available to probe the integrity of amorphous nanostructures in complex media. In biochemical buffers, drug colloids can readily be defined by dynamic light scattering (DLS); however these techniques become limited in the presence of serum due to scattering from serum proteins themselves, which is only further complicated as serum-content is increased[206]. Alternatively, FRET pairs can be absorbed into the self-assembled colloids, where they can report on their gross structural integrity[30,156,205]. Accordingly, we designed such a strategy to study colloidal drug aggregate stability in serum-containing media in vitro. Cholesterol-modified BODIPY dyes can be readily incorporated during colloid formation due to the hydrophobic and amorphous nature of drug aggregates[14,205]. These dyes have substantial fluorescence intensity within drug colloids but have very low intensity when not associated with a drug aggregate or when colloids are disrupted with detergents (Figure 4.1). Thus, we investigated the presence and stability of colloidal aggregates of fulvestrant, in high-serum conditions exploiting the fluorescence intensity changes of a BODIPY FRET pair.

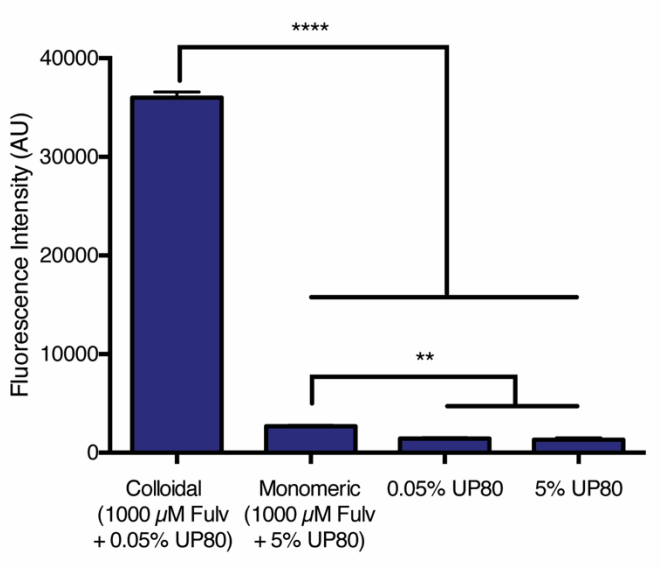

Figure 4.1. Fluorescence intensity of BODIPY FRET pair is significantly increased when incorporated in colloids. Colloidal fulvestrant formulated with 0.05% UP80 had a significantly higher FRET fluorescence intensity compared to monomeric fulvestrant or UP80-only controls. BODIPY FRET (10 µM) was incorporated into each formulation with 2% DMSO in PBS. ** $p < 0.01$, **** $p < 0.0001$ by one-way ANOVA with Tuckey's post-hoc (n = 3, mean ± SD)

We first investigated the effects of dilution and media composition on the critical aggregation concentration of fulvestrant. In protein-free media, many colloid-forming compounds, including fulvestrant, aggregate at low micromolar concentrations, typically measured by light scattering (Figure 4.2)[201]. To measure the CAC of fulvestrant in serum-containing media, colloids were formulated with 10 µM BODIPY FRET pair in PBS with 0.01% UP80 and subsequently diluted 10-fold into media of varying serum content. Using fluorescence intensity as a measure of the amount of colloids present following dilution, allowed the CAC to be determined (Figure 4.3A and 4.4). The CAC of fulvestrant increased with serum content (Figure 4.3B), perhaps owing to serum proteins themselves sequestering drug monomers, bile acids, and other detergent-like molecules in serum[207]. This equilibrium shift requires a higher amount of free drug for colloid formation to occur. Naturally, for colloids to influence drug fate in vivo they must be present, and this can only be predicted by CAC measurements in relevant, serum-containing media.

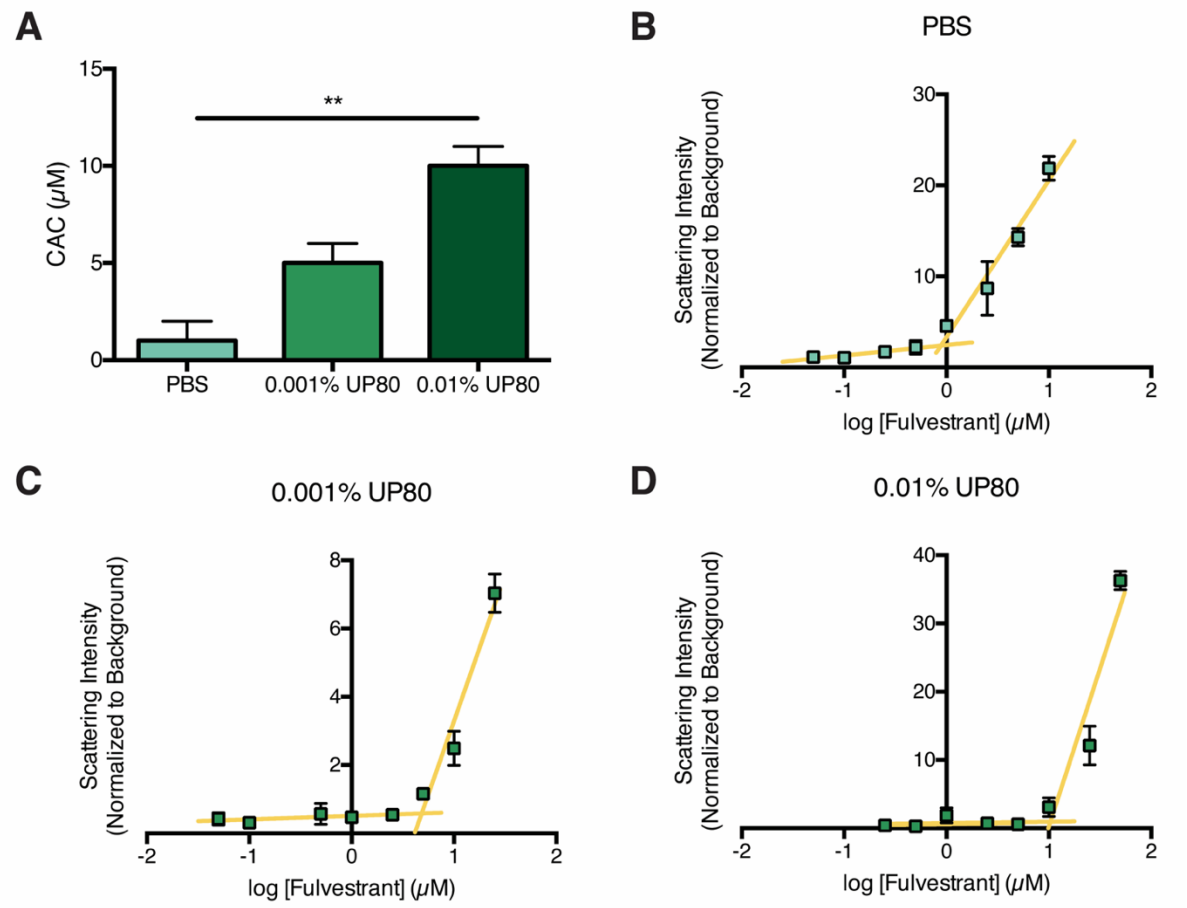

Figure 4.2. (A) CAC of fulvestrant increases with increasing UP80. Critical aggregation concentration of fulvestrant was measured in (B) PBS or PBS with (C) 0.001% UP80 and (D) 0.01% UP80. ** $p < 0.01$ between all groups by one-way ANOVA with Tuckey's post-hoc (n = 3, mean ± SD).

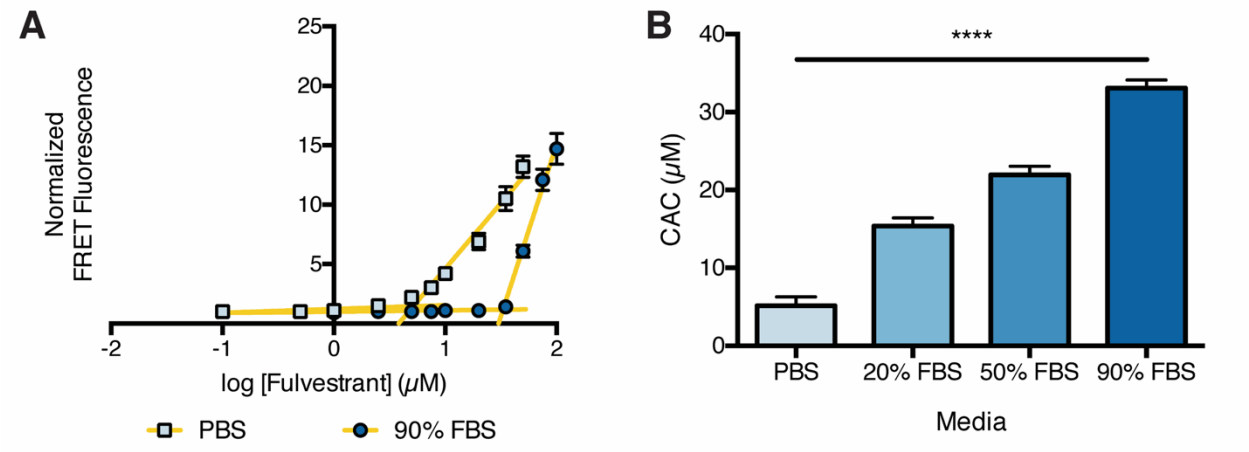

Figure 4.3. Critical aggregation concentration of fulvestrant depends on serum-content of media. (A) Fulvestrant colloids with 10 µM BODIPY FRET pair and 0.01% UP80 as a stabilizing excipient were diluted (10-fold) into PBS or 90% FBS. Fluorescence intensity was used to measure the remaining colloids. (B) CAC of fulvestrant in serum-containing media. **** $p < 0.0001$ between all groups by one-way ANOVA with Tuckey's post-hoc (n = 3, mean ± SD).

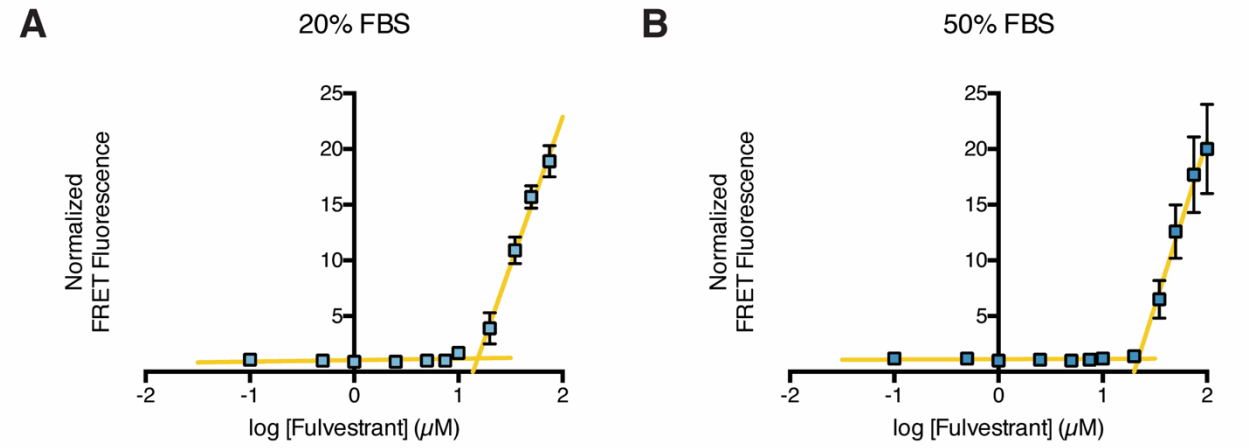

Figure 4.4. Critical aggregation concentration of fulvestrant measured following 10-fold dilution into (A) 20% FBS and (B) 50% FBS. Fulvestrant colloids were formulated in PBS with 0.01% UP80 and 10 µM BODIPY FRET pair. (n = 3, mean ± SD)

Drug colloids, which will ordinarily flocculate and precipitate over several hours, require a stabilizing excipient to remain in buffer and serum-containing media for longer times[201]. We investigated the role of excipients in stabilizing fulvestrant colloids in high-serum conditions,

which mimic the in vivo environment. Here, using the same hydrophobic dyes, which lose fluorescence intensity as they become released when the colloids disassemble or precipitate[19,205], we measured the stability of colloids in complex protein media. Fulvestrant colloids were formulated at 500 μM with 10 μM of the BODIPY FRET pair and a range of UP80 concentrations, and subsequently diluted 10-fold into serum-containing media (Figure 4.5); this paradigm results in a final concentration of 50 μM which is above the CAC in each of the tested media. Without UP80, colloids quickly disappeared from the liquid phase and were not detectable after 10 h. A low amount of UP80 (0.001% or 0.01%) provided some stability to colloids, but only the formulation with an initial 0.1% UP80 was fully stable over the entire 48-h period in the highest amount of serum, with no sign of diminishing signal. At low concentrations of UP80 there is likely insufficient surface coverage of the colloid, which results in flocculation, protein adsorption, colloid destabilization, and eventual precipitation[194,208]. These observations are consistent with other studies where nanoparticle PEGylation and PEG surface density influence serum stability[101,155].

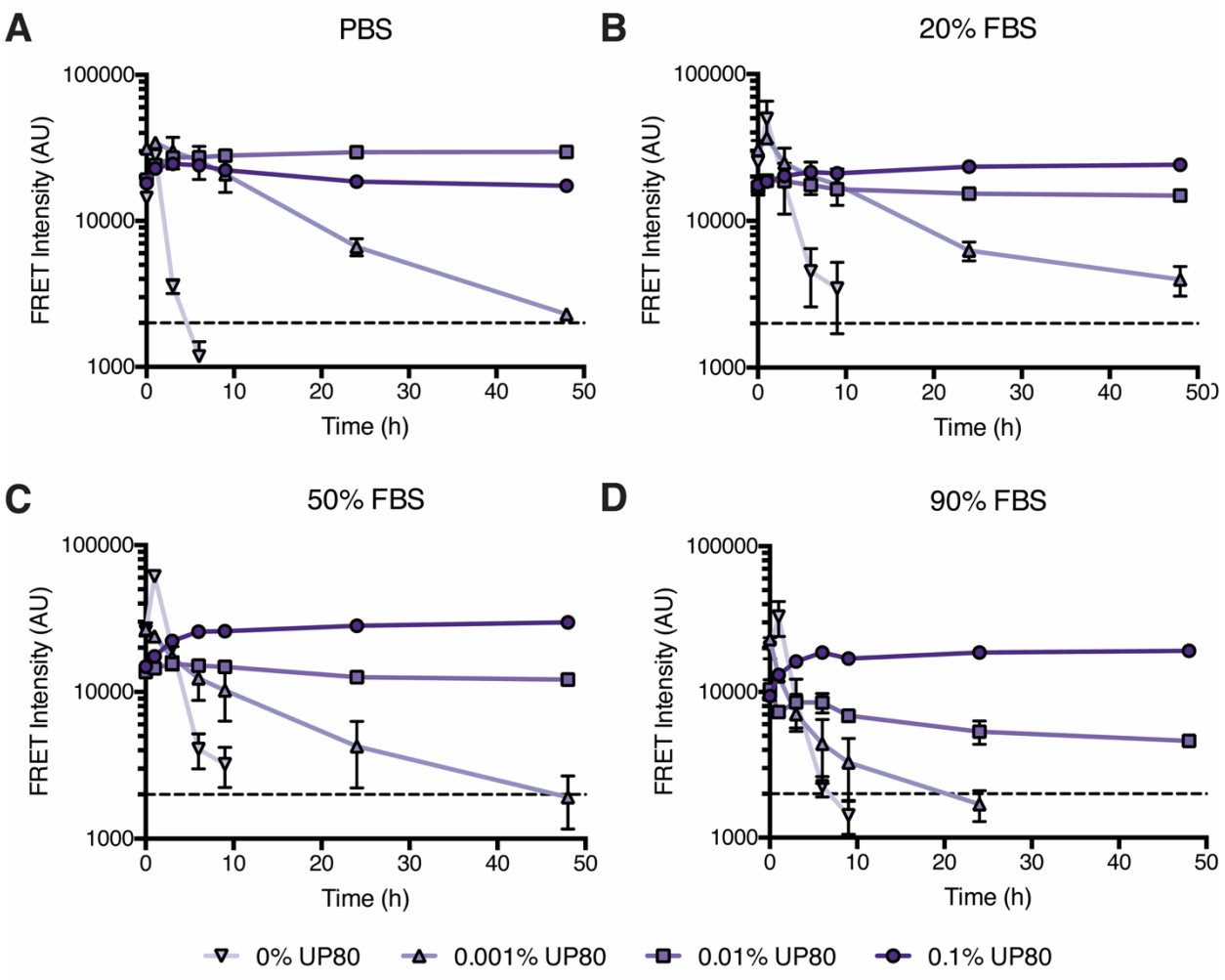

Figure 4.5. Fulvestrant colloids require excipients to remain stable in buffered solutions and serum-containing media. Fulvestrant (500 µM) colloids with the BODIPY FRET pair (10 µM) and UP80 were diluted (10-fold) into (A) PBS, (B) 20% FBS, (C) 50% FBS, or (D) 90% FBS. Stability was measured over time by monitoring FRET fluorescence. Dashed line indicates baseline fluorescence of dye-only controls. (n = 3, mean ± SD)

We hypothesized that serum-stable fulvestrant-UP80 colloids would increase the circulation of fulvestrant compared to a solubilized monomeric form of the drug, similar to other drug nanoparticles. As colloid formation can be disrupted by detergents, we used 5% UP80 to yield a fully solubilized, monomeric form of fulvestrant (Figure 4.6A). Tumor-bearing mice were intravenously administered 6 mg/kg fulvestrant (formulated at 1250 µM) as either a stable colloids(with 0.03% UP80, Figure 4.6B) or a monomeric solubilized-drug solution (with 5% UP80). Plasma drug concentrations were quantified at various time points by high performance liquid chromatography with tandem mass spectrometry (HPLC-MS/MS) to obtain a

pharmacokinetic profile of fulvestrant (Figure 4.7A and 4.7B). Based on a noncompartmental pharmacokinetic analysis, fulvestrant colloids had a plasma half-life ($t_{1/2}$) that was almost four times longer than monomeric fulvestrant (Figure 4.7C). As only a modest increase in exposure (as seen from the area under the curve, AUC) and a decrease in drug clearance (Cl) was observed, the extended half-life of the colloidal fulvestrant is mainly due to its three-fold increased volume of distribution (V_z). We hypothesize that the UP80-stabilized colloidal fulvestrant likely reduced drug binding to plasma proteins, resulting in increased distribution to other organ tissues. In contrast, in the monomeric form, plasma proteins can sequester free fulvestrant in circulation[209], resulting in a reduced volume of distribution. This is corroborated by the biodistribution data, which show higher tissue accumulation of colloidal fulvestrant (Figure 4.8).

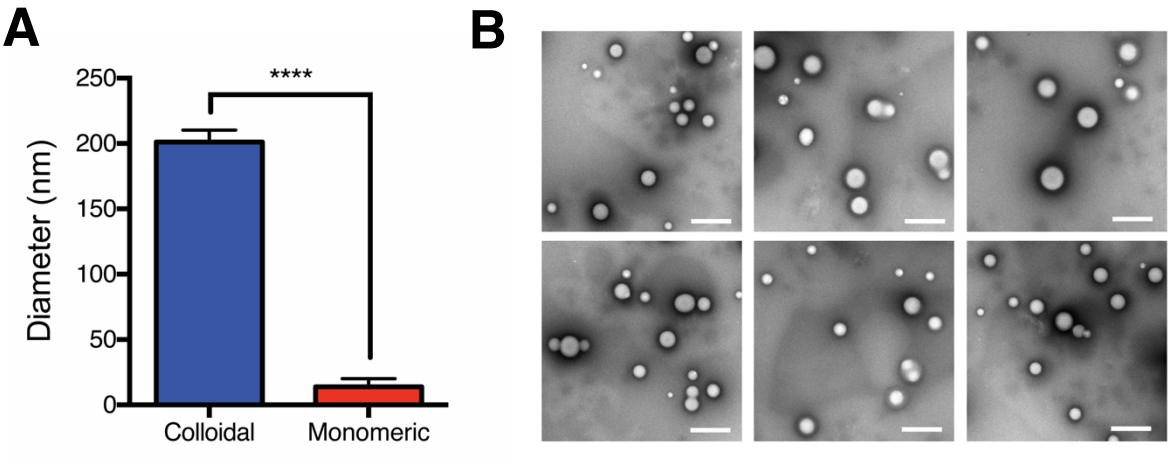

Figure 4.6. (A) Diameter of fulvestrant colloidal and monomeric formulations used for in vivo PK study. 1250 µM fulvestrant (6 mg/kg) was formulated with 0.03% UP80 (colloidal) or 5% UP80 (monomeric) and 2% DMSO in PBS. Diameter of monomeric formulation corresponds to that of UP80 micelles. **** $p < 0.0001$ (n = 3, mean ± SD). (B) Representative transmission electron micrographs of UP80-stabilized fulvestrant colloids (1250 µM fulvestrant, 0.03% UP80). Negative staining of grids with 1% ammonium molybdate. Scale bar represents 500 nm.

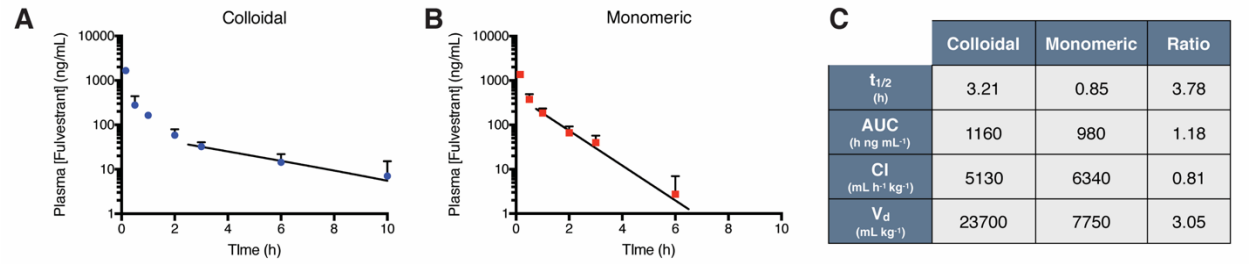

C

	Colloidal	Monomeric	Ratio
$t_{1/2}$ (h)	3.21	0.85	3.78
AUC (h ng mL^{-1})	1160	980	1.18
Cl (mL h^{-1} kg^{-1})	5130	6340	0.81
V_d (mL kg^{-1})	23700	7750	3.05

Figure 4.7. Stable colloidal aggregates improves half-life of fulvestrant after intravenous administration. Plasma concentration of fulvestrant (initial dose, ID = 6 mg/kg, formulated at 1250 µM) administered as (A) stable colloids (0.03% UP80) or (B) monomer (5% UP80). Trend line denotes exponential decay fitting of lambda elimination phase. (C) Pharmacokinetic parameters of fulvestrant show almost 4-fold increase in drug half-life with colloids compared to monomer. (n = 3-6, mean + SD)

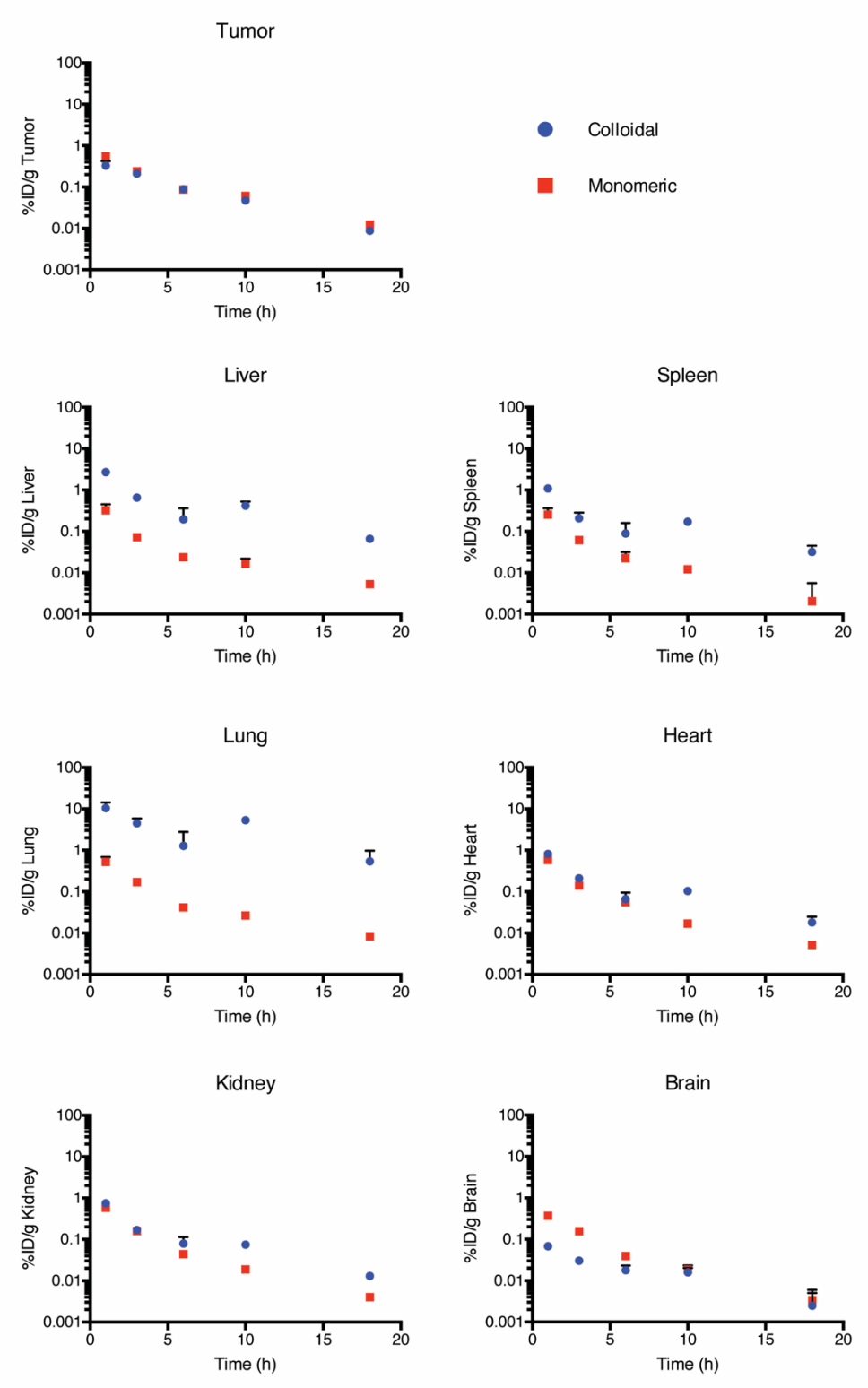

Figure 4.8. Biodistribution of fulvestrant (1250 µM, 6 mg/kg) administered as colloid (0.03% UP80) or monomeric (5% UP80) formulations. (n=3, mean + SD)

We next investigated whether the in vivo PK trends observed for stable fulvestrant colloids could be extended to another colloid-forming compound. We previously developed stabilized colloids of the investigational prodrug, PPD, using an amphiphilic polymer, PLAC-PEG[205]. Colloidal or monomeric PPD (Figure 4.9) were intravenously delivered to naive NSG mice and plasma drug concentrations were measured by HPLC-MS/MS (Figure 4.10A and 4.10B). The colloidal PPD had a 2-fold greater plasma half-life than monomeric PPD (Figure 4.10C). This corresponded to a 2-fold decrease in drug clearance and a 2-fold increase in drug exposure (AUC). PPD is a prodrug that is activated by carboxylesterases overexpressed in some human tumors[67,68,210]; however, rodent plasma also has high levels of these enzymes[211,212]. Thus, we postulate that PPD-PLAC-PEG colloids limit access of the prodrug to plasma carboxylesterase activity, preventing degradation and accounting for the lower clearance and greater circulation observed.

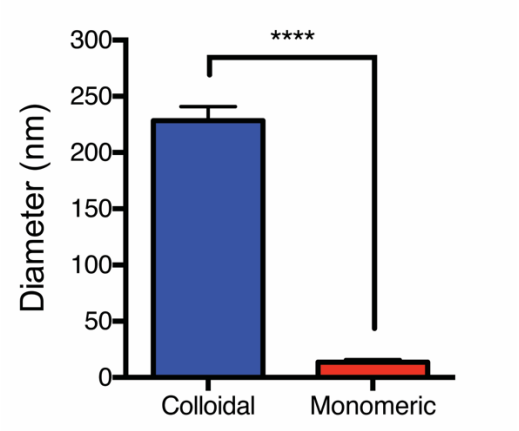

Figure 4.9. Diameter of PPD colloidal and monomeric formulations used for in vivo pharmacokinetics study. 500 µM PPD (2 mg/kg) was formulated with 0.04% PLAC-PEG (colloidal) or 5% UP80 (monomeric) and 2% DMSO in PBS. Diameter of monomeric formulation corresponds to that of UP80 micelles. **** $p < 0.0001$ (n = 3, mean ± SD)

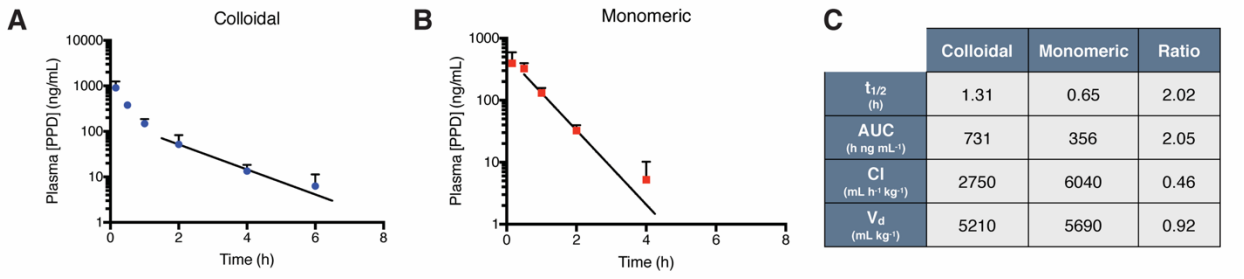

C

	Colloidal	Monomeric	Ratio
$t_{1/2}$ (h)	1.31	0.65	2.02
AUC (h ng mL^{-1})	731	356	2.05
Cl (mL h^{-1} kg^{-1})	2750	6040	0.46
V_d (mL kg^{-1})	5210	5690	0.92

Figure 4.10 Pharmacokinetic profileof the investigational prodrug, PPD, is improved by colloidal aggregates. Plasma concentration of PPD (ID = 2 mg/kg, formulated at 500 µM) administered as (A) colloids(0.04% PLAC-PEG) or (B) solubilized monomer(5% UP80). Trend line denotes exponential decay fitting of the lambda elimination phase. (C) Pharmacokinetic parameters of noncompartmental analysis show improvement in colloidal PPD half-life due to decreased clearance, resulting in increased AUC. (n = 3-6, mean + SD)

Three key observations emerge from this study. First, the critical aggregation concentration of a colloid-forming compound is serum content-dependent. Furthermore, colloidal drug aggregates may be co-formulated with excipients, improving their stability in high-serum media from a few hours to several days, likely due to reduced protein adsorption[205]. This, in turn, allows them to be injected in vivo where stable colloidal aggregate can extend the circulation half-life over their monomeric counterparts. Second, these studies were enabled by our use of hydrophobic dyes embedded within the colloids to measure colloidal stability. Whereas dynamic light scattering has found wide use in identifying, quantifying, and characterizing colloidal aggregates in buffered solutions[3,14,206], it cannot be used in high-serum media. The incorporation of fluorophores may find broad use for characterizing colloidal aggregates in many biological milieus. Finally, it is useful to note that colloidal aggregation overcomes the major limitation of poor drug loading for many current nanoparticle formulations. While many traditional nanoparticles are limited to loadings of 5-15%[213,214], colloidal drug aggregates offer the opportunity to increase loadings to 50-90%. The stabilized fulvestrant and PPD aggregates used in this study have drug loadings of 70% and 50%, respectively. Importantly, these high drug loadings are achieved without chemical modification of the drug. The PLAC-PEG polymer used in this study for stabilizing PPD has also been investigated as a micellar carrier of docetaxel, a drug that does not form colloidal aggregates[135,215]. Interestingly, while similar pharmacokinetic trends were observed for both PPD and docetaxel, a significantly higher drug loading was achieved for colloid-forming PPD. Thus, colloidal aggregation can be combined with

conventional micellar and liposomal formulations, taking advantage of decades of research that has identified many nanocarrier design principles[92,216].

Certain caveats bear airing. While the pharmacokinetic data demonstrate that colloids can extend the circulation of fulvestrant and PPD, these differences were only observed at the later time points. This leaves opportunity to improve the stability of colloidal drug aggregates such that significant changes to drug pharmacokinetics are observed at earlier time points. Our results also suggest that the extent and mechanisms by which stable drug colloids influence pharmacokinetics are dependent on the formulation itself. Drug-dependent processes such as plasma protein adsorption, metabolism and tissue distribution may contribute to these differences. The two excipients used to stabilize fulvestrant and PPD likely also contribute to the differences observed as they may elicit the formation of different protein coronas, which has been shown to influence in vivo circulation[101,217]. Further studies will be required to determine how the changes to pharmacokinetics observed herein influence drug efficacy and how stable colloidal aggregates of other drug-excipient combinations might behave in vivo.

These caveats should not obscure the principal observations from this work. While the in vitro implications of colloidal aggregates have been intensely studied[4,9,14,41], investigations on the in vivo consequences of small molecule aggregation have been rare. This study suggests that serum-stable colloidal drug aggregates do indeed influence drug fate and furthermore that they may be intentionally designed to do so. It is conceivable that such a colloidal formulation strategy may be adapted to benefit the many drugs that aggregate at relevant concentrations.

4.5 Acknowledgments

This work was supported by grants from the Canadian Cancer Society Research Institute (to MSS and BKS), the US National Institutes of General Medical Sciences (GM71630 to BKS and MSS), and the US National Cancer Institute (CA143549 to THK). ANG and JL were supported, in part, by the Natural Sciences and Engineering Research Council Postgraduate Research Scholarships. The authors wish to thank Peter Poon for assistance with animal experiments, Dr. Armand Keating (Princess Margaret Hospital) for help in establishing the mouse tumor model, Steven Doyle and Battista Calvieri (University of Toronto Microscopy Imaging Laboratory) for assistance with TEM imaging, and members of both Shoichet laboratories for thoughtful discussions.

5 Thesis Discussion

Colloidal aggregation has been well accepted as the single major contributor towards false hits in drug screening and the number of clinical used drugs that are being identified as aggregators is also increasing. A number of in vitro properties of drug colloids have been identified: their formation and presence in a number of biologically relevant media[5,39], their ability of adsorb proteins thereby inactivating bound enzymes[4], their ability to limit drug diffusion across membranes[41], and their inability to enter cells thereby rendering drugs ineffective in cytotoxicity assays[7,9]. Notwithstanding these consequences of aggregation, drug colloids offer opportunities to formulate drug-rich nanoparticles comprising unmodified active drugs, with loadings an order of magnitude higher than most conventional micellar or liposomal nanoparticles formulations. Despite this potential, drug colloids are inherently unstable resulting in crystallization and precipitation, limiting their utility.

This thesis developed strategies whereby colloidal drug aggregates can be stabilized. Utilizing colloid-forming chemotherapeutics in proof-of-concept formulations, we developed two methods to stabilize colloids in buffered and serum-containing media. First, in Chapter 2 we exploited the inherent ability of drug colloids to strongly adsorb proteins to their surface; by forming a protein corona on the surface of the colloids, we were able to provide a steric shell that stabilized drug colloids. Furthermore, we demonstrated that the corona could comprise a bioactive antibody, which led to selective internalization by target cells. Next, in Chapter 3 we investigated the use of amphiphilic polymers to stabilize drug colloids wherein the hydrophobic polymer segments would interact with the hydrophobic colloids and the hydrophilic polymer segments would extend into the aqueous phase. In addition to sterically stabilizing colloids, the hydrophilic polymer segments prevented the adsorption of proteins to the colloid surface and were required for stability in serum-containing media. Finally, in Chapter 4, we measured, for the first time, the critical aggregation concentration (CAC) of a colloid-forming compound in in vivo mimicking, high-serum media and demonstrated the need for stabilizing excipients under these conditions. We further demonstrated that serum-stable colloids could improve the circulation time of chemotherapeutics compared to solubilized monomeric formulations. We further determined that the CAC is dependent on the serum-content of the medium and this must be taken into consideration as intravenously injected formulations undergo a significant dilution and change of media composition. Herein, we discuss the impact of these findings to our understanding of

colloidal aggregation and the implications of stable colloidal drug aggregates as they relate to nanoparticle-mediated drug delivery.

5.1 Exploiting a nuisance phenomenon for drug formulations

Colloidal aggregation is a significant challenge in high-throughput drug screening[1,2]. At this early stage of drug discovery, small molecule fragment libraries comprising millions of compounds are screened to identify chemical modulators of an enzyme of interest[218]. The presence of colloidal aggregates leads to the adsorption of the enzyme and local unfolding, which results in the apparent inactivation of the enzyme[4]. While it may appear that the compound is a "hit", this is not a true chemical inhibition, but rather a physical, non-specific inhibition. Colloidal aggregation emerged as the single largest contributor to false hits at this stage of drug discovery; many compounds in these screening libraries, as many as 3% of them, will aggregate and up to 95% of "hits" can be a result of aggregation[1,2]. While aggregation is prevalent among screening library compounds, there are also a number of clinically used drugs that aggregate[7,21,201]. Herein we have demonstrated methods by which these colloidal drug aggregates might be stabilized to yield drug-rich nanoparticle formulations, thereby turning a nuisance drug screening phenomenon into a potentially useful formulation strategy.

Stable colloidal drug aggregates are able to overcome a major limitation of conventional nanoparticle formulations (i.e. micelles or liposomes); being self-assembled aggregates of drug, the final formulations have drug loadings increased by an order of magnitude (50-90% loadings vs. 5-10% loadings). Many other attempts to create high drug-loaded nanoparticle formulations have required the chemical modification of the active drug[93]. Couvreur et al. have functionalized many small molecules (e.g. doxorubicin, paclitaxel, adenosine, etc.) with the natural triterpene squalene to facilitate drug self-assembly into drug rich nano-particles[147,148,219]. Self-assembly will also occur with amphiphilic drugs; anthracyclines, such as doxorubicin and daunorubicin comprising hydrophobic anthraquinone and hydrophilic amino-sugar groups, are known to exist as oligomeric structures under certain conditions[220]. Others have also specifically conjugated hydrophobic and hydrophilic drugs together to form amphiphilic conjugates; Yan et al. have developed conjugates of the hydrophilic drugs chlorambucil and floxuridine with the hydrophobic drugs irinotecan and bendamustine, respectively[94,221].

While these conjugation strategies are able to yield high drug-loaded particles, they require modification of drugs with a second molecule of equal or greater size (500 – 1000 Da). These

modifications can have significant repercussions, such as reducing target binding affinity and potency[65,222]. Cleavable strategies to mitigate these effects but must be thoroughly tested, typically after the drug development process. An elegant extension of this work would be to search for colloidal aggregators during the drug discovery and lead optimization process. Once true hits of high throughput screening have been identified, medicinal chemistry approaches are used to generate and optimize lead candidates with better drug-like properties[223,224]. False hits during this process are even more costly than those at the HTS stage; as a result, the criteria used to generate and evaluate lead candidates must be very stringent[10]. The physicochemical properties of the compound are a significant part of these criteria as dose-limiting solubility, poor absorption and poor metabolic profiles must be avoided. A number of chemical permutations may have superior potency, but are eliminated from consideration, due to poor physicochemical properties that would typically limit formulation and delivery options[65,224-226]. Should some of these poorly soluble lead candidates be colloid-forming compounds, we have now presented viable formulation strategies such that these compounds can be further investigated rather than discarded.

5.2 Drug colloid stabilization strategies – one size does not fit all

The development of two methods to stabilize drug colloids was a central outcome of this thesis. In Chapter 2, we developed methods for controlled protein corona formation that stabilized drug colloids. In Chapter 3 we demonstrated that amphiphilic surfactants could also stabilize drug colloids by reducing protein adsorption to the colloid surface. In both cases, the stabilizer (protein or surfactant) increased steric repulsive forces between colloidal particles, preventing their flocculation and eventual precipitation[155,227].

Both of these strategies were amenable to stabilizing multiple colloid-forming compounds, however the extent of the conferred stability was dependent on both the colloid-forming compound and stabilizer investigated. We demonstrated that fulvestrant colloids could be stabilized by three proteins: bovine serum albumin (BSA), human immunoglobulin G, and the clinically used antibody, trastuzumab. While all three proteins were able to control and maintain the size of fulvestrant colloids, each did so over different protein concentration ranges; BSA was required in the least amount while the antibodies were required in higher concentrations. We also demonstrated that, in addition to stabilizing fulvestrant colloids, BSA could also stabilize colloids of sorafenib, vemurafenib and chlorotrianisene. Again, we observed that different

amounts of BSA resulted in different sized colloids for each compound. These differences likely result from differences in how the proteins interact with the colloidal surface; this is driven by the properties of both the colloidal surface and the protein itself[98]. In terms of the proteins, the tertiary and quaternary structure give proteins vastly different surface domains and dictate how a protein interacts with nanoparticle surfaces[228]. BSA for example has many hydrophobic pockets, responsible for endogenous lipid transport, but also plays a crucial role in lipophilic drug transport[169,209,229]. These hydrophobic pockets could also facilitate interactions with the hydrophobic colloidal surface[228,230]. The antibodies are post-translationally glycosylated and more hydrophilic, necessary for improved protein stability and in vivo function[170,171]. Their more hydrophilic nature could contribute to less efficient binding to the colloid surface and require more unfolding of the protein in order to interact with the colloid. Recent studies have demonstrated how the surface characteristics of nanoparticle, namely the chemical composition and zeta potential, influence antibody adsorption and how adsorption can be modulating by controlling the pH[231].

In Chapter 3, we investigated the ability of a number of surfactants to stabilize colloids of fulvestrant and PPD: UP80, PLAC-PEG, Brij 58 and L23, Pluronics F127 and 68, and vitamin E-PEG. Again, while all of these surfactants were able to stabilize fulvestrant and PPD colloids, each formulation resulted in different degrees of stability. With PPD, most surfactants stabilized colloids to similar extents, however with fulvestrant colloids, each surfactant tested resulted in varying amounts of stability, with UP80 performing the best. Again, here the properties of the colloid itself and how the surfactants interact with the drug dictate the success of stabilization.

These results suggest that there is not a one-size-fits-all strategy for stabilizing colloidal aggregates. This is consistent with other attempts to stabilize colloidal aggregates and even more generally with other nanoparticle-drug formulations. Taylor et al. have investigated the ability of polymeric excipients to stabilize colloids formed upon dissolution of amorphous solid dispersions[232]. In studying colloids of ritonavir, they were able to classify a diverse set of polymers (e.g. poly(vinylpyrrolidone), poly(acrylic acid), sodium dodecyl sulfate, polysorbate 80, hydroxypropyl methyl cellulose, cellulose acetate, etc.) into those that stabilized colloidal sizes and/or inhibited crystallization of the colloidal core, and those that did neither[19]. When comparing polysaccharide-based polymers, they observed that some polymers promoted crystallization and while others prevented it. They hypothesized that the differential localization of the polymers within the colloid core or at the surface could contribute to these differences.

McLaughlin et al. developed a method by which drug colloids could be stabilized by co-aggregation with the azo dyes Congo red and Evans blue[36]. We demonstrated that this strategy was very successful at stabilizing aggregates of sorafenib and vemurafenib. This strategy however was not successful at stabilizing drug colloids of fulvestrant, lapatinib or nilotinib, perhaps due to suboptimal packing of the azo dyes and these drugs within the colloid[233]. Furthermore, even with sorafenib colloids, Congo red and Evans blue were required at different concentrations to achieve similar levels of stability. The importance of drug-stabilizer compatibility is not a concept limited to colloidal drug aggregates. The importance of these interactions has also been observed with conventional micellar and liposomal formulations[196,197]. Many studies have investigated the modification of both the carrier and the drug to improve loading and stability. A number of studies have modified polymeric micelles with functional side groups that promote drug packing and stability[142,234-236]. Conversely, Mulder et al. and Sengupta et al. modified drugs to improve miscibility with the carrier for improved stability of polymeric micelles and lipid nanoparticles[200,237].

As more colloid-forming compounds are investigated and stabilizers of increasing chemical diversity are explored, generalizable rules that dictate stabilization mechanisms may be generated. This is an extremely challenging endeavor, as even after more than a decade of research, efforts to generate algorithms that are predictive of colloid formation itself have only been somewhat successful. Aggregate Advisor (http://advisor.bkslab.org) is one such tool that can aide in identifying compounds that potentially form colloids[183]; while the database is based on 10,000 known observations of colloidal aggregation, even this tool has false hits, both positive and negative. Recently, Shamay et al. developed a predictive algorithm to determine which drugs might stably assemble with their indocyanine dye-based nanoparticles using molecular descriptors of drugs[233]. The development, and more importantly the optimization, of such models will aid in generalizing formulation strategies to fully exploit colloidal drug aggregation.

5.3 In vitro stability of colloidal drug aggregates

An important aspect of any drug formulation is its stability under relevant conditions. A drug formulation transitions through a series of conditions during storage, administration, and circulation in vivo. Important to note, is that when evaluating colloidal stability in vitro, the criteria for stability must become more stringent with decreasing media complexity. In vivo,

most nanoparticle formulations have half-lives on hour-timescales[96]. Thus, when assaying nanoparticle formulations in vitro we must require multi-day stability in serum-containing media and stability over even longer timescales in buffered solutions if we can hope to have any stability in vivo.

In this thesis we focused on the stability of colloidal drug aggregate formulations under physiological conditions. Previous studies have demonstrated that colloids are present in serum-containing media commonly used for in vitro cell culture (10% serum)[7,39]. However, the serum concentrations in vivo are much higher; the acellular plasma component comprises 55% of the blood volume[97,238]. Thus, if the colloids are to remain stably circulating in blood, they must not interact with the cellular blood components but be stable in the plasma fraction (recapitulated by 100% serum in vitro). Very few studies have investigated the properties and stability of nanoparticle formulations under such high serum-content, mainly due to the interference of serum components with common techniques for nanoparticle analysis; background scattering of serum proteins preclude many common light scattering methodologies[206].

One key finding of this thesis is the effect of dilution and physiologically relevant concentrations of serum on the CAC of a colloid-forming compound. We demonstrated that with increasing serum-content, the CAC of fulvestrant increased. This is consistent with the notion that fulvestrant, like many hydrophobic drugs, strongly binds to serum proteins, specifically albumin[209]. With increasing serum, there is an increasing fraction of the drug that is bound to albumin and cannot participate in colloid formation. Thus, a higher amount of drug is required to reach the onset of colloid formation. These studies were only possible by the inclusion of a fluorescent probe into stably formulated fulvestrant colloid. Analytical techniques are still limited to readily the measure the onset of colloid formation directly in serum containing media.

In addition to measuring the onset of aggregation, stability measurements of particle formulations are extremely important as it is the presence of intact particles that modulates the pharmacokinetics and in vivo fate of a drug. Hammond et al. developed a size exclusion chromatography method whereby polymeric micelles could be separated from serum proteins and the remaining intact micelle population could be quantified using a spectrophotometric measurements[154]. In Chapter 3, we were able to use this method to probe the stability of fulvestrant-UP80 and PPD-PLAC-PEG colloids in 20% serum where due to their size, intact colloids eluted prior to serum proteins. The inherent absorbance of PPD permitted a probe-free

method of measuring intact colloids. However, the incorporation of a fluorescent FRET pair was required for assaying of fulvestrant colloids. In Chapter 4, we investigated the stability of fulvestrant colloids higher serum-content media more closely mimicking the in vivo environment (50% and 90% serum). Such high concentrations of serum proteins would overload many standard separation columns, preventing the use of size exclusion chromatography methods. However, the use of a FRET pair can still allow for measurement of intact colloidal particles without separation from serum proteins. Such strategies have already been employed for the study of micelles[30], and can be extended to investigate properties of many other colloid-forming compounds in complex media.

Another important aspect controlling colloidal drug aggregate stability is dilution of the formulation. Typically, when formulations are administered as a bolus intravenous injection, up to 10% of the blood volume can be injected[239]; this leads to at least a 10-fold dilution. As the presence of colloids is dictated by the CAC, the final concentration must be above the CAC of the compound in that specific medium if the presence of colloids is desired. In Chapter 4, we measured the CAC of fulvestrant colloids after dilution into various media showing that the concentration required for aggregation positively correlated with the serum concentration. We further investigated the stability of UP80-stabilized fulvestrant colloids upon dilution into serum-containing media validating that UP80 was required to generate colloids that were stable for multiple days in vitro. Such dilution experiments are critical for concentration-dependent self-assembled nanoparticles such as drug colloids and micelles, in contrast to solid nanoparticles (e.g. gold and silica nanoparticles). This is especially important when considering clinical translation of these types of formulations due to the high blood volume of humans and the dose required to maintain concentrations above the CAC. This is further complicated by the fact that infusions are typically used to deliver drugs intravenously. Nano-formulations in the clinic, such as Doxil, Vyxeos and Abraxane, are all administered by intravenous infusion; in fact, Abraxane has been shown to rapidly dissociated into soluble albumin-paclitaxel complexes such that there are no nanoparticles remaining in solution during administration[240]. Further studies are required to assess the feasibility of translating the colloidal drug aggregate formulations developed herein.

5.4 In vivo fate of drug colloids

The goal of nanoparticle formulations is to improve the in vivo fate of their drug payload. The body presents a number of physiological barriers towards foreign compounds; should these

barriers be overcome, there is opportunity to improve the efficacy of therapeutic agents[96]. The absorption, distribution, metabolism and excretion (ADME) of an active small molecule drug ultimately dictates its efficacy; sufficient concentrations of drug must reach the target tissue to elicit an effect without excess drug reaching off-target tissues resulting in toxicities[241]. Nanoparticle formulations can significantly alter these four processes, and with appropriate engineering, can be used to modulate drug pharmacokinetics and biodistribution as desired[242,243]. In general, most nanoparticle formulations aim to extend the circulation half-life of the cargo drug and thus the exposure (as measured by the area under the curve). The literature is filled with examples of preclinical nanoparticles formulations that have improved the pharmacokinetics of drugs of interest[135,148,244]; while translation of nanomedicines is limited[87,245], improvements to pharmacokinetic profiles of chemotherapeutics have been observed in a clinical setting as well[246-248].

In Chapter 4, we investigated the in vivo fate of fulvestrant-UP80 and PPD-PLAC-PEG stable colloidal drug aggregates. Herein, we used liquid chromatography with tandem mass spectrometry (LC-MS/MS) to quantify the drug concentration in plasma and tissue samples. LC-MS/MS provides a probe-free method for quantifying amounts of a specific analyte by measuring the molecular mass of both the parent drug ion and a daughter fragment ion[249]; these counts are compared to an internal standard that is spiked into all samples. The high specificity offered by LC-MS/MS methods, through measurements of unique parent and daughter ion pairs, requires the development of validated methods for each analyte of interest; this can limit its applications in monitoring drug metabolites as the exact metabolite must be known and isolated for preparation of a standard curve. However, this strategy can be useful to quantify amounts of specific compounds and their metabolites. While radiolabeling methods require external probes, that can ultimately convolute the fate of the compounds themselves[250], these methods can be used investigate clearance routes and approximate mass balances, as all metabolites will retain their radioactivity. Ultimately a combination of these two methods can provide a complete picture of the in vivo ADME of a drug.

For both fulvestrant and PPD, plasma circulation times of the drugs were enhanced by formulation as stable colloidal aggregates. In both cases, differences between colloidal and monomeric formulations were observed at late time points. While these observations demonstrate potential benefits of colloidal formulations, they also suggest that there remains opportunity to improve these formulations. Formulations that modulate the pharmacokinetics at

early time points would be of interest and could lead to improved tumor accumulation, which was not observed in these studies. Interestingly, the mechanisms contributing to the observed enhanced circulation appear to be different for both formulations. Due to its lipophilicity, fulvestrant is typically highly protein bound; however, formulation as stable drug colloids appears to have reduced protein binding leading to increased distribution to organ tissues. Similarly, PPD formulated as stable drug colloids has reduced interaction with endogenous plasma carboxylesterases, which would convert the prodrug into an active metabolite[210]; this leads to decreased clearance and enhanced circulation.

For many formulations, improved circulation corresponds to increased accumulation at the target site potentially leading to increased efficacy[251]. Important to note is that for non-targeted therapeutics (e.g. taxanes), extended plasma circulation can result in increased toxicity to blood cells (e.g. neutropenia and thrombocytopenia)[252,253]; thus, the off-target toxicities of a drug must be considered when tuning formulations for the desired pharmacokinetic profiles. Further investigation is required to determine if the observed improvements to drug pharmacokinetics when formulated as stable colloids leads to increased efficacy. Most clinically used nanoparticles have been approved on the basis of improved tolerability, rather than improved efficacy[83,240]; even in this regard, stable colloidal drug aggregates can be formulated with much less excipient than solubilized drug solutions (0.03% UP80 vs. 5% UP80 for fulvestrant formulations) reducing excipient-associated toxicities. Thus, colloidal drug aggregates still present an advantage to conventional solubilized formulations.

The initial excitement of nanoparticle drug delivery surrounded the potential of nanoparticles to accumulate in the tumor via the enhanced permeability and retention effect due to the leaky tumor vasculature and poor lymphatic drainage[119,121]. This concept has been highly debated in recent years. While the EPR effect has been demonstrated in human tumors, its inter- and intra-tumor heterogeneity and the inadequate recapitulation of human disease in mouse models have hindered translation of this concept to the clinic[118,121,133,134]. We did aim to investigate the potential tumor accumulation of our stable fulvestrant colloids in an orthotopic xenograft model of breast cancer. Tumor xenografts of an estrogen-dependent breast cancer cell line (MCF-7), relevant for fulvestrant, were established in NOD scid gamma (NSG) mice. In our study, we did not observe increased fulvestrant concentrations in tumors when delivered as colloidal formulations. A number of factors could have contributed to this; we did not verify that the tumor model used was sufficiently vascularized to observe enhanced accumulation. Furthermore,

tumors were established using Matrigel to facilitate cell engraftment, however Matrigel has been shown to reduce retention of nanoparticles in some xenograft tumor models[254]. Notwithstanding these caveats, the biodistribution profile observed is consistent with the pharmacokinetic profile and with the circulation of intact particles. Fulvestrant concentrations in the liver and spleen were higher for colloidal formulation compared to monomeric formulation; these organs of the mononuclear phagocyte system are known to clear particulate formulations[96,255]. Increased drug concentrations in these organs suggest that perhaps stable colloidal particles were being cleared and that optimization of the formulation would be of interest in the future. Tissue-resident macrophages are typically responsible for clearance of nanoparticles. In the liver, macrophages in the liver sinusoid (e.g. Kupffer cells) are mainly responsible for this process and it has been shown that depletion of these cells can improve the pharmacokinetics of nanoparticles and tumor accumulation [109,255]. Furthermore, the lung presents the first (and some of the smallest) capillary bed which intravenously administered nanoparticles encounter, serving as a mechanism of first-pass clearance[96]. While typically particles smaller than 3 μm are not significantly retained in the lungs, fulvestrant colloids appear to accumulate in the lungs, perhaps due to changes in interactions with plasma proteins and could provide a mechanism of lung targeting, warranting further investigation[256]. Taking inspiration from the nanoparticle literature, which has demonstrated the benefits of increasing amounts of PEG or the use of zwitterionic polymers to promote long circulation properties, would be an elegant extension of this work to further modulate the in vivo properties of drug colloids[101,257].

6 Conclusions

Over the course of this thesis, two methods to stabilize colloidal drug aggregates were developed and the in vivo fate of stable colloidal aggregate formulations was investigated. Firstly, we exploited the protein adsorption properties of colloidal aggregates to form a controlled corona which stabilized drug colloids. Furthermore, we demonstrated that coronas comprising targeted antibodies could elicit specific internalization by target cells. Secondly, we showed that co-aggregation with polymeric surfactants also stabilized drug colloids; surfactants significantly reduced adsorption of proteins to the colloids, specifically those most prominent in blood. Both stabilization methods yielded aggregates with multi-day stability in buffered solution and serum-containing media. We demonstrated that the CAC of a colloid-forming compound was significantly influenced by the protein content of its environment. With stable formulations in hand, we investigated the in vivo fate of drug colloids; colloids stable under in vivo-mimicking conditions were able to extend the plasma circulation half-life compared to solubilized monomeric formulations. These findings demonstrate the potential utility of stabilized colloidal aggregates as drug delivery formulations, warranting further studies on how to turn this drug screening nuisance into a formulation strategy.

6.1 Achievement of Objectives

The hypothesis driving this work was:

Controlled formulation of colloidal drug aggregates with proteins and polymers will improve their in vitro serum stability and in vivo pharmacokinetics.

Achievement of the objectives originally outlined in Chapter 1 are summarized below:

1. To design stable antibody-modified drug colloids for targeted in vitro delivery

    - Protein adsorption was able to stabilize fulvestrant colloidal aggregates in a concentration-dependent manner.

    - Fulvestrant colloids were stabilized with multiple proteins (albumin, immunoglobulin G and trastuzumab) and albumin was able to stabilize multiple drug colloids.

    - Protein corona formation stabilized fulvestrant colloids in 20% serum over 48 hours.

- Protein coronas comprising a targeted antibody, trastuzumab, elicited specific uptake by HER2-overexpressing cells leading to significant decrease to cell viability.

These data were presented in Chapter 2 and published in *ACS Applied Materials and Interfaces* [204].

2. To enhance the stability of colloidal drug aggregates with polymeric excipients

    - Fulvestrant and PPD colloidal aggregates were stabilized by multiple polymeric surfactants achieving multi-day stability in buffered solutions.

    - Formulations of fulvestrant-UP80 and PPD-PLAC-PEG were stable in up to 20% serum over 48 hours.

    - The presence of surfactants significantly reduced adsorption of the main blood proteins, namely albumin, immunoglobulin G and fibrinogen.

    - Formulation as colloid drug aggregates significantly changed the internalization pathway of fulvestrant and PPD by cells in vitro in a serum-dependent manner.

These data were presented in Chapter 3 and published in *Molecular Pharmaceutics* [205].

3. To investigate the in vivo utility of stable colloidal drug formulations

    - The CAC of fulvestrant after dilution into media was positively-correlated with the serum-content.

    - UP80 was able to stabilize fulvestrant colloids after dilution into media mimicking the in vivo environment (90% serum).

    - Stable fulvestrant-UP80 colloids increased plasma circulation half-life of fulvestrant by increasing distribution to organ tissues compared to monomeric formulation.

    - Stable PPD-PLAC-PEG colloids resulted in increased in vivo plasma circulation half-life by decreasing clearance of PPD compared to monomeric formulation.

These data were presented in Chapter 4.

6.2 Recommendations for Future Work

6.2.1 Drug release from stable colloidal drug aggregates

In Chapters 2 and 3 we developed stable colloidal drug aggregate formulations. However, for any formulation to be efficacious, the drug payload must be released at the target site. In regard to colloidal drug aggregates, this means that stable drug colloids must disassemble releasing monomeric drug, which can then freely diffuse through biological membranes and bind to its intracellular target receptor. Such release strategies should exploit local environmental stimuli such that drug release only occurs at the target site. In the context of nanoparticle drug delivery formulations, a number of stimuli have been investigated to trigger release at the target site, including pH, redox potential, temperature, and ultrasound, among others[216,258].

Exploiting changes to local pH has been extensively investigated for cancer nanomedicines. Many of these strategies take advantage of the decreased pH of the tumor microenvironment or the endo-lysosomal compartment[127,259]. One method to exploit this change in pH is to incorporate ionizable groups into the carrier; Bae et al. designed a poly(histidine)-PEG polymer that self-assembled into micelles at neutral pH due to the hydrophobicity of the uncharged histidine side groups[260]. These residues, having a pKa of ~6, will ionize under acidic conditions rendering the polymer more hydrophilic resulting in micelle disruption and drug release[261]. Ionizable groups can also be used to disrupt the endosomal membrane itself resulting in the release of endosomal contents into the cytosol; this has been particularly useful for the delivery of membrane-impermeable therapeutics, such as oligonucleotides[262-264]. Change to pH can also be used to trigger degradation of the carrier itself through incorporation of acid-labile bonds[265].

Redox-sensitive nanocarriers often take advantage of the increased glutathione concentrations of the intra-tumor environment and within cancer cells. Similar to pH-sensitive carriers, the increased redox potential can be used to trigger drug release form the carrier, carrier disassembly or carrier degradation. Temperature-sensitive strategies have mostly been explored with liposomal formulations, through the use of thermo-sensitive components that result in pore formation in the bilayer, facilitating drug release[266]. While early clinical trials of such formulations (e.g. ThermoDox®) failed, opportunity and interest in using temperature as a stimulus is re-emerging as advances in localized hyperthermia technologies are being made[266,267].

In the context of colloidal drug aggregation, a number of these strategies might be employed to trigger drug release at the target site, warranting further investigation. Taylor et al. have demonstrated that the onset of aggregation is dependent on the pH for weakly basic drugs (e.g. clotrimazole and nicardipine)[21]. They observed an increase in the CAC of these compounds with decreasing pH. Strategies employing redox and temperature stimuli need to be further investigated and likely will be drug-dependent.

6.2.2 In vivo tracking of colloidal drug aggregates

In Chapter 4, we investigated the in vivo fate of fulvestrant and PPD when delivered as colloidal or monomeric formulations. Using LC-MS/MS we were able to quantify the plasma and tissue concentrations of these drugs. This allowed for determination of pharmacokinetic parameters of fulvestrant and PPD using a non-compartmental analysis. However, the LC-MS/MS method used was limited in that it was unable to distinguish between drug remaining as intact colloids versus released free or protein-bound drug. While formulations of fulvestrant and PPD as colloid drug aggregates changed their pharmacokinetics, we were unable to determine the pharmacokinetic parameters for the intact colloid itself. In vivo tracking of intact colloidal aggregates would provide significant insight into their biological fate, as well as allow for optimization of formulation parameters to achieve the desired pharmacokinetic profile.

We were able to incorporate hydrophobically-modified dyes as a FRET pair into colloidal formulations of fulvestrant to investigate their in vitro serum-stability. A similar strategy can be employed to investigate the in vivo stability, circulation and distribution of intact colloids[268]. Intravital imaging would allow real-time visualization of fluorescently-labeled nanoparticles in circulation and allow investigation of the in vivo drug release kinetics[257,269-271]; this allows for quantification of the distribution phase of the pharmacokinetic profile for intact colloids. Intravital imaging modalities can also be used to investigate mechanisms of extravasation of nanoparticles from circulation into tumor and organ tissues[268,272,273]. Such methods would provide insight into how different formulation parameters modulate the interactions with the diseased pathophysiology; in cancer, these methods can be used to evaluate tumor-dependent heterogeneity, vascular permeability, and drug formulation penetration[117,274,275].

6.2.3 Co-aggregates for combination drug delivery

As the biological drivers of cancer and mechanisms of drug resistance are further elucidated, and the genetic profiling of tumors and patients becoming mainstream, novel combinations of

orthogonal therapies have emerged[276-279]. Nanoparticles offer a modality for delivery of synergistic combinations of therapies[280]; nanoparticles also allow for ratiometric drug loading allowing for synergistic doses of these multiple drugs[281]. One recent success, Vyxeos (Jazz Pharmaceuticals), is a synergistic combination of cytarabine and daunorubicin co-encapsulated in a liposome for the treatment of acute myeloid leukemia[137].

Colloidal aggregates have the potential to be adapted for combination drug delivery. In Chapter 2 we demonstrated how therapeutic antibodies, like trastuzumab, could be used to stabilize colloids of fulvestrant. This approach could be extended to other therapeutically relevant antibody-drug and protein-drug combinations. Additionally, when multiple colloid-forming compounds are present in solution, they may co-aggregate to form mixed aggregates of both compounds[32,36]. Here the amount of each compound could be varied to achieve a desired ratio, one that may be synergistic for disease treatment. With the formulation strategies developed herein, stable aggregates of multiple compound could be generated and used for treatment of diseases. Such combination therapies would be of interest outside of oncology as well.

6.2.4 Application of colloidal aggregates for other diseases

While there have been many limitations in the clinical translation of nanomedicines targeting solid tumors[240], there continues to be active preclinical and clinical stage development of formulations to improve therapeutic outcomes[83,84]. The application of nanoparticle drug formulations for other diseases and treatment strategies have also emerged as promising avenues for clinical translation.

Due to the propensity of nanoparticles to accumulate in the liver, there have been successes in utilizing nanoparticles to deliver therapeutics for hepatic diseases[282]. The recently-approved siRNA therapeutic, patisiran (Alnylam Pharmaceutics Inc.), utilizes liver-targeted lipid nanoparticles for the treatment of hereditary transthyretin amyloidosis[283]. There has also been growing interest in the application of nanomedicine for the treatment of cardiovascular diseases[284,285], inflammatory diseases[286,287], ischemia[147], viral infections[288], and recent immunotherapy efforts[289]. In some diseases where the pathophysiology is mediated by monocytes and macrophages, the innate uptake of nanoparticles by these cells can facilitate therapeutic delivery. For example, in HIV infections, infected macrophages can act as carriers of the virus to other tissues including the central nervous system; nanoparticle-mediated antiretroviral delivery to macrophages has been investigated as potential therapeutic strategy[290].

In this regard, the diversity of compounds that form colloidal aggregates easily lends itself to exploring the application of stable colloidal aggregates for the treatment of various diseases. Clinically used non-oncology drugs that form colloidal aggregates include anti-fungals (e.g. clotrimazole and itraconazole), ion-channel inhibitors (e.g. nicardipine and glyburide), and anti-retroviral compounds (e.g. ritonavir and etravirine). As the list of known drugs that form colloidal aggregates continues to grow, applications of stabilized colloidal formulations can be investigated for the treatment of a variety of diseases.

Appendix A: Abbreviations

ADC	antibody-drug conjugate
ADME	absorption distribution metabolism excretion
AUC	area under the curve
BODIPY	boron-dipyrromethene
BSA	bovine serum albumin
CAC	critical aggregation concentration
CES2	carboxylesterase 2
Cl	drug clearance
CMC	critical micelle concentration
DLS	dynamic light scattering
DMSO	dimethylsulfoxide
EPR	enhanced permeability and retention
FBS	fetal bovine serum
FPLC	fast protein liquid chromatography
FRET	Forster Resonance energy transfer
HER2	human epidermal growth factor receptor 2
HPLC-MS/MS	high performance liquid chromatography with tandem mass spectrometry
HTS	high-throughput screen
IgG	immunoglobulin G

IV	intravenous
NNRTI	non-nucleoside reverse transcriptase inhibitors
NSG	NOD scid gamma (non-obese diabetic, severe combined immunodeficient, *Il2rg*^{null})
PBS	phosphate buffered saline
PEG	poly(ethylene glycol)
PK	pharmacokinetics
PLAC-PEG	poly(D,L-lactide-*co*-2-methyl-2-carboxytrimethylene carbonate)-g-poly(ethylene glycol)
PPD	pentyloxycarbonyl-(*p*-aminobenzyl)doxazolidinylcarbamate
SDS-PAGE	sodium dodecyl sulfate polyacrylamide gel electrophoresis
SIF	simulated intestinal fluid
TEM	transmission electron microscopy
THF	tetrahydrofuran
TOF-SIMS	time-of-flight secondary ion mass spectrometry
UP80	ultra pure polysorbate 80
V_z	volume of distribution
XPS	x-ray photoelectron spectroscopy

Appendix B: Non-compartmental pharmacokinetic analysis

Pharmacokinetic models aim to describe the temporal and spatial distribution of a drug in the body. While spatiotemporal models are ideal, they are very complex and thus compartmental models are used to reduce the order of these models and use temporal changes to model spatial heterogeneity. Non-compartmental analysis (NCA) does not require the assumption of specific compartments and is typically used when the extent of drug exposure and pharmacokinetic parameters are of interest. NCA allows for the determination of these parameters through the generation of algebraic expressions, as opposed to compartmental models which require solutions to linear and non-linear differential equations.

The degree of drug exposure is measured by the area under the curve (AUC) of the plasma concentration vs. time plot:

$$AUC = \int_0^{T_{last}} C(t)dt$$

This measurement is usually performed computationally using the trapezoid rule.

The lambda phase elimination constant (λ_z) is determined through a linear regression of the last n points of the log(concentration) vs. time plot that satisfy the conditions: $t \geq T_{max}$ and $C \leq C_{max}$, and generates the highest R^2.

With the AUC and λ_z, other pharmacokinetic parameters can be calculated algebraically. The elimination half-life of the compound ($t_{1/2}$) is calculated as follows:

$$t_{1/2} = \frac{\ln(2)}{\lambda_z}$$

Clearance (Cl) of the drug is calculated using the initial dose administered (D):

$$Cl = \frac{D}{AUC}$$

Volume of distribution (V_z) can be calculated from:

$$V_d = \frac{D}{AUC * \lambda_z}$$

Appendix C: Colloid interactions with blood cells

This thesis investigated the influence of colloidal aggregate formulations on the plasma circulation of fulvestrant and PPD. In these studies, blood was collected from mice after intravenous administration of drug colloids and subsequently centrifuged to separate the plasma and cellular fractions. While many hydrophobic drugs, like fulvestrant, are highly plasma protein bound, this does not preclude colloidal aggregates from interacting with blood cells. Incubation of colloids with blood ex vivo was used to assess the extent of drug partitioning within the blood fractions.

We isolated blood from C47Bl6/J mice and spiked with a fulvestrant colloids (500 µM, 0.01% UP80 in PBS). After incubation for 15 min or 1 h, samples were centrifuged to isolate plasma and cellular fractions; an aliquot of whole blood was isolated prior to centrifugation. Fulvestrant concentration in these samples were quantified by LC-MS/MS.

A small amount of fulvestrant was present in the cellular fraction, however the amount of fulvestrant in whole blood or plasma was not significantly different. These results indicate that sampling of plasma for in vivo studies presented in Chapter 4 should account for the majority of fulvestrant in circulation. Many nanoparticle formulations use PEGylated polymers, such as UP80 and PLAC-PEG used in this thesis, to prevent non-specific interactions and uptake by off-target cells, including those in the blood[96,97].

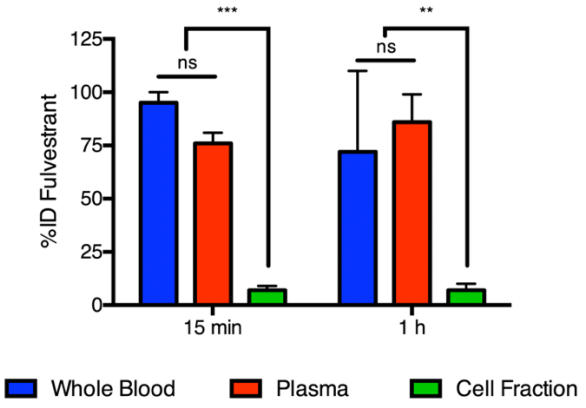

Figure B.1 Majority of fulvestrant remains in the plasma fraction of whole blood. Quantification of fulvestrant by LC-MS/MS after centrifugation of blood for 5 min at 2000x *g*. ** p<0.01, *** p<0.001 by two-way ANOVA. (n=3 biological replicates, mean + SD)

References

(1) Shoichet, B. K. Screening in a Spirit Haunted World. *Drug Discov. Today* **2006**, *11* (13-14), 607–615.

(2) Aldrich, C.; Bertozzi, C.; Georg, G. I.; Kiessling, L.; Lindsley, C.; Liotta, D.; Merz, K. M. J.; Schepartz, A.; Wang, S. The Ecstasy and Agony of Assay Interference Compounds. *J. Med. Chem.* **2017**, *60* (6), 2165–2168.

(3) McGovern, S. L.; Caselli, E.; Grigorieff, N.; Shoichet, B. K. A Common Mechanism Underlying Promiscuous Inhibitors From Virtual and High-Throughput Screening. *J. Med. Chem.* **2002**, *45* (8), 1712–1722.

(4) McGovern, S. L.; Helfand, B. T.; Feng, B.; Shoichet, B. K. A Specific Mechanism of Nonspecific Inhibition. *J. Med. Chem.* **2003**, *46* (20), 4265–4272.

(5) Coan, K. E.; Shoichet, B. K. Stoichiometry and Physical Chemistry of Promiscuous Aggregate-Based Inhibitors. *J. Am. Chem. Soc.* **2008**, *130* (29), 9606–9612.

(6) McGovern, S. L.; Shoichet, B. Kinase Inhibitors: Not Just for Kinases Anymore. *J. Med. Chem.* **2003**, *46*, 1478–1483.

(7) Owen, S. C.; Doak, A. K.; Wassam, P.; Shoichet, M. S.; Shoichet, B. K. Colloidal Aggregation Affects the Efficacy of Anticancer Drugs in Cell Culture. *ACS Chem. Biol.* **2012**, *7* (8), 1429–1435.

(8) Seidler, J.; McGovern, S. L.; Doman, T. N.; Shoichet, B. K. Indentification and Prediction of Promiscuous Aggregating Inhibitors Among Known Drugs. *J. Med. Chem.* **2003**, *46*, 4477–4486.

(9) Owen, S. C.; Doak, A. K.; Ganesh, A. N.; Nedyalkova, L.; McLaughlin, C. K.; Shoichet, B. K.; Shoichet, M. S. Colloidal Drug Formulations Can Explain "Bell-Shaped" Concentration-Response Curves. *ACS Chem. Biol.* **2014**, *9* (3), 777–784.

(10) Bleicher, K. H.; Bohm, H. J.; Muller, K.; Alanine, A. I. Hit and Lead Generation: Beyond High-Throughput Screening. *Nat. Rev. Drug Discov.* **2003**, *2* (5), 369–378.

(11) Feng, B. Y.; Simeonov, A.; Jadhav, A.; Babaoglu, K.; Inglese, J.; Shoichet, B. K.; Austin, C. P. A High-Throughput Screen for Aggregation-Based Inhibition in a Large Compound Library. *J. Med. Chem.* **2007**, *50* (10), 2385–2390.

(12) Shoichet, B. K. Interpreting Steep Dose-Response Curves in Early Inhibitor Discovery. *J. Med. Chem.* **2006**, *49* (25), 7274–7277.

(13) Coan, K. E.; Maltby, D. A.; Burlingame, A. L.; Shoichet, B. K. Promiscuous Aggregate-Based Inhibitors Promote Enzyme Unfolding. *J. Med. Chem.* **2009**, *52* (7), 2067–2075.

(14) Ilevbare, G. A.; Taylor, L. S. Liquid-Liquid Phase Separation in Highly Supersaturated Aqueous Solutions of Poorly Water-Soluble Drugs: Implications for Solubility Enhancing Formulations. *Cryst. Growth Des.* **2013**, *13* (4), 1497–1509.

(15) Mosquera-Giraldo, L. I.; Taylor, L. S. Glass-Liquid Phase Separation in Highly Supersaturated Aqueous Solutions of Telaprevir. *Mol. Pharm.* **2015**, *12* (2), 496–503.

(16) Zhao, C. L.; Winnik, M. A.; Riess, G.; Croucher, M. D. Fluorescence Probe Techniques Used to Study Micelle Formation in Water-Soluble Block Copolymers. *Langmuir* **1990**, *6* (2), 514–516.

(17) Wilhelm, M.; Zhao, C. L.; Wang, Y. C.; Xu, R. L.; Winnik, M. A.; Mura, J. L.; Riess, G.; Croucher, M. D. Polymer Micelle Formation .3. Poly(Styrene-Ethylene Oxide) Block Copolymer Micelle Formation in Water - a Fluorescence Probe Study. *Macromolecules* **1991**, *24* (5), 1033–1040.

(18) Goddard, E. D.; Turro, N. J.; Kuo, P. L.; Ananthapadmanabhan, K. P. Fluorescence Probes for Critical Micelle Concentration Determination. *Langmuir* **1985**, *1* (3), 352–355.
(19) Ilevbare, G. A.; Liu, H.; Pereira, J.; Edgar, K. J.; Taylor, L. S. Influence of Additives on the Properties of Nanodroplets Formed in Highly Supersaturated Aqueous Solutions of Ritonavir. *Mol. Pharm.* **2013**, *10* (9), 3392–3403.
(20) Purohit, H. S.; Taylor, L. S. Phase Separation Kinetics in Amorphous Solid Dispersions Upon Exposure to Water. *Mol. Pharm.* **2015**, *12* (5), 1623–1635.
(21) Indulkar, A. S.; Box, K. J.; Taylor, R.; Ruiz, R.; Taylor, L. S. pH-Dependent Liquid-Liquid Phase Separation of Highly Supersaturated Solutions of Weakly Basic Drugs. *Mol. Pharm.* **2015**, *12* (7), 2365–2377.
(22) Almeida e Sousa, L.; Reutzel-Edens, S. M.; Stephenson, G. A.; Taylor, L. S. Assessment of the Amorphous "Solubility" of a Group of Diverse Drugs Using New Experimental and Theoretical Approaches. *Mol. Pharm.* **2015**, *12* (2), 484–495.
(23) Duan, D.; Torosyan, H.; Elnatan, D.; McLaughlin, C. K.; Logie, J.; Shoichet, M. S.; Agard, D. A.; Shoichet, B. K. Internal Structure and Preferential Protein Binding of Colloidal Aggregates. *ACS Chem. Biol.* **2017**, *12* (1), 282–290.
(24) Brick, M. C.; Palmer, H. J.; Whitesides, T. H. Formation of Colloidal Dispersions of Organic Materials in Aqueous Media by Solvent Shifting. *Langmuir* **2003**, *19* (16), 6367–6380.
(25) Harmon, P.; Galipeau, K.; Xu, W.; Brown, C.; Wuelfing, W. P. Mechanism of Dissolution-Induced Nanoparticle Formation From a Copovidone-Based Amorphous Solid Dispersion. *Mol. Pharm.* **2016**, *13* (5), 1467–1481.
(26) Indulkar, A. S.; Gao, Y.; Raina, S. A.; Zhang, G. G.; Taylor, L. S. Exploiting the Phenomenon of Liquid-Liquid Phase Separation for Enhanced and Sustained Membrane Transport of a Poorly Water-Soluble Drug. *Mol. Pharm.* **2016**, *13* (6), 2059–2069.
(27) Indulkar, A. S.; Waters, J. E.; Mo, H.; Gao, Y.; Raina, S. A.; Zhang, G. G. Z.; Taylor, L. S. Origin of Nanodroplet Formation Upon Dissolution of an Amorphous Solid Dispersion: a Mechanistic Isotope Scrambling Study. *J. Pharm. Sci.* **2017**, *106* (8), 1998–2008.
(28) Murdande, S. B.; Pikal, M. J.; Shanker, R. M.; Bogner, R. H. Solubility Advantage of Amorphous Pharmaceuticals: I. a Thermodynamic Analysis. *J. Pharm. Sci.* **2010**, *99* (3), 1254–1264.
(29) Emerson, M. F.; Holtzer, A. On the Ionic Strength Dependence of Micelle Number. II. *J. Phys. Chem.* **1967**, *71* (6), 1898–1907.
(30) Owen, S. C.; Chan, D. P. Y.; Shoichet, M. S. Polymeric Micelle Stability. *Nano Today* **2012**, *7* (1), 53–65.
(31) Raina, S. A.; Zhang, G. G.; Alonzo, D. E.; Wu, J.; Zhu, D.; Catron, N. D.; Gao, Y.; Taylor, L. S. Impact of Solubilizing Additives on Supersaturation and Membrane Transport of Drugs. *Pharm. Res.* **2015**, *32* (10), 3350–3364.
(32) Feng, B. Y.; Shoichet, B. K. Synergy and Antagonism of Promiscuous Inhibition in Multiple-Compound Mixtures. *J. Med. Chem.* **2006**, *49* (7), 2151–2154.
(33) Frenkel, Y. V.; Clark, A. D. J.; Das, K.; Wang, Y. H.; Lewi, P. J.; Janssen, P. A.; Arnold, E. Concentration and pH Dependent Aggregation of Hydrophobic Drug Molecules and Relevance to Oral Bioavailability. *J. Med. Chem.* **2005**, *48* (6), 1974–1983.
(34) Trasi, N. S.; Taylor, L. S. Thermodynamics of Highly Supersaturated Aqueous Solutions of Poorly Water-Soluble Drugs-Impact of a Second Drug on the Solution

Phase Behavior and Implications for Combination Products. *J. Pharm. Sci.* **2015**, *104* (8), 2583–2593.

(35) Giannetti, A. M.; Koch, B. D.; Browner, M. F. Surface Plasmon Resonance Based Assay for the Detection and Characterization of Promiscuous Inhibitors. *J. Med. Chem.* **2008**, *51* (3), 574–580.

(36) McLaughlin, C. K.; Duan, D.; Ganesh, A. N.; Torosyan, H.; Shoichet, B. K.; Shoichet, M. S. Stable Colloidal Drug Aggregates Catch and Release Active Enzymes. *ACS Chem. Biol.* **2016**, *11* (4), 992–1000.

(37) Ryan, A. J.; Gray, N. M.; Lowe, P. N.; Chung, C. W. Effect of Detergent on "Promiscuous" Inhibitors. *J. Med. Chem.* **2003**, *46* (16), 3448–3451.

(38) Feng, B. Y.; Shoichet, B. K. A Detergent-Based Assay for the Detection of Promiscuous Inhibitors. *Nat. Protoc.* **2006**, *1* (2), 550–553.

(39) Coan, K. E.; Shoichet, B. K. Stability and Equilibria of Promiscuous Aggregates in High Protein Milieus. *Molecular bioSystems* **2007**, *3* (3), 208–213.

(40) Liu, H. Y.; Wang, Z.; Regni, C.; Zou, X.; Tipton, P. A. Detailed Kinetic Studies of an Aggregating Inhibitor; Inhibition of Phosphomannomutase/Phosphoglucomutase by Disperse Blue 56. *Biochemistry* **2004**, *43* (27), 8662–8669.

(41) Raina, S. A.; Zhang, G. G. Z.; Alonzo, D. E.; Wu, J.; Zhu, D.; Catron, N. D.; Gao, Y.; Taylor, L. S. Enhancements and Limits in Drug Membrane Transport Using Supersaturated Solutions of Poorly Water Soluble Drugs. *J. Pharm. Sci.* **2014**, *103* (9), 2736–2748.

(42) Alexis, F.; Pridgen, E.; Molnar, L. K.; Farokhzad, O. C. Factors Affecting the Clearance and Biodistribution of Polymeric Nanoparticles. *Mol. Pharm* **2008**, *5* (4), 505–515.

(43) Lesniak, A.; Fenaroli, F.; Monopoli, M. P.; Aberg, C.; Dawson, K. A.; Salvati, A. Effects of the Presence or Absence of a Protein Corona on Silica Nanoparticle Uptake and Impact on Cells. *ACS Nano* **2012**, *6* (7), 5845–5857.

(44) Walkey, C. D.; Olsen, J. B.; Song, F.; Liu, R.; Guo, H.; Olsen, D. W.; Cohen, Y.; Emili, A.; Chan, W. C. Protein Corona Fingerprinting Predicts the Cellular Interaction of Gold and Silver Nanoparticles. *ACS Nano* **2014**, *8* (3), 2439–2455.

(45) Doak, A. K.; Wille, H.; Prusiner, S. B.; Shoichet, B. K. Colloid Formation by Drugs in Simulated Intestinal Fluid. *J. Med. Chem.* **2010**, *53* (10), 4259–4265.

(46) Frenkel, Y. V.; Gallicchio, E.; Das, K.; Levy, R. M.; Arnold, E. Molecular Dynamics Study of Non-Nucleoside Reverse Transcriptase Inhibitor 4-[[4-[[4-[(E)-2-Cyanoethenyl]-2,6-Dimethylphenyl]Amino]-2-Pyrimidinyl]Amino]Benz Onitrile (TMC278/Rilpivirine) Aggregates: Correlation Between Amphiphilic Properties of the Drug and Oral Bioavailability. *J. Med. Chem.* **2009**, *52* (19), 5896–5905.

(47) Clark, M. A.; Jepson, M. A.; Hirst, B. H. Exploiting M Cells for Drug and Vaccine Delivery. *Adv. Drug Deliv. Rev.* **2001**, *50* (1-2), 81–106.

(48) Ensign, L. M.; Cone, R.; Hanes, J. Oral Drug Delivery with Polymeric Nanoparticles: the Gastrointestinal Mucus Barriers. *Adv. Drug Deliv. Rev.* **2012**, *64* (6), 557–570.

(49) DeVita, V. T.; Chu, E. A History of Cancer Chemotherapy. *Cancer Res.* **2008**, *68* (21), 8643–8653.

(50) Hurley, L. H. DNA and Its Associated Processes as Targets for Cancer Therapy. *Nat. Rev. Cancer* **2002**, *2* (3), 188–200.

(51) Jordan, M. A.; Wilson, L. Microtubules as a Target for Anticancer Drugs. *Nat. Rev. Cancer* **2004**, *4* (4), 253–265.

(52) Chabner, B. A.; Roberts, T. G. Chemotherapy and the War on Cancer. *Nat. Rev. Cancer* **2005**, *5* (1), 65–72.

(53) Ali, S.; Coombes, R. C. Endocrine-Responsive Breast Cancer and Strategies for Combating Resistance. *Nat. Rev. Cancer* **2002**, *2* (2), 101–112.
(54) Osborne, C. K.; Wakeling, A.; Nicholson, R. I. Fulvestrant: an Oestrogen Receptor Antagonist with a Novel Mechanism of Action. *Br. J. Cancer* **2004**, *90 Suppl 1*, S2–S6.
(55) Johnston, S. R.; Dowsett, M. Aromatase Inhibitors for Breast Cancer: Lessons From the Laboratory. *Nat. Rev. Cancer* **2003**, *3* (11), 821–831.
(56) Wakeling, A. E.; Dukes, M.; Bowler, J. A Potent Specific Pure Antiestrogen with Clincal Potential. *Cancer Res.* **1991**, *51*, 3867–3873.
(57) Scott, S. M.; Brown, M.; Come, S. E. Emerging Data on the Efficacy and Safety of Fulvestrant, a Unique Antiestrogen Therapy for Advanced Breast Cancer. *Expert opinion on drug safety* **2011**, *10* (5), 819–826.
(58) Arora, A.; Scholar, E. M. Role of Tyrosine Kinase Inhibitors in Cancer Therapy. *J. Pharmacol. Exp. Ther.* **2005**, *315* (3), 971–979.
(59) Hynes, N. E.; Lane, H. A. ERBB Receptors and Cancer: the Complexity of Targeted Inhibitors. *Nat. Rev. Cancer* **2005**, *5* (5), 341–354.
(60) Slamon, D. J.; Clark, G. M.; Wong, S. G.; Levin, W. J.; Ullrich, A.; McGuire, W. L. Human Breast Cancer: Correlation of Relapse and Survival with Amplification of the HER-2/Neu Oncogene. *Science* **1987**, *235* (4785), 177–182.
(61) Filardo, E. J. Epidermal Growth Factor Receptor (EGFR) Transactivation by Estrogen via the G-Protein-Coupled Receptor, GPR30: a Novel Signaling Pathway with Potential Significance for Breast Cancer. *J. Steroid Biochem. Mol. Biol.* **2002**, *80* (2), 231–238.
(62) Nahta, R.; Hortobagyi, G. N.; Esteva, F. J. Growth Factor Receptors in Breast Cancer: Potential for Therapeutic Intervention. *Oncologist* **2003**, *8* (1), 5–17.
(63) Xia, W.; Mullin, R. J.; Keith, B. R.; Liu, L. H.; Ma, H.; Rusnak, D. W.; Owens, G.; Alligood, K. J.; Spector, N. L. Anti-Tumor Activity of GW572016: a Dual Tyrosine Kinase Inhibitor Blocks EGF Activation of EGFR/erbB2 and Downstream Erk1/2 and AKT Pathways. *Oncogene* **2002**, *21* (41), 6255–6263.
(64) Zhou, H.; Kim, Y. S.; Peletier, A.; McCall, W.; Earp, H. S.; Sartor, C. I. Effects of the EGFR/HER2 Kinase Inhibitor GW572016 on EGFR- and HER2-Overexpressing Breast Cancer Cell Line Proliferation, Radiosensitization, and Resistance. *Int. J. Radiat. Oncol. Biol. Phys.* **2004**, *58* (2), 344–352.
(65) Rautio, J.; Meanwell, N. A.; Di, L.; Hageman, M. J. The Expanding Role of Prodrugs in Contemporary Drug Design and Development. *Nat. Rev. Drug Discov.* **2018**, *17* (8), 559–587.
(66) Burkhart, D. J.; Barthel, B. L.; Post, G. C.; Kalet, B. T.; Nafie, J. W.; Shoemaker, R. K.; Koch, T. H. Design, Synthesis, and Preliminary Evaluation of Doxazolidine Carbamates as Prodrugs Activated by Carboxylesterases. *J. Med. Chem.* **2006**, *49* (24), 7002–7012.
(67) Barthel, B. L.; Torres, R. C.; Hyatt, J. L.; Edwards, C. C.; Hatfield, M. J.; Potter, P. M.; Koch, T. H. Identification of Human Intestinal Carboxylesterase as the Primary Enzyme for Activation of a Doxazolidine Carbamate Prodrug. *J. Med. Chem.* **2008**, *51* (2), 298–304.
(68) Barthel, B. L.; Zhang, Z.; Rudnicki, D. L.; Coldren, C. D.; Polinkovsky, M.; Sun, H.; Koch, G. G.; Chan, D. C. F.; Koch, T. H. Preclinical Efficacy of a Carboxylesterase 2-Activated Prodrug of Doxazolidine. *J. Med. Chem.* **2009**, *52* (23), 7678–7688.
(69) Scott, A. M.; Wolchok, J. D.; Old, L. J. Antibody Therapy of Cancer. *Nat. Rev. Cancer* **2012**, 1–10.

(70) Hudis, C. A. Trastuzumab — Mechanism of Action and Use in Clinical Practice. *N. Engl. J. Med.* **2007**, *357* (1), 39–51.
(71) Weiner, L. M.; Surana, R.; Wang, S. Monoclonal Antibodies: Versatile Platforms for Cancer Immunotherapy. *Nat. Rev. Immunol.* **2010**, *10* (5), 317–327.
(72) Gotwals, P.; Cameron, S.; Cipolletta, D.; Cremasco, V.; Crystal, A.; Hewes, B.; Mueller, B.; Quaratino, S.; Sabatos-Peyton, C.; Petruzzelli, L.; et al. Prospects for Combining Targeted and Conventional Cancer Therapy with Immunotherapy. *Nat. Rev. Cancer* **2017**, *17* (5), 286–301.
(73) Gelderblom, H.; Verweij, J.; Nooter, K.; Sparreboom, A. Cremophor EL: the Drawbacks and Advantages of Vehicle Selection for Drug Formulation. *European journal of cancer* **2001**, *37* (13), 1590–1598.
(74) Strickley, R. G. Solubilizing Excipients in Oral and Injectable Formulations. *Pharm. Res.* **2004**, *21* (2), 201–230.
(75) Vasconcelos, T.; Sarmento, B.; Costa, P. Solid Dispersions as Strategy to Improve Oral Bioavailability of Poor Water Soluble Drugs. *Drug Discov. Today* **2007**, *12* (23-24), 1068–1075.
(76) Beck, A.; Goetsch, L.; Dumontet, C.; Corvaïa, N. Strategies and Challenges for the Next Generation of Antibody–Drug Conjugates. *Nat. Rev. Drug Discov.* **2017**, *16* (5), 315–337.
(77) Sievers, E. L.; Senter, P. D. Antibody-Drug Conjugates in Cancer Therapy. *Annu. Rev. Med.* **2013**, *64* (1), 15–29.
(78) Carter, P. J.; Lazar, G. A. Next Generation Antibody Drugs: Pursuit of the "High-Hanging Fruit." *Nat. Rev. Drug Discov.* **2017**, *17* (3), 197–223.
(79) Lyon, R. P.; Bovee, T. D.; Doronina, S. O.; Burke, P. J.; Hunter, J. H.; Neff-LaFord, H. D.; Jonas, M.; Anderson, M. E.; Setter, J. R.; Senter, P. D. Reducing Hydrophobicity of Homogeneous Antibody-Drug Conjugates Improves Pharmacokinetics and Therapeutic Index. *Nat. Biotechnol.* **2015**, *33* (7), 733–735.
(80) Saleh, M. N.; Sugarman, S.; Murray, J.; Ostroff, J. B.; Healey, D.; Jones, D.; Daniel, C. R.; LeBherz, D.; Brewer, H.; Onetto, N.; et al. Phase I Trial of the Anti–Lewis Y Drug Immunoconjugate BR96-Doxorubicin in Patients with Lewis Y–Expressing Epithelial Tumors. *J. Clin. Oncol.* **2000**, *18* (11), 2282–2292.
(81) Tolcher, A. W.; Sugarman, S.; Gelmon, K. A.; Cohen, R.; Saleh, M.; Isaacs, C.; Young, L.; Healey, D.; Onetto, N.; Slichenmyer, W. Randomized Phase II Study of BR96-Doxorubicin Conjugate in Patients with Metastatic Breast Cancer. *Journal of Clinical Oncology* **2016**, *17* (2), 478–478.
(82) Wang, A. Z.; Langer, R.; Farokhzad, O. C. Nanoparticle Delivery of Cancer Drugs. *Annu. Rev. Med.* **2012**, *63*, 185–198.
(83) Shi, J.; Kantoff, P. W.; Wooster, R.; Farokhzad, O. C. Cancer Nanomedicine: Progress, Challenges and Opportunities. *Nat. Rev. Cancer* **2017**, *17* (1), 20–37.
(84) D'Mello, S. R.; Cruz, C. N.; Chen, M.-L.; Kapoor, M.; Lee, S. L.; Tyner, K. M. The Evolving Landscape of Drug Products Containing Nanomaterials in the United States. *Nat. Nanotechnol.* **2017**, *12* (6), 523–529.
(85) Allen, T. M. Liposomal Drug Delivery. *Current Opinion in Colloid and Interface Science* **1996**, *1*, 645–651.
(86) Torchilin, V. P. Recent Advances with Liposomes as Pharmaceutical Carriers. *Nat. Rev. Drug Discov.* **2005**, *4* (2), 145–160.
(87) Stirland, D. L.; Nichols, J. W.; Miura, S.; Bae, Y. H. Mind the Gap: a Survey of How Cancer Drug Carriers Are Susceptible to the Gap Between Research and Practice. *J. Control. Release* **2013**, *172* (3), 1045–1064.

(88) Jones, M.; Leroux, J. Polymeric Micelles - a New Generation of Colloidal Drug Carriers. *European Journal of Pharmaceutics and Biopharmaceutics* **1999**, *48* (2), 101–111.
(89) Duncan, R. The Dawning Era of Polymer Therapeutics. *Nat. Rev. Drug Discov.* **2003**, *2* (5), 347–360.
(90) Kenth, S.; Sylvestre, J. P.; Fuhrmann, K.; Meunier, M.; Leroux, J. C. Fabrication of Paclitaxel Nanocrystals by Femtosecond Laser Ablation and Fragmentation. *J. Pharm. Sci.* **2011**, *100* (3), 1022–1030.
(91) Gao, L.; Liu, G.; Ma, J.; Wang, X.; Zhou, L.; Li, X. Drug Nanocrystals: in Vivo Performances. *J. Control. Release* **2012**, *160* (3), 418–430.
(92) Dawidczyk, C. M.; Kim, C.; Park, J. H.; Russell, L. M.; Lee, K. H.; Pomper, M. G.; Searson, P. C. State-of-the-Art in Design Rules for Drug Delivery Platforms: Lessons Learned From FDA-Approved Nanomedicines. *J. Control. Release* **2014**, *187*, 133–144.
(93) Ma, W.; Cheetham, A. G.; Cui, H. Building Nanostructures with Drugs. *Nano Today* **2016**, *11* (1), 13–30.
(94) Huang, P.; Wang, D.; Su, Y.; Huang, W.; Zhou, Y.; Cui, D.; Zhu, X.; Yan, D. Combination of Small Molecule Prodrug and Nanodrug Delivery: Amphiphilic Drug-Drug Conjugate for Cancer Therapy. *J. Am. Chem. Soc.* **2014**, *136* (33), 11748–11756.
(95) Reddy, L. H.; Couvreur, P. Squalene: a Natural Triterpene for Use in Disease Management and Therapy. *Adv. Drug Deliv. Rev.* **2009**, *61* (15), 1412–1426.
(96) Bertrand, N.; Leroux, J. C. The Journey of a Drug-Carrier in the Body: an Anatomo-Physiological Perspective. *J. Control. Release* **2012**, *161* (2), 152–163.
(97) Lazarovits, J.; Chen, Y. Y.; Sykes, E. A.; Chan, W. C. W. Nanoparticle–Blood Interactions: the Implications on Solid Tumour Targeting. *Chem. Commun.* **2015**, *51* (14), 2756–2767.
(98) Lundqvist, M.; Stigler, J.; Elia, G.; Lynch, I.; Cedervall, T.; Dawson, K. A. Nanoparticle Size and Surface Properties Determine the Protein Corona with Possible Implications for Biological Impacts. *Proc. Natl. Acad. Sci.* **2008**, *105* (38), 14265–14270.
(99) Cedervall, T.; Lynch, I.; Lindman, S.; Berggard, T.; Thulin, E.; Nilsson, H.; Dawson, K. A.; Linse, S. Understanding the Nanoparticle-Protein Corona Using Methods to Quantify Exchange Rates and Affinities of Proteins for Nanoparticles. *Proc. Natl. Acad. Sci.* **2007**, *104* (7), 2050–2055.
(100) Walkey, C. D.; Olsen, J. B.; Guo, H.; Emili, A.; Chan, W. C. Nanoparticle Size and Surface Chemistry Determine Serum Protein Adsorption and Macrophage Uptake. *J. Am. Chem. Soc.* **2012**, *134* (4), 2139–2147.
(101) Bertrand, N.; Grenier, P.; Mahmoudi, M.; Lima, E. M.; Appel, E. A.; Dormont, F.; Lim, J.-M.; Karnik, R.; Langer, R.; Farokhzad, O. C. Mechanistic Understanding of in Vivo Protein Corona Formation on Polymeric Nanoparticles and Impact on Pharmacokinetics. *Nat. Commun.* **2017**, *8* (1), 772.
(102) Blanco, E.; Shen, H.; Ferrari, M. Principles of Nanoparticle Design for Overcoming Biological Barriers to Drug Delivery. *Nat. Biotechnol.* **2015**, *33* (9), 941–951.
(103) Gabizon, A.; Papahadjopoulos, D. Liposome Formulations with Prolonged Circulation Time in Blood and Enhanced Uptake by Tumors. *Proc. Natl. Acad. Sci.* **1988**, *85* (18), 6949–6953.
(104) Gabizon, A.; Shmeeda, H.; Barenholz, Y. Pharmacokinetics of Pegylated Liposomal Doxorubicin: Review of Animal and Human Studies. *Clin. Pharmacokinet.* **2003**, *42* (5), 419–436.

(105) Hu, C.-M. J.; Zhang, L.; Aryal, S.; Cheung, C.; Fang, R. H.; Zhang, L.; Zhang, L. Erythrocyte Membrane-Camouflaged Polymeric Nanoparticles as a Biomimetic Delivery Platform. *Proc. Natl. Acad. Sci.* **2011**, *108* (27), 10980–10985.

(106) Lyass, O.; Uziely, B.; Ben-Yosef, R.; Tzemach, D.; Heshing, N. I.; Lotem, M.; Brufman, G.; Gabizon, A. Correlation of Toxicity with Pharmacokinetics of Pegylated Liposomal Doxorubicin (Doxil) in Metastatic Breast Carcinoma. *Cancer* **2000**, *89* (5), 1037–1047.

(107) Solomon, R.; Gabizon, A. A. Clinical Pharmacology of Liposomal Anthracyclines: Focus on Pegylated Liposomal Doxorubicin. *Clinical Lymphoma and Myeloma* **2008**, *8* (1), 21–32.

(108) Soo Choi, H.; Liu, W.; Misra, P.; Tanaka, E.; Zimmer, J. P.; Itty Ipe, B.; Bawendi, M. G.; Frangioni, J. V. Renal Clearance of Quantum Dots. *Nat. Biotechnol.* **2007**, *25* (10), 1165–1170.

(109) Tavares, A. J.; Poon, W.; Zhang, Y.-N.; Dai, Q.; Besla, R.; Ding, D.; Ouyang, B.; Li, A.; Chen, J.; Zheng, G.; et al. Effect of Removing Kupffer Cells on Nanoparticle Tumor Delivery. *Proc. Natl. Acad. Sci.* **2017**, *114* (51), E10871–E10880.

(110) Gustafson, H. H.; Holt-Casper, D.; Grainger, D. W.; Ghandehari, H. Nanoparticle Uptake: the Phagocyte Problem. *Nano Today* **2015**, *10* (4), 487–510.

(111) Matsumura, Y.; Maeda, H. A New Concept for Macromolecular Therapeutics in Cancer Chemotherapy: Mechanism of Tumortropic Accumulation of Proteins and the Antitumor Agent Smancs. *Cancer Res.* **1986**, *46*, 6387–6392.

(112) Jain, R. K. Molecular Regulation of Vessel Maturation. *Nat. Med.* **2003**, *9* (6), 685–693.

(113) Maeda, H.; Nakamura, H.; Fang, J. The EPR Effect for Macromolecular Drug Delivery to Solid Tumors: Improvement of Tumor Uptake, Lowering of Systemic Toxicity, and Distinct Tumor Imaging in Vivo. *Adv. Drug Deliv. Rev.* **2013**, *65* (1), 71–79.

(114) Torchilin, V. Tumor Delivery of Macromolecular Drugs Based on the EPR Effect. *Adv. Drug Deliv. Rev.* **2011**, *63* (3), 131–135.

(115) Maeda, H.; Wu, J.; Sawa, T.; Matsumura, Y.; Hori, K. Tumor Vascular Permeability and the EPR Effect in Macromolecular Therapeutics: a Review. *J. Control. Release* **2000**, *65* (1–2), 271–284.

(116) Tang, L.; Gabrielson, N. P.; Uckun, F. M.; Fan, T. M.; Cheng, J. Size-Dependent Tumor Penetration and in Vivo Efficacy of Monodisperse Drug-Silica Nanoconjugates. *Mol. Pharm.* **2013**, *10* (3), 883–892.

(117) Cabral, H.; Matsumoto, Y.; Mizuno, K.; Chen, Q.; Murakami, M.; Kimura, M.; Terada, Y.; Kano, M. R.; Miyazono, K.; Uesaka, M.; et al. Accumulation of Sub-100 Nm Polymeric Micelles in Poorly Permeable Tumours Depends on Size. *Nat. Nanotechnol.* **2011**, *6* (12), 815–823.

(118) Harrington, K. J.; Mohammadtaghi, S.; Uster, P. S.; Glass, D.; Peters, A. M.; Vile, R. G.; Stewart, J. S. W. Effective Targeting of Solid Tumors in Patients with Locally Advanced Cancers by Radiolabeled Pegylated Liposomes. *Clin. Cancer Res.* **2001**, *7* (2), 243–254.

(119) Nichols, J. W.; Bae, Y. H. EPR: Evidence and Fallacy. *J. Control. Release* **2014**, *190*, 451–464.

(120) Ojha, T.; Pathak, V.; Shi, Y.; Hennink, W. E.; Moonen, C. T. W.; Storm, G.; Kiessling, F.; Lammers, T. Pharmacological and Physical Vessel Modulation Strategies to Improve EPR-Mediated Drug Targeting to Tumors. *Adv. Drug Deliv. Rev.* **2017**, *119*, 44–60.

(121) Golombek, S. K.; May, J.-N.; Theek, B.; Appold, L.; Drude, N.; Kiessling, F.; Lammers, T. Tumor Targeting via EPR: Strategies to Enhance Patient Responses. *Adv. Drug Deliv. Rev.* **2018**, 1–22.

(122) Park, K. Questions on the Role of the EPR Effect in Tumor Targeting. *J. Control. Release* **2013**, *172* (1), 391.

(123) Hollis, C. P.; Weiss, H. L.; Leggas, M.; Evers, B. M.; Gemeinhart, R. A.; Li, T. Biodistribution and Bioimaging Studies of Hybrid Paclitaxel Nanocrystals: Lessons Learned of the EPR Effect and Image-Guided Drug Delivery. *J. Control. Release* **2013**, *172* (1), 12–21.

(124) Torchilin, V. P. Multifunctional Nanocarriers. *Adv. Drug Deliv. Rev.* **2012**, *64*, 302–315.

(125) Owen, S. C.; Patel, N.; Logie, J.; Pan, G.; Persson, H.; Moffat, J.; Sidhu, S. S.; Shoichet, M. S. Targeting HER2+ Breast Cancer Cells: Lysosomal Accumulation of Anti-HER2 Antibodies Is Influenced by Antibody Binding Site and Conjugation to Polymeric Nanoparticles. *J. Control. Release* **2013**, *172* (2), 395–404.

(126) Dreaden, E. C.; Morton, S. W.; Shopsowitz, K. E.; Choi, J. H.; Deng, Z. J.; Cho, N. J.; Hammond, P. T. Bimodal Tumor-Targeting From Microenvironment Responsive Hyaluronan Layer-by-Layer (LbL) Nanoparticles. *ACS Nano* **2014**, *8* (8), 8374–8382.

(127) Yameen, B.; Choi, W. I.; Vilos, C.; Swami, A.; Shi, J.; Farokhzad, O. C. Insight Into Nanoparticle Cellular Uptake and Intracellular Targeting. *J. Control. Release* **2014**, *190*, 485–499.

(128) Kukowska-Latallo, J. F.; Candido, K. A.; Cao, Z.; Nigavekar, S. S.; Majoros, I. J.; Thomas, T. P.; Balogh, L. P.; Khan, M. K.; Baker, J. R. Nanoparticle Targeting of Anticancer Drug Improves Therapeutic Response in Animal Model of Human Epithelial Cancer. *Cancer Res.* **2005**, *65* (12), 5317–5324.

(129) Byrne, J. D.; Betancourt, T.; Brannon-Peppas, L. Active Targeting Schemes for Nanoparticle Systems in Cancer Therapeutics. *Adv. Drug Deliv. Rev.* **2008**, *60* (15), 1615–1626.

(130) Miura, Y.; Takenaka, T.; Toh, K.; Wu, S.; Nishihara, H.; Kano, M. R.; Ino, Y.; Nomoto, T.; Matsumoto, Y.; Koyama, H.; et al. Cyclic RGD-Linked Polymeric Micelles for Targeted Delivery of Platinum Anticancer Drugs to Glioblastoma Through the Blood-Brain Tumor Barrier. *ACS Nano* **2013**, *7* (10), 8583–8592.

(131) Ruoslahti, E. Peptides as Targeting Elements and Tissue Penetration Devices for Nanoparticles. *Adv. Mater.* **2012**, *24* (28), 3747–3756.

(132) Valetti, S.; Maione, F.; Mura, S.; Stella, B.; Desmaele, D.; Noiray, M.; Vergnaud, J.; Vauthier, C.; Cattel, L.; Giraudo, E.; et al. Peptide-Functionalized Nanoparticles for Selective Targeting of Pancreatic Tumor. *J. Control. Release* **2014**, *192*, 29–39.

(133) Wilhelm, S.; Tavares, A. J.; Dai, Q.; Ohta, S.; Audet, J.; Dvorak, H. F.; Chan, W. C. W. Analysis of Nanoparticle Delivery to Tumours. *Nat. Rev. Mater.* **2016**, 1–12.

(134) Lammers, T.; Kiessling, F.; Ashford, M.; Hennink, W.; Crommelin, D.; Storm, G. Cancer Nanomedicine: Is Targeting Our Target? *Nat. Rev. Mater.* **2016**, *1* (9), 434–2.

(135) Logie, J.; Ganesh, A. N.; Aman, A. M.; Al-Awar, R. S.; Shoichet, M. S. Preclinical Evaluation of Taxane-Binding Peptide-Modified Polymeric Micelles Loaded with Docetaxel in an Orthotopic Breast Cancer Mouse Model. *Biomaterials* **2017**, *123*, 39–47.

(136) Dai, Q.; Wilhelm, S.; Ding, D.; Syed, A. M.; Sindhwani, S.; Zhang, Y.; Chen, Y. Y.; MacMillan, P.; Chan, W. C. W. Quantifying the Ligand-Coated Nanoparticle Delivery to Cancer Cells in Solid Tumors. *ACS Nano* **2018**, acsnano.8b03900.

(137) Lancet, J. E.; Uy, G. L.; Cortes, J. E.; Newell, L. F.; Lin, T. L.; Ritchie, E. K.; Stuart, R. K.; Strickland, S. A.; Hogge, D.; Solomon, S. R.; et al. Final Results of a Phase III Randomized Trial of CPX-351 Versus 7+3 in Older Patients with Newly Diagnosed High Risk (Secondary) AML. *J. Clin. Oncol.* **2016**, *34* (15_suppl), 7000–7000.

(138) Ke, P. C.; Lin, S.; Parak, W. J.; Davis, T. P.; Caruso, F. A Decade of the Protein Corona. *ACS Nano* **2017**, *11* (12), 11773–11776.

(139) Björnmalm, M.; Thurecht, K. J.; Michael, M.; Scott, A. M.; Caruso, F. Bridging Bio-Nano Science and Cancer Nanomedicine. *ACS Nano* **2017**, *11* (10), 9594–9613.

(140) Park, K. Facing the Truth About Nanotechnology in Drug Delivery. *ACS Nano* **2013**, *7* (9), 7442–7447.

(141) Hubbell, J. A.; Langer, R. Translating Materials Design to the Clinic. *Nat. Mater.* **2013**, *12* (11), 963–966.

(142) Logie, J.; McLaughlin, C. K.; Tam, R. Y.; Shoichet, M. S. Innovative Use of the Taxol Binding Peptide Overcomes Key Challenges of Stable and High Drug Loading in Polymeric Nanomicelles. *Chem. Commun.* **2015**, *51* (60), 12000–12003.

(143) McCombs, J. R.; Owen, S. C. Antibody Drug Conjugates: Design and Selection of Linker, Payload and Conjugation Chemistry. *AAPS J* **2015**, *17* (2), 339–351.

(144) McGovern, S. L.; Caselli, E.; Grigorieff, N.; Shoichet, B. K. A Common Mechanism Underlying Promiscuous Inhibitors From Virtual and High-Throughput Screening. *J. Med. Chem.* **2002**, *45* (8), 1712–1722.

(145) Sassano, M. F.; Doak, A. K.; Roth, B. L.; Shoichet, B. K. Colloidal Aggregation Causes Inhibition of G Protein-Coupled Receptors. *J. Med. Chem.* **2013**, *56* (6), 2406–2414.

(146) Kim, S.; Shi, Y.; Kim, J. Y.; Park, K.; Cheng, J. X. Overcoming the Barriers in Micellar Drug Delivery: Loading Efficiency, in Vivo Stability, and Micelle-Cell Interaction. *Expert Opin. Drug Deliv.* **2010**, *7* (1), 49–62.

(147) Gaudin, A.; Yemisci, M.; Eroglu, H.; Lepetre-Mouelhi, S.; Turkoglu, O. F.; Donmez-Demir, B.; Caban, S.; Sargon, M. F.; Garcia-Argote, S.; Pieters, G.; et al. Squalenoyl Adenosine Nanoparticles Provide Neuroprotection After Stroke and Spinal Cord Injury. *Nat. Nanotechnol.* **2014**, *9* (12), 1054–1062.

(148) Maksimenko, A.; Dosio, F.; Mougin, J.; Ferrero, A.; Wack, S.; Reddy, L. H.; Weyn, A. A.; Lepeltier, E.; Bourgaux, C.; Stella, B.; et al. A Unique Squalenoylated and Nonpegylated Doxorubicin Nanomedicine with Systemic Long-Circulating Properties and Anticancer Activity. *Proc. Natl. Acad. Sci.* **2014**, *111* (2), E217–E226.

(149) D'Addio, S. M.; Prud'homme, R. K. Controlling Drug Nanoparticle Formation by Rapid Precipitation. *Adv. Drug Deliv. Rev.* **2011**, *63* (6), 417–426.

(150) Barua, S.; Yoo, J. W.; Kolhar, P.; Wakankar, A.; Gokarn, Y. R.; Mitragotri, S. Particle Shape Enhances Specificity of Antibody-Displaying Nanoparticles. *Proc. Natl. Acad. Sci.* **2013**, *110* (9), 3270–3275.

(151) Barua, S.; Mitragotri, S. Synergistic Targeting of Cell Membrane, Cytoplasm, and Nucleus of Cancer Cells Using Rod-Shaped Nanoparticles. *ACS Nano* **2013**, *7* (11), 9558–9570.

(152) Cortez, C.; Tomaskovic-Crook, E.; Johnston, A. P.; Scott, A. M.; Nice, E. C.; Heath, J. K.; Caruso, F. Influence of Size, Surface, Cell Line, and Kinetic Properties on the Specific Binding of A33 Antigen-Targeted Multilayered Particles and Capsules to Colorectal Cancer Cells. *ACS Nano* **2007**, *1* (2), 93–102.

(153) Sodhi, R. N. S. Time-of-Flight Secondary Ion Mass Spectrometry (TOF-SIMS):-Versatility in Chemical and Imaging Surface Analysis. *Analyst* **2004**, *129* (6), 483–487.

(154) Zhao, X.; Poon, Z.; Engler, A. C.; Bonner, D. K.; Hammond, P. T. Enhanced Stability of Polymeric Micelles Based on Postfunctionalized Poly(Ethylene Glycol)-B-Poly(Gamma-Propargyl L-Glutamate): the Substituent Effect. *Biomacromolecules* **2012**, *13* (5), 1315–1322.

(155) Logie, J.; Owen, S. C.; McLaughlin, C. K.; Shoichet, M. S. PEG-Graft Density Controls Polymeric Nanoparticle Micelle Stability. *Chem Mater* **2014**, *26* (9), 2847–2855.

(156) Gaudin, A.; Tagit, O.; Sobot, D.; Lepetre-Mouelhi, S.; Mougin, J.; Martens, T. F.; Braeckmans, K.; Nicolas, V.; Desmaele, D.; de Smedt, S. C.; et al. Transport Mechanisms of Squalenoyl-Adenosine Nanoparticles Across the Blood-Brain Barrier. *Chem Mater* **2015**, *27* (10), 3636–3647.

(157) Rimawi, M. F.; Schiff, R.; Osborne, C. K. Targeting HER2 for the Treatment of Breast Cancer. *Annu. Rev. Med.* **2015**, *66* (1), 111–128.

(158) Maxfield, F. R.; McGraw, T. E. Endocytic Recycling. *Nat. Rev. Mol. Cell Biol.* **2004**, *5* (2), 121–132.

(159) Holliday, D.; Speirs, V. Choosing the Right Cell Line for Breast Cancer Research. *Breast Cancer Res.* **2011**, *13* (4), 215.

(160) Monopoli, M. P.; Aberg, C.; Salvati, A.; Dawson, K. A. Biomolecular Coronas Provide the Biological Identity of Nanosized Materials. *Nat. Nanotechnol.* **2012**, *7* (12), 779–786.

(161) Mahmoudi, M.; Lynch, I.; Ejtehadi, M. R.; Monopoli, M. P.; Bombelli, F. B.; Laurent, S. Protein-Nanoparticle Interactions: Opportunities and Challenges. *Chem. Rev.* **2011**, *111* (9), 5610–5637.

(162) Lindman, S.; Lynch, I.; Thulin, E.; Nilsson, H.; Dawson, K. A.; Linse, S. Systematic Investigation of the Thermodynamics of HSA Adsorption to N-Iso-Propylacrylamide/N-Tert-Butylacrylamide Copolymer Nanoparticles. Effects of Particle Size and Hydrophobicity. *Nano Letters* **2007**, *7* (4), 914–920.

(163) Monopoli, M. P.; Walczyk, D.; Campbell, A.; Elia, G.; Lynch, I.; Bombelli, F. B.; Dawson, K. A. Physical-Chemical Aspects of Protein Corona: Relevance to in Vitro and in Vivo Biological Impacts of Nanoparticles. *J. Am. Chem. Soc.* **2011**, *133* (8), 2525–2534.

(164) Moerz, S. T.; Kraegeloh, A.; Chanana, M.; Kraus, T. Formation Mechanism for Stable Hybrid Clusters of Proteins and Nanoparticles. *ACS Nano* **2015**, *9* (7), 6696–6705.

(165) Brewer, S. H.; Glomm, W. R.; Johnson, M. C.; Knag, M. K.; Franzen, S. Probing BSA Binding to Citrate-Coated Gold Nanoparticles and Surfaces. *Langmuir* **2005**, *21* (20), 9303–9307.

(166) Wertz, C. F.; Santore, M. M. Effect of Surface Hydrophobicity on Adsorption and Relaxation Kinetics of Albumin and Fibrinogen: Single-Species and Competitive Behavior. *Langmuir* **2001**, *17* (10), 3006–3016.

(167) Jeyachandran, Y. L.; Mielczarski, E.; Rai, B.; Mielczarski, J. A. Quantitative and Qualitative Evaluation of Adsorption/Desorption of Bovine Serum Albumin on Hydrophilic and Hydrophobic Surfaces. *Langmuir* **2009**, *25* (19), 11614–11620.

(168) Kim, J.; Somorjai, G. A. Molecular Packing of Lysozyme, Fibrinogen, and Bovine Serum Albumin on Hydrophilic and Hydrophobic Surfaces Studied by Infrared−Visible Sum Frequency Generation and Fluorescence Microscopy. *J. Am. Chem. Soc.* **2003**, *125* (10), 3150–3158.

(169) He, X. M.; Carter, D. C. Atomic Structure and Chemistry of Human Serum Albumin. *Nature* **1992**, *358* (6383), 209–215.

(170) Walsh, G.; Jefferis, R. Post-Translational Modifications in the Context of Therapeutic Proteins. *Nat. Biotechnol.* **2006**, *24* (10), 1241–1252.
(171) Beck, A.; Wagner-Rousset, E.; Bussat, M. C.; Lokteff, M.; Klinguer-Hamour, C.; Haeuw, J. F.; Goetsch, L.; Wurch, T.; Van Dorsselaer, A.; Corvaia, N. Trends in Glycosylation, Glycoanalysis and Glycoengineering of Therapeutic Antibodies and Fc-Fusion Proteins. *Curr. Pharm. Biotechnol.* **2008**, *9* (6), 482–501.
(172) Gebauer, J. S.; Malissek, M.; Simon, S.; Knauer, S. K.; Maskos, M.; Stauber, R. H.; Peukert, W.; Treuel, L. Impact of the Nanoparticle–Protein Corona on Colloidal Stability and Protein Structure. *Langmuir* **2012**, *28* (25), 9673–9679.
(173) Au, K. M.; Armes, S. P. Heterocoagulation as a Facile Route to Prepare Stable Serum Albumin-Nanoparticle Conjugates for Biomedical Applications: Synthetic Protocols and Mechanistic Insights. *ACS Nano* **2012**, *6* (9), 8261–8279.
(174) Fuhrmann, K.; Gauthier, M. A.; Leroux, J. C. Targeting of Injectable Drug Nanocrystals. *Mol. Pharm.* **2014**, *11* (6), 1762–1771.
(175) Yan, Y.; Gause, K. T.; Kamphuis, M. M. J.; Ang, C.-S.; O'Brien-Simpson, N. M.; Lenzo, J. C.; Reynolds, E. C.; Nice, E. C.; Caruso, F. Differential Roles of the Protein Corona in the Cellular Uptake of Nanoporous Polymer Particles by Monocyte and Macrophage Cell Lines. *ACS Nano* **2013**, *7* (12), 10960–10970.
(176) Kiss, L.; Walter, F. R.; Bocsik, A.; Veszelka, S.; Ozsvári, B.; Puskás, L. G.; Szabó-Révész, P.; Deli, M. A. Kinetic Analysis of the Toxicity of Pharmaceutical Excipients Cremophor EL and RH40 on Endothelial and Epithelial Cells. *J. Pharm. Sci.* **2013**, *102* (4), 1173–1181.
(177) Bravo González, R. C.; Huwyler, J.; Boess, F.; Walter, I.; Bittner, B. In Vitro Investigation on the Impact of the Surface-Active Excipients Cremophor EL, Tween 80 and Solutol HS 15 on the Metabolism of Midazolam. *Biopharm Drug Dispos* **2004**, *25* (1), 37–49.
(178) Peer, D.; Karp, J. M.; Hong, S.; Farokhzad, O. C.; Margalit, R.; Langer, R. Nanocarriers as an Emerging Platform for Cancer Therapy. *Nat. Nanotechnol.* **2007**, *2* (12), 751–760.
(179) Cabral, H.; Kataoka, K. Progress of Drug-Loaded Polymeric Micelles Into Clinical Studies. *J. Control. Release* **2014**, *190*, 465–476.
(180) Luque-Michel, E.; Imbuluzqueta, E.; Sebastián, V.; Blanco-Prieto, M. J. Clinical Advances of Nanocarrier-Based Cancer Therapy and Diagnostics. *Expert Opin. Drug Deliv.* **2017**, *14* (1), 75–92.
(181) Eetezadi, S.; Ekdawi, S. N.; Allen, C. The Challenges Facing Block Copolymer Micelles for Cancer Therapy: in Vivo Barriers and Clinical Translation. *Adv. Drug Deliv. Rev.* **2015**, *91*, 7–22.
(182) Shen, G.; Xing, R.; Zhang, N.; Chen, C.; Ma, G.; Yan, X. Interfacial Cohesion and Assembly of Bioadhesive Molecules for Design of Long-Term Stable Hydrophobic Nanodrugs Toward Effective Anticancer Therapy. *ACS Nano* **2016**, *10* (6), 5720–5729.
(183) Irwin, J. J.; Duan, D.; Torosyan, H.; Doak, A. K.; Ziebart, K. T.; Sterling, T.; Tumanian, G.; Shoichet, B. K. An Aggregation Advisor for Ligand Discovery. *J. Med. Chem.* **2015**, *58* (17), 7076–7087.
(184) Jackson, M. J.; Toth, S. J.; Kestur, U. S.; Huang, J.; Qian, F.; Hussain, M. A.; Simpson, G. J.; Taylor, L. S. Impact of Polymers on the Precipitation Behavior of Highly Supersaturated Aqueous Danazol Solutions. *Mol. Pharm.* **2014**, *11* (9), 3027–3038.
(185) Kalepu, S.; Nekkanti, V. Insoluble Drug Delivery Strategies: Review of Recent Advances and Business Prospects. *Acta Pharmaceutica Sinica B* **2015**, *5* (5), 442–453.

(186) Liu, Y.; Hu, Y.; Huang, L. Influence of Polyethylene Glycol Density and Surface Lipid on Pharmacokinetics and Biodistribution of Lipid-Calcium-Phosphate Nanoparticles. *Biomaterials* **2014**, *35* (9), 3027–3034.

(187) Owens, D. E.; Peppas, N. A. Opsonization, Biodistribution, and Pharmacokinetics of Polymeric Nanoparticles. *Int. J. Pharmaceutics* **2006**, *307* (1), 93–102.

(188) Overbeek, J. T. G. Recent Developments in the Understanding of Colloid Stability. *J. Colloid Interface Sci.* **1977**, *58* (2), 408–422.

(189) Latere Dwan'Isa, J. P.; Rouxhet, L.; Préat, V.; Brewster, M. E.; Ariën, A. Prediction of Drug Solubility in Amphiphilic Di-Block Copolymer Micelles: the Role of Polymer-Drug Compatibility. *Pharmazie* **2007**, *62* (7), 499–504.

(190) Marsac, P. J.; Shamblin, S. L.; Taylor, L. S. Theoretical and Practical Approaches for Prediction of Drug-Polymer Miscibility and Solubility. *Pharm. Res.* **2006**, *23* (10), 2417–2426.

(191) Zaccone, A.; Wu, H.; Lattuada, M.; Morbidelli, M. Correlation Between Colloidal Stability and Surfactant Adsorption/Association Phenomena Studied by Light Scattering. *J. Phys. Chem. B* **2008**, *112* (21), 6733–6733.

(192) Santander-Ortega, M. J.; Jodar-Reyes, A. B.; Csaba, N.; Bastos-Gonzalez, D.; Ortega-Vinuesa, J. L. Colloidal Stability of Pluronic F68-Coated PLGA Nanoparticles: a Variety of Stabilisation Mechanisms. *J. Colloid Interface Sci.* **2006**, *302* (2), 522–529.

(193) Liu, J.; Zeng, F.; Allen, C. Influence of Serum Protein on Polycarbonate-Based Copolymer Micelles as a Delivery System for a Hydrophobic Anti-Cancer Agent. *J. Control. Release* **2005**, *103* (2), 481–497.

(194) Gref, R.; Luck, M.; Quellec, P.; Marchand, M.; Dellacherie, E.; Harnisch, S.; Blunk, T.; Muller, R. H. "Stealth" Corona-Core Nanoparticles Surface Modified by Polyethylene Glycol (PEG): Influences of the Corona (PEG Chain Length and Surface Density) and of the Core Composition on Phagocytic Uptake and Plasma Protein Adsorption. *Colloids and Surfaces B: Biointerfaces* **2000**, *18* (3-4), 301–313.

(195) Tacar, O.; Sriamornsak, P.; Dass, C. R. Doxorubicin: an Update on Anticancer Molecular Action, Toxicity and Novel Drug Delivery Systems. *Journal of Pharmacy and Pharmacology* **2012**, *65* (2), 157–170.

(196) Letchford, K.; Liggins, R.; Burt, H. Solubilization of Hydrophobic Drugs by Methoxy Poly(Ethylene Glycol)-Block-Polycaprolactone Diblock Copolymer Micelles: Theoretical and Experimental Data and Correlations. *J. Pharm. Sci.* **2008**, *97* (3), 1179–1190.

(197) Liu, J.; Xiao, Y.; Allen, C. Polymer–Drug Compatibility: a Guide to the Development of Delivery Systems for the Anticancer Agent, Ellipticine. *J. Pharm. Sci.* **2004**, *93* (1), 132–143.

(198) Yang, C.; Tan, J. P. K.; Cheng, W.; Attia, A. B. E.; Ting, C. T. Y.; Nelson, A.; Hedrick, J. L.; Yang, Y.-Y. Supramolecular Nanostructures Designed for High Cargo Loading Capacity and Kinetic Stability. *Nano Today* **2010**, *5* (6), 515–523.

(199) Gou, J.; Feng, S.; Xu, H.; Fang, G.; Chao, Y.; Zhang, Y.; Xu, H.; Tang, X. Decreased Core Crystallinity Facilitated Drug Loading in Polymeric Micelles Without Affecting Their Biological Performances. *Biomacromolecules* **2015**, *16* (9), 2920–2929.

(200) Zhao, Y.; Fay, F. C. O.; Hak, S.; Perez-Aguilar, J. M.; Sanchez-Gaytan, B. L.; Goode, B.; Duivenvoorden, R. E. L.; de Lange Davies, C.; y, A. B. O. R. O.; Weinstein, H.; et al. Augmenting Drug-Carrier Compatibility Improves Tumour Nanotherapy Efficacy. *Nat. Commun.* **2016**, *7*, 1–11.

(201) Ganesh, A. N.; Donders, E. N.; Shoichet, B. K.; Shoichet, M. S. Colloidal Aggregation: From Screening Nuisance to Formulation Nuance. *Nano Today* **2018**, *19* (C), 188–200.
(202) Duan, D.; Doak, A. K.; Nedyalkova, L.; Shoichet, B. K. Colloidal Aggregation and the in Vitro Activity of Traditional Chinese Medicines. *ACS Chem. Biol.* **2015**, *10* (4), 978–988.
(203) Wilson, V.; Lou, X.; Osterling, D. J.; Stolarik, D. F.; Jenkins, G.; Gao, W.; Zhang, G. G. Z.; Taylor, L. S. Relationship Between Amorphous Solid Dispersion in Vivo Absorption and in Vitro Dissolution: Phase Behavior During Dissolution, Speciation, and Membrane Mass Transport. *J. Control. Release* **2018**, *292*, 172–182.
(204) Ganesh, A. N.; McLaughlin, C. K.; Duan, D.; Shoichet, B. K.; Shoichet, M. S. A New Spin on Antibody-Drug Conjugates: Trastuzumab-Fulvestrant Colloidal Drug Aggregates Target HER2-Positive Cells. *ACS Appl. Mater. Interfaces* **2017**, *9* (14), 12195–12202.
(205) Ganesh, A. N.; Logie, J.; McLaughlin, C. K.; Barthel, B. L.; Koch, T. H.; Shoichet, B. K.; Shoichet, M. S. Leveraging Colloidal Aggregation for Drug-Rich Nanoparticle Formulations. *Mol. Pharm.* **2017**, *14* (6), 1852–1860.
(206) Fischer, K.; Schmidt, M. Pitfalls and Novel Applications of Particle Sizing by Dynamic Light Scattering. *Biomaterials* **2016**, *98* (c), 79–91.
(207) Krebs, H. Chemical Composition of Blood Plasma and Serum. *Annu. Rev. Biochem.* **1950**, No. 19, 409–430.
(208) Riley, T.; Govender, T.; Stolnik, S.; Xiong, C. D.; Garnett, M. C.; Illum, L.; Davis, S. S. Colloidal Stability and Drug Incorporation Aspects of Micellar-Like PLA–PEG Nanoparticles. *Colloids and Surfaces B: Biointerfaces* **1999**, *16* (1-4), 147–159.
(209) Zhang, F.; Xue, J.; Shao, J.; Jia, L. Compilation of 222 Drugs' Plasma Protein Binding Data and Guidance for Study Designs. *Drug Discov. Today* **2012**, *17* (9-10), 475–485.
(210) Barthel, B. L.; Rudnicki, D. L.; Kirby, T. P.; Colvin, S. M.; Burkhart, D. J.; Koch, T. H. Synthesis and Biological Characterization of Protease-Activated Prodrugs of Doxazolidine. *J. Med. Chem.* **2012**, *55* (14), 6595–6607.
(211) Rudakova, E. V.; Boltneva, N. P.; Makhaeva, G. F. Comparative Analysis of Esterase Activities of Human, Mouse, and Rat Blood. *Bulletin of Experimental Biology and Medicine* **2011**, *152* (1), 73–75.
(212) Li, B.; Sedlacek, M.; Manoharan, I.; Boopathy, R.; Duysen, E. G.; Masson, P.; Lockridge, O. Butyrylcholinesterase, Paraoxonase, and Albumin Esterase, but Not Carboxylesterase, Are Present in Human Plasma. *Biochemical Pharmacology* **2005**, *70* (11), 1673–1684.
(213) Kumar, V.; Prud'homme, R. K. Thermodynamic Limits on Drug Loading in Nanoparticle Cores. *J. Pharm. Sci.* **2008**, *97* (11), 4904–4914.
(214) Chu, K. S.; Schorzman, A. N.; Finniss, M. C.; Bowerman, C. J.; Peng, L.; Luft, J. C.; Madden, A. J.; Wang, A. Z.; Zamboni, W. C.; DeSimone, J. M. Nanoparticle Drug Loading as a Design Parameter to Improve Docetaxel Pharmacokinetics and Efficacy. *Biomaterials* **2013**, *34* (33), 8424–8429.
(215) Ho, K. S.; Aman, A. M.; Al-awar, R. S.; Shoichet, M. S. Amphiphilic Micelles of Poly(2-Methyl-2-Carboxytrimethylene Carbonate-Co-D,L-Lactide)-Graft-Poly(Ethylene Glycol) for Anti-Cancer Drug Delivery to Solid Tumours. *Biomaterials* **2012**, *33* (7), 2223–2229.
(216) Torchilin, V. P. Multifunctional, Stimuli-Sensitive Nanoparticulate Systems for Drug Delivery. *Nat. Rev. Drug Discov.* **2014**, *13* (11), 813–827.

(217) Perry, J. L.; Reuter, K. G.; Kai, M. P.; Herlihy, K. P.; Jones, S. W.; Luft, J. C.; Napier, M.; Bear, J. E.; DeSimone, J. M. PEGylated PRINT Nanoparticles: the Impact of PEG Density on Protein Binding, Macrophage Association, Biodistribution, and Pharmacokinetics. *Nano Letters* **2012**, *12* (10), 5304–5310.

(218) Macarron, R.; Banks, M. N.; Bojanic, D.; Burns, D. J.; Cirovic, D. A.; Garyantes, T.; Green, D. V. S.; Hertzberg, R. P.; Janzen, W. P.; Paslay, J. W.; et al. Impact of High-Throughput Screening in Biomedical Research. *Nat. Rev. Drug Discov.* **2011**, *10* (3), 188–195.

(219) Caron, J.; Maksimenko, A.; Wack, S.; Lepeltier, E.; Bourgaux, C.; Morvan, E.; Leblanc, K.; Couvreur, P.; Desmaele, D. Improving the Antitumor Activity of Squalenoyl-Paclitaxel Conjugate Nanoassemblies by Manipulating the Linker Between Paclitaxel and Squalene. *Adv. Healthcare Mater.* **2013**, *2* (1), 172–185.

(220) Menozzi, M.; Valentini, L.; Vannini, E.; Arcamone, F. Self-Association of Doxorubicin and Related Compounds in Aqueous Solution. *J. Pharm. Sci.* **1984**, *73* (6), 766–770.

(221) Zhang, T.; Huang, P.; Shi, L.; Su, Y.; Zhou, L.; Zhu, X.; Yan, D. Self-Assembled Nanoparticles of Amphiphilic Twin Drug From Floxuridine and Bendamustine for Cancer Therapy. *Mol. Pharm.* **2015**, *12* (7), 2328–2336.

(222) Svetlana O Doronina; Brian A Mendelsohn; Tim D Bovee; Charles G Cerveny; Stephen C Alley; Damon L Meyer; Ezogelin Oflazoglu; Brian E Toki; Russell J Sanderson; Roger F Zabinski; et al. Enhanced Activity of Monomethylauristatin F Through Monoclonal Antibody Delivery: Effects of Linker Technology on Efficacy and Toxicity. *Bioconjug. Chem.* **2005**, *17* (1), 114–124.

(223) Zhao, H. Scaffold Selection and Scaffold Hopping in Lead Generation: a Medicinal Chemistry Perspective. *Drug Discov. Today* **2007**, *12* (3-4), 149–155.

(224) Leeson, P. D.; Springthorpe, B. The Influence of Drug-Like Concepts on Decision-Making in Medicinal Chemistry. *Nat. Rev. Drug Discov.* **2007**, *6* (11), 881–890.

(225) Bickerton, G. R.; Paolini, G. V.; Besnard, J.; Muresan, S.; Hopkins, A. L. Quantifying the Chemical Beauty of Drugs. *Nat. Chem.* **2012**, *4* (2), 90–98.

(226) Lobenberg, R. Modern Bioavailability, Bioequivalence and Biopharmaceutics Classification System. New Scientific Approaches to International Regulatory Standards. *European Journal of Pharmaceutics and Biopharmaceutics* **2000**, *50* (1), 3–12.

(227) Otsuka, H.; Nagasaki, Y.; Kataoka, K. PEGylated Nanoparticles for Biological and Pharmaceutical Applications. *Adv. Drug Deliv. Rev.* **2003**, *55* (3), 403–419.

(228) Lynch, I.; Dawson, K. A. Protein-Nanoparticle Interactions. *Nano Today* **2008**, *3* (1-2), 40–47.

(229) Kratz, F. Albumin as a Drug Carrier: Design of Prodrugs, Drug Conjugates and Nanoparticles. *J. Control. Release* **2008**, *132* (3), 171–183.

(230) Roach, P.; Farrar, D.; Perry, C. C. Interpretation of Protein Adsorption: Surface-Induced Conformational Changes. *J. Am. Chem. Soc.* **2005**, *127* (22), 8168–8173.

(231) Tonigold, M.; Simon, J.; Estupiñán, D.; Kokkinopoulou, M.; Reinholz, J.; Kintzel, U.; Kaltbeitzel, A.; Renz, P.; Domogalla, M. P.; Steinbrink, K.; et al. Pre-Adsorption of Antibodies Enables Targeting of Nanocarriers Despite a Biomolecular Corona. *Nat. Nanotechnol.* **2018**, 1–13.

(232) Ilevbare, G. A.; Liu, H. Y.; Edgar, K. J.; Taylor, L. S. Maintaining Supersaturation in Aqueous Drug Solutions: Impact of Different Polymers on Induction Times. *Cryst. Growth Des.* **2013**, *13* (2), 740–751.

(233) Shamay, Y.; Shah, J.; Işık, M.; Mizrachi, A.; Leibold, J.; Tschaharganeh, D. F.; Roxbury, D.; Budhathoki-Uprety, J.; Nawaly, K.; Sugarman, J. L.; et al. Quantitative Self-Assembly Prediction Yields Targeted Nanomedicines. *Nat. Mater.* **2018**, *17* (4), 361–368.

(234) Shi, Y.; van Steenbergen, M. J.; Teunissen, E. A.; Novo, L.; Gradmann, S.; Baldus, M.; van Nostrum, C. F.; Hennink, W. E. Π–Π Stacking Increases the Stability and Loading Capacity of Thermosensitive Polymeric Micelles for Chemotherapeutic Drugs. *Biomacromolecules* **2013**, *14* (6), 1826–1837.

(235) Nakanishi, T.; Fukushima, S.; Okamoto, K.; Suzuki, M.; Matsumura, Y.; Yokoyama, M.; Okano, T.; Sakurai, Y.; Kataoka, K. Development of the Polymer Micelle Carrier System for Doxorubicin. *J. Control. Release* **2001**, *74* (1-3), 295–302.

(236) Mikhail, A. S.; Allen, C. Poly(Ethylene Glycol)-B-Poly(E-Caprolactone) Micelles Containing Chemically Conjugated and Physically Entrapped Docetaxel: Synthesis, Characterization, and the Influence of the Drug on Micelle Morphology. *Biomacromolecules* **2010**, *11* (5), 1273–1280.

(237) Kulkarni, A.; Pandey, P.; Rao, P.; Mahmoud, A.; Goldman, A.; Sabbisetti, V.; Parcha, S.; Natarajan, S. K.; Chandrasekar, V.; Dinulescu, D.; et al. Algorithm for Designing Nanoscale Supramolecular Therapeutics with Increased Anticancer Efficacy. *ACS Nano* **2016**, *10* (9), 8154–8168.

(238) Krebs, H. Chemical Composition of Blood Plasma and Serum. *Annu. Rev. Biochem.* **1950**.

(239) Workman, P.; Aboagye, E. O.; Balkwill, F.; Balmain, A.; Bruder, G.; Chaplin, D. J.; Double, J. A.; Everitt, J.; Farningham, D. A. H.; Glennie, M. J.; et al. Guidelines for the Welfare and Use of Animals in Cancer Research. *Br. J. Cancer* **2010**, *102* (11), 1555–1577.

(240) Youn, Y. S.; Bae, Y. H. Perspectives on the Past, Present, and Future of Cancer Nanomedicine. *Adv. Drug Deliv. Rev.* **2018**, 1–9.

(241) Eddershaw, P. J.; Beresford, A. P.; Bayliss, M. K. ADME/PK as Part of a Rational Approach to Drug Discovery. *Drug Discov. Today* **2000**, *5* (9), 409–414.

(242) Ernsting, M. J.; Murakami, M.; Roy, A.; Li, S.-D. Factors Controlling the Pharmacokinetics, Biodistribution and Intratumoral Penetration of Nanoparticles. *J. Control. Release* **2013**, *172* (3), 782–794.

(243) Moghimi, S. M.; Hunter, A. C.; Andresen, T. L. Factors Controlling Nanoparticle Pharmacokinetics: an Integrated Analysis and Perspective. *Annu. Rev. Pharmacol. Toxicol.* **2012**, *52* (1), 481–503.

(244) Shi, Y.; van der Meel, R.; Theek, B.; Oude Blenke, E.; Pieters, E. H.; Fens, M. H.; Ehling, J.; Schiffelers, R. M.; Storm, G.; van Nostrum, C. F.; et al. Complete Regression of Xenograft Tumors Upon Targeted Delivery of Paclitaxel via Pi-Pi Stacking Stabilized Polymeric Micelles. *ACS Nano* **2015**, *9* (4), 3740–3752.

(245) van der Meel, R.; Lammers, T.; Hennink, W. E. Cancer Nanomedicines: Oversold or Underappreciated? *Expert Opinion on Drug Delivery* **2016**, *14* (1), 1–5.

(246) Hamaguchi, T.; Matsumura, Y.; Suzuki, M.; Shimizu, K.; Goda, R.; Nakamura, I.; Nakatomi, I.; Yokoyama, M.; Kataoka, K.; Kakizoe, T. NK105, a Paclitaxel-Incorporating Micellar Nanoparticle Formulation, Can Extend in Vivo Antitumour Activity and Reduce the Neurotoxicity of Paclitaxel. *Br. J. Cancer* **2005**, *92* (7), 1240–1246.

(247) Sparreboom, A.; Scripture, C. D.; Trieu, V.; Williams, P. J.; De, T.; Yang, A.; Beals, B.; Figg, W. D.; Hawkins, M.; Desai, N. Comparative Preclinical and Clinical Pharmacokinetics of a Cremophor-Free, Nanoparticle Albumin-Bound Paclitaxel

(ABI-007) and Paclitaxel Formulated in Cremophor (Taxol). *Clin. Cancer Res.* **2005**, *11* (11), 4136–4143.

(248) Gabizon, A.; Catane, R.; Uziely, B.; Kaufman, B.; Safra, T.; Cohen, R.; Martin, F.; Huang, A.; Barenholz, Y. Prolonged Circulation Time and Enhanced Accumulatino in Malignant Exudates of Doxorubicin Encapsulated in Polyethylene-Glycol Coated Liposomes. *Cancer research* **1994**, *54*, 987–992.

(249) Pitt, J. J. Principles and Applications of Liquid Chromatography-Mass Spectrometry in Clinical Biochemistry. *Clin. Biochem. Rev.* **2009**, *30* (1), 19–34.

(250) Isin, E. M.; Elmore, C. S.; Nilsson, G. N.; Thompson, R. A.; Weidolf, L. Use of Radiolabeled Compounds in Drug Metabolism and Pharmacokinetic Studies. *Chem. Res. Toxicol.* **2012**, *25* (3), 532–542.

(251) Smith, D. A.; Di, L.; Kerns, E. H. The Effect of Plasma Protein Binding on in Vivo Efficacy: Misconceptions in Drug Discovery. *Nat. Rev. Drug Discov.* **2010**, *9* (12), 929–939.

(252) Herbst, R. S.; Khuri, F. R. Mode of Action of Docetaxel – a Basis for Combination with Novel Anticancer Agents. *Cancer Treatment Reviews* **2003**, *29* (5), 407–415.

(253) Chen, A. L.; Pavlick, A. Docetaxel More Active Than Paclitaxel as Second-Line Therapy for Metastatic Breast Cancer. *The Women's Oncology Review* **2011**, *6* (1-2), 99–100.

(254) Shuhendler, A. J.; Prasad, P.; Cai, P.; Hui, K. K. W.; Henderson, J. T.; Rauth, A. M.; Wu, X. Y. Matrigel Alters the Pathophysiology of Orthotopic Human Breast Adenocarcinoma Xenografts with Implications for Nanomedicine Evaluation. *Nanomedicine* **2013**, *9* (6), 795–805.

(255) Zhang, Y.-N.; Poon, W.; Tavares, A. J.; McGilvray, I. D.; Chan, W. C. W. Nanoparticle–Liver Interactions: Cellular Uptake and Hepatobiliary Elimination. *J. Control. Release* **2016**, *240*, 332–348.

(256) Brenner, J. S.; Pan, D. C.; Myerson, J. W.; Marcos-Contreras, O. A.; Villa, C. H.; Patel, P.; Hekierski, H.; Chatterjee, S.; Tao, J.-Q.; Parhiz, H.; et al. Red Blood Cell-Hitchhiking Boosts Delivery of Nanocarriers to Chosen Organs by Orders of Magnitude. *Nat. Commun.* **2018**, *9* (1), 2684.

(257) Jackson, M. A.; Werfel, T. A.; Curvino, E. J.; Yu, F.; Kavanaugh, T. E.; Sarett, S. M.; Dockery, M. D.; Kilchrist, K. V.; Jackson, A. N.; Giorgio, T. D.; et al. Zwitterionic Nanocarrier Surface Chemistry Improves siRNA Tumor Delivery and Silencing Activity Relative to Polyethylene Glycol. *ACS Nano* **2017**, *11* (6), 5680–5696.

(258) Wang, Y.; Kohane, D. S. External Triggering and Triggered Targeting Strategies for Drug Delivery. *Nat. Rev. Mater.* **2017**, *2* (6), 17020–14.

(259) Vaupel, P.; Kallinowski, F.; Okunieff, P. Blood Flow, Oxygen and Nutrient Supply, and Metabolic Microenvironment of Human Tumors: a Review. *Cancer Res.* **1989**, *49* (23), 6449–6465.

(260) Lee, E. S.; Shin, H. J.; Na, K.; Bae, Y. H. Poly(L-Histidine)–PEG Block Copolymer Micelles and pH-Induced Destabilization. *J. Control. Release* **2003**, *90* (3), 363–374.

(261) Kim, D.; Lee, E. S.; Oh, K. T.; Gao, Z. G.; Bae, Y. H. Doxorubicin-Loaded Polymeric Micelle Overcomes Multidrug Resistance of Cancer by Double-Targeting Folate Receptor and Early Endosomal pH. *Small* **2008**, *4* (11), 2043–2050.

(262) Semple, S. C.; Akinc, A.; Chen, J.; Sandhu, A. P.; Mui, B. L.; Cho, C. K.; Sah, D. W. Y.; Stebbing, D.; Crosley, E. J.; Yaworski, E.; et al. Rational Design of Cationic Lipids for siRNA Delivery. *Nat. Biotechnol.* **2010**, *28* (2), 172–176.

(263) Kanasty, R.; Dorkin, J. R.; Vegas, A.; Anderson, D. Delivery Materials for siRNA Therapeutics. *Nat. Mater.* **2013**, *12* (11), 967–977.

(264) Hajj, K. A.; Whitehead, K. A. Tools for Translation: Non-Viral Materials for Therapeutic mRNA Delivery. *Nat. Rev. Mater.* **2017**, *2* (10), 17056.
(265) Gao, W.; Chan, J. M.; Farokhzad, O. C. pH-Responsive Nanoparticles for Drug Delivery. *Mol. Pharm* **2010**, *7* (6), 1913–1920.
(266) Dou, Y.; Hynynen, K.; Allen, C. To Heat or Not to Heat: Challenges with Clinical Translation of Thermosensitive Liposomes. *J. Control. Release* **2017**, *249*, 63–73.
(267) Dunne, M.; Hynynen, K.; Allen, C. Thermosensitive Nanomedicines Could Revolutionize Thermal Therapy in Oncology. *Nano Today* **2017**, *16*, 9–13.
(268) Matsumoto, Y.; Nichols, J. W.; Toh, K.; Nomoto, T.; Cabral, H.; Miura, Y.; Christie, R. J.; Yamada, N.; Ogura, T.; Kano, M. R.; et al. Vascular Bursts Enhance Permeability of Tumour Blood Vessels and Improve Nanoparticle Delivery. *Nat. Nanotechnol.* **2016**, *11* (6), 533–538.
(269) Synatschke, C. V.; Nomoto, T.; Cabral, H.; Förtsch, M.; Toh, K.; Matsumoto, Y.; Miyazaki, K.; Hanisch, A.; Schacher, F. H.; Kishimura, A.; et al. Multicompartment Micelles with Adjustable Poly(Ethylene Glycol) Shell for Efficient in Vivo Photodynamic Therapy. *ACS Nano* **2014**, *8* (2), 1161–1172.
(270) Bouchaala, R.; Mercier, L.; Andreiuk, B.; Mély, Y.; Vandamme, T.; Anton, N.; Goetz, J. G.; Klymchenko, A. S. Integrity of Lipid Nanocarriers in Bloodstream and Tumor Quantified by Near-Infrared Ratiometric FRET Imaging in Living Mice. *J. Control. Release* **2016**, *236*, 57–67.
(271) Christie, R. J.; Miyata, K.; Matsumoto, Y.; Nomoto, T.; Menasco, D.; Lai, T. C.; Pennisi, M.; Osada, K.; Fukushima, S.; Nishiyama, N.; et al. Effect of Polymer Structure on Micelles Formed Between siRNA and Cationic Block Copolymer Comprising Thiols and Amidines. *Biomacromolecules* **2011**, *12* (9), 3174–3185.
(272) Yen, H.-C.; Cabral, H.; Mi, P.; Toh, K.; Matsumoto, Y.; Liu, X.; Koori, H.; Kim, A.; Miyazaki, K.; Miura, Y.; et al. Light-Induced Cytosolic Activation of Reduction-Sensitive Camptothecin-Loaded Polymeric Micelles for Spatiotemporally Controlled in Vivo Chemotherapy. *ACS Nano* **2014**, *8* (11), 11591–11602.
(273) Rapoport, N.; Gupta, R.; Kim, Y.-S.; O'Neill, B. E. Polymeric Micelles and Nanoemulsions as Tumor-Targeted Drug Carriers: Insight Through Intravital Imaging. *J. Control. Release* **2015**, *206*, 153–160.
(274) Mikhail, A. S.; Eetezadi, S.; Ekdawi, S. N.; Stewart, J.; Allen, C. Image-Based Analysis of the Size- and Time-Dependent Penetration of Polymeric Micelles in Multicellular Tumor Spheroids and Tumor Xenografts. *Int. J. Pharmaceutics* **2014**, *464* (1-2), 168–177.
(275) Ekdawi, S. N.; Stewart, J. M. P.; Dunne, M.; Stapleton, S.; Mitsakakis, N.; Dou, Y. N.; Jaffray, D. A.; Allen, C. Spatial and Temporal Mapping of Heterogeneity in Liposome Uptake and Microvascular Distribution in an Orthotopic Tumor Xenograft Model. *J. Control. Release* **2015**, *207*, 101–111.
(276) Holohan, C.; Van Schaeybroeck, S.; Longley, D. B.; Johnston, P. G. Cancer Drug Resistance: an Evolving Paradigm. *Nat. Rev. Cancer* **2013**, *13* (10), 714–726.
(277) Knight, Z. A.; Lin, H.; Shokat, K. M. Targeting the Cancer Kinome Through Polypharmacology. *Nat. Rev. Cancer* **2010**, *10* (2), 130–137.
(278) Al-Lazikani, B.; Banerji, U.; Workman, P. Combinatorial Drug Therapy for Cancer in the Post-Genomic Era. *Nat. Biotechnol.* **2012**, *30* (7), 679–692.
(279) Foucquier, J.; Guedj, M. Analysis of Drug Combinations: Current Methodological Landscape. *Pharmacol. Res. Perspect.* **2015**, *3* (3), e00149.

(280) Zhang, R. X.; Wong, H. L.; Xue, H. Y.; Eoh, J. Y.; Wu, X. Y. Nanomedicine of Synergistic Drug Combinations for Cancer Therapy - Strategies and Perspectives. *J. Control. Release* **2016**, *240*, 489–503.

(281) Shin, H.-C.; Alani, A. W. G.; Cho, H.; Bae, Y.; Kolesar, J. M.; Kwon, G. S. A 3-in-1 Polymeric Micelle Nanocontainer for Poorly Water-Soluble Drugs. *Mol. Pharm.* **2011**, *8* (4), 1257–1265.

(282) Reddy, L. H.; Couvreur, P. Nanotechnology for Therapy and Imaging of Liver Diseases. *Journal of Hepatology* **2011**, *55* (6), 1461–1466.

(283) Adams, D.; Gonzalez-Duarte, A.; O'Riordan, W. D.; Yang, C.-C.; Ueda, M.; Kristen, A. V.; Tournev, I.; Schmidt, H. H.; Coelho, T.; Berk, J. L.; et al. Patisiran, an RNAi Therapeutic, for Hereditary Transthyretin Amyloidosis. *N. Engl. J. Med.* **2018**, *379* (1), 11–21.

(284) Giménez, V. M. M.; Kassuha, D. E.; Manucha, W. Nanomedicine Applied to Cardiovascular Diseases: Latest Developments:. *Therapeutic Advances in Cardiovascular Disease* **2017**, *11* (4), 133–142.

(285) Godin, B.; Sakamoto, J. H.; Serda, R. E.; Grattoni, A.; Bouamrani, A.; Ferrari, M. Emerging Applications of Nanomedicine for the Diagnosis and Treatment of Cardiovascular Diseases. *Trends in Pharmacological Sciences* **2010**, *31* (5), 199–205.

(286) Eichaker, L. R.; Cho, H.; Duvall, C. L.; Werfel, T. A.; Hasty, K. A. Future Nanomedicine for the Diagnosis and Treatment of Osteoarthritis. *Nanomedicine* **2014**, *9* (14), 2203–2215.

(287) Zhang, Q.; Dehaini, D.; Zhang, Y.; Zhou, J.; Chen, X.; Zhang, L.; Fang, R. H.; Gao, W.; Zhang, L. Neutrophil Membrane-Coated Nanoparticles Inhibit Synovial Inflammation and Alleviate Joint Damage in Inflammatory Arthritis. *Nat. Nanotechnol.* **2018**, *11*, 1.

(288) Neves, das, J.; Amiji, M. M.; Bahia, M. F.; Sarmento, B. Nanotechnology-Based Systems for the Treatment and Prevention of HIV/AIDS. *Adv. Drug Deliv. Rev.* **2010**, *62* (4-5), 458–477.

(289) Liu, Z.; Jiang, W.; Nam, J.; Moon, J. J.; Kim, B. Y. S. Immunomodulating Nanomedicine for Cancer Therapy. *Nano Letters* **2018**, acs.nanolett.8b02340.

(290) Kirtane, A. R.; Langer, R.; Traverso, G. Past, Present, and Future Drug Delivery Systems for Antiretrovirals. *J. Pharm. Sci.* **2016**, *105*, 3471–3482.

Copyright Acknowledgements

Portions of Chapter 1 are reprinted with permission from Elsevier from the following publication:

> Ganesh, A.N., Donders, E.N., Shoichet, B.K., and Shoichet, M.S. (2018) Colloidal aggregation: From screening nuisance to formulation nuance. *Nano Today*. 19:188-200.

Chapter 2 is reprinted with permission from American Chemical Society from the following publication:

> Ganesh, A.N., McLaughlin, C.K., Duan, D., Shoichet, B.K., and Shoichet, M.S. (2017) A new spin on antibody-drug conjugates: trastuzumab-fulvestrant colloidal drug aggregates target HER2-positive cells. *ACS Applied Materials and Interfaces*, 9: 12195-12202.

Chapter 3 is reprinted with permission from American Chemical Society from the following publication:

> Ganesh, A.N.[#], Logie, J.[#], McLaughlin, C.K.[#], Barthel, B.L., Koch, T.H., Shoichet, B.K., and Shoichet, M.S. (2017) Leveraging colloidal aggregation for drug rich nanoparticle formulations. *Molecular Pharmaceutics*. 14: 1852-1860.